Hypercapnia Impairs Cell Junction Formation By Promoting TRAF2 E3 Ligase-Mediated Ubiquitination And Endocytosis Of The Na,K-ATPase β-Subunit In Alveolar Epithelial Cells

Inaugural Dissertation
submitted to the
Faculty of Medicine
in partial fulfillment of the requirements
for the PhD-Degree
of the Faculties of Veterinary Medicine and Medicine
of the Justus Liebig University Giessen

by
Gabrielli, Nieves María
of
Buenos Aires, Argentina

Giessen 2013

From the Department of Internal Medicine II
Director: Prof. Dr. Werner Seeger
of the Faculty of Medicine of the Justus Liebig University Giessen

First Supervisor and Committee Member: Prof. Dr. Werner Seeger
Second Supervisor and Committee Member: Prof. Dr. Martin Diener
Committee Member (Chair): Prof. Dr. Klaus-Dieter Schlüter
Committee Member: Prof. Dr. Wolfgang M. Kübler

Date of Doctoral Defense: November 20, 2013

Declaration

I declare that I have completed this dissertation single-handedly unauthorized help of a second party and only with the assistance acknowledged therein. I have appropriately acknowledged and referenced text passages that are derived literally from or are based on the content published or unpublished work of others, and all information that verbal communications. I have abided by the principles of good scientific conduct laid down in the charter of the Justus Liebig University of carrying out the investigations described in the dissertation.

Gabrielli, Nieves María

Giessen

Dedicated to my parents

Table of Contents

List of Abbreviations

A	alanine
A549	human adenocarcinoma alveolar epithelial cell line
ALI	acute lung injury
AMP	adenosine monophosphate
AMPK	AMP-activated protein kinase
ARDS	acute respiratory distress syndrome
ATI cells	alveolar epithelial type I cells
ATII cells	alveolar epithelial type II cells
ATP	adenosine triphosphate
Bis	bisindolylmaleimide I, hydrochloride
BSA	bovine serum albumin
$C_{12}E_{10}$	decaethyleneglycol dodecylether
Ca^{+}	calcium ion
cDNA	copy DNA
Chlor	chloroquine
CHO	Chinese Hamster Ovary cells
CHX	cycloheximide
cyt	cytoplasmic
CO_2	carbon dioxide
CP	core particle
C-terminal	carboxyl-terminal
Ctrl	control
D	aspartate
DMEM	Dulbecco's Modified Eagle's *Medium*
DMSO	dimethylsulfoxide
DNA	deoxyribonucleic acids
dNTP	desoxiNTP
DPBS	Dulbecco´s Phosphate-Buffered Saline
DTT	dithiothreitol
E1	ubiquitin-activating enzyme
E2	ubiquitin-conjugating enzyme
E3	ubiquitin ligase

E-cadherin	epithelial cadherin
EDTA	ethylene diamine tetraacetic acid
EGTA	ethylene glycol tetraacetic acid
ENaC	epithelial sodium channel
ER	endoplasmic reticulum
ERAD	endoplasmic reticulum-associated degradation
ERK	extracellular signal-regulated kinase
ESCRT	endosomal sorting complexes required for transport
FBS	fetal bovine serum
FCS	fetal calf serum
FiO_2	fraction of inspired oxygen
FITC	fluorescein isothiocyanate
GFP	green fluorescence protein
GST	glutathione S-transferase
HA	hemagglutinin
HECT	homologous to E6-AP carboxyl terminus
HeLa	Henrietta Lacks cells
His	histidine
HRP	horseradish peroxidase
IB	Western immunoblotting
IF	immunofluorescence
IgG	immunoglobulin G
IP	immunoprecipitation
K	lysine
K^+	potassium ion
kb	kilobase
LB	Luria-Bertani
MDCK	Madin-Darby canine kidney
Mg^+	magnesium ion
mmHg	millimeters of mercury
mRIPA	modified radioimmunoprecipitation assay buffer
mRNA	messenger RNA
MSV	Maloney sarcoma virus
Na,K-ATPase	sodium/potassium pump

NEM	N-ethilmaneimide
NF-κβ	nuclear factor κβ
NO_2	nitrogen dioxide
N-terminal	amino-terminal
NTP	nucleotide triphosphate
O_2	dioxygen
PaO_2	arterial partial pressure of oxygen
PBS	phosphate-buffered saline
PCR	polymerase chain reaction
PEEP	positive end-expiratory pressure
pH_e	extracellular pH
pH_i	intracellular pH
PKC-ζ	protein kinase C-ζ
P-substrate	phosphorylated substrate
R	arginine
RING	really interesting new gene
RNA	ribonucleic acid
ROS	reactive oxygen species
RP	regulatory particle
RPMI 1640	Roswell Park Memorial Institute 1640 medium
S	serine
S1P	sphingosine-1-phosphate
SDS-PAGE	sodium dodecyl sulfate-polyacrilamide gel electrophoresis
si	small interfering
Sphk	sphingosine kinase
TAE buffer	tris/acetic acid/EDTA buffer
TER	transepithelial electrical resistance
TGN	*trans*-Golgi network
TJ	tight junctions
TNF	tumor necrosis factor
TNFR	TNF receptor
TRAF2	TNF receptor-associated factor 2
T-TBS	tween 20-tris-buffer saline
Ub	ubiquitin

UBE	ubiquitin-activating enzyme
v-ATPase	vacuolar ATPase
wt	wild-type
YFP	yellow fluorescence protein
Zn^{2+}	zinc ion
ZO	zonula occludens

Summary

INTRODUCTION: In patients with acute respiratory distress syndrome (ARDS) disruption of the epithelial barrier results in accumulation of edema fluid in the airspaces, impairing gas exchange and leading to elevated CO_2 levels (hypercapnia). Moreover, lung-protective mechanical ventilation in patients often results in further hypercapnia. The formation of new cell-cell contacts after ARDS is essential for the re-establishment of an intact and functional alveolar epithelium, capable of clearing lung edema and performing gas exchange. The Na,K-ATPase β-subunit is a cell-adhesion molecule with a key role in the formation and stability of cell junctions and therefore might be important in the repair of the alveolar epithelium. However, the effects of hypercapnia on the stability of the Na,K-ATPase β-subunit and on the re-organization of adherens junctions have not been studied before. In the present work we tested the hypothesis that hypercapnia inhibits cell-cell contact formation by promoting the down-regulation of the Na,K-ATPase β-subunit. We aimed to elucidate the molecular mechanism underlying the (dis)regulation of adherens junction formation by hypercapnia.

METHODS AND RESULTS: Exposing alveolar epithelial cells to elevated CO_2 at constant extracellular pH of 7.4 led to the ubiquitination of the Na,K-ATPase β-subunit at the plasma membrane which resulted in a significant reduction of the protein abundance at the cell surface, as determined by cell-surface biotinylation and confocal microscopy. Internalization of the Na,K-ATPase β-subunit was followed by proteasome-dependent degradation of the protein, as assessed by pulse-chase experiments with impermeable biotin. The simultaneous mutations of lysines 5 and 7 of the Na,K-ATPase β-subunit to arginine prevented hypercapnia-induced ubiquitination and endocytosis of the protein, demonstrating that ubiquitin chains covalently-attached to the Na,K-ATPase β-subunit during hypercapnia act as an endocytosis signal. Mutation of serine 11 of the Na,K-ATPase β-subunit to alanine prevented hypercapnia-induced ubiquitination and degradation of the protein. In contrast, mutation of serine 11 to aspartate which mimics phosphorylation did not prevent hypercapnia-induced effects, suggesting that phosphorylation of the Na,K-ATPase β-subunit at serine 11 is a prerequisite for the ubiquitination of the protein. Coimmunoprecipitation and *in vitro* interaction studies showed that the serine/threonine kinase protein kinase C-ζ (PKC-ζ), known to be activated by hypercapnia, interacted with the Na,K-ATPase β-subunit and this interaction was dependent on the serine 11 of the Na,K-ATPase β-subunit. Moreover, PKC-ζ activity was

required for the hypercapnia-mediated effects, since the chemical inhibition or knock-down of the kinase prevented the endocytosis of the Na,K-ATPase β-subunit under hypercapnic conditions. By the use of a protein-interaction microarray we identified the E3 ligase TRAF2 as an interactive partner for Na,K-ATPase β-subunit. This interaction was further confirmed by coimmunoprecipitation and *in vitro* interaction studies. TRAF2 led to ubiquitination of the Na,K-ATPase β-subunit *in vitro* and *in vivo*. Moreover, knock-down of TRAF2 prevented the hypercapnia-induced endocytosis of the Na,K-ATPase β-subunit, demonstrating that TRAF2 is the E3 ligase that mediates the Na,K-ATPase β-subunit ubiquitination in hypercapnia. Most importantly, by cell aggregation assays we demonstrated that hypercapnia led to impaired cell junction formation, effect that was prevented by the simultaneous mutations of lysines 5 and 7 of the Na,K-ATPase β-subunit, demonstrating that hypercapnia-mediated down-regulation of the Na,K-ATPase β-subunit at the plasma membrane is the underlying mechanism by which hypercapnia inhibits cell-cell adhesion.

CONCLUSIONS: Here we report a novel mechanism by which hypercapnia affects the function of the alveolar epithelium. We provide evidence that hypercapnia (independently of pH) promotes ubiquitination of the Na,K-ATPase β-subunit at the plasma membrane leading to the endocytosis of the protein, which results in reduced ability of alveolar cells to form intercellular junctions. We demonstrate that ubiquitination depends on PKC-ζ activity and we identify TRAF2 as the E3 ligase that mediates the hypercapnia-induced ubiquitination of the Na,K-ATPase β-subunit. Thus, hypercapnia may impair restoration of the alveolo-capillary barrier in patients with ARDS upon hypercapnia by the down-regulation of the Na,K-ATPase β-subunit.

Zusammenfassung

EINLEITUNG: Die Schädigung der epithelialen Schranke in Patienten mit akutem Lungenversagen (engl. acute respiratory distress syndrome, ARDS) führt zur Ausbildung alveolärer Ödeme und folglich zu erhöhten CO_2-Leveln (Hyperkapnie). Zudem kann die lungenprotektive Beatmung mit geringen Tidalvolumen Hyperkapnie induzieren. Zur Auflösung von ARDS ist daher die Ausbildung neuer Zell-Zell-Kontakte für die Wiederherstellung eines intakten und funktionalen alveolären Epitheliums, das zur Resorption der Ödemflüssigkeit und Aufnahme des normalen Gasaustausches in der Lage ist, essenziell. Die β-Untereinheit der Na,K-ATPase ist ein Zelladhäsionsmolekül und spielt eine Schlüsselrolle in Ausbildung und Aufrechterhaltung von Zell-Zell-Kontakten und kann daher auch als wichtige Komponente für die Wiederherstellung der alveolo-kapillaren Schranke von Interesse sein. Allerdings ist bisher nicht bekannt, inwieweit erhöhte CO_2-Level einen Einfluss auf die Stabilität der Na,K-ATPase β-Untereinheit und die Reorganisation von Adherens Junctions haben. In der vorliegenden Arbeit sollte daher untersucht werden, ob und über welche molekularen Mechanismen Hyperkapnie die Regulation von Adherens Junctions reguliert und ob die Ausbildung von Zell-Zell-Kontakten durch eine Herunterregulation der Na,K-ATPase β-Untereinheit inhibiert wird.

METHODEN AND ERGEBNISSE: Oberflächen-Biotinylierung und konfokale Mikroskopie humane alveolarer epithelialer A549 Zellen zeigen, dass die Behandlung mit hohen CO_2-Konzentration 120mmHg) zu einer schnellen Ubiquitinierung der an der Plasmamembran befindlichen Na,K-ATPase β-Untereinheit, und in Folge dessen zu einer signifikanten Reduktion der Häufigkeit dieser Untereinheit an der Plasmamembran führt. Pulse-Chase Experimente mit nicht-zellpermeablem Biotin demonstrieren, dass nach der Hyperkapnie-induzierten Internalisierung der Na,K-ATPase β-Untereinheit eine proteosomale Degradation des Proteins folgt. Die gleichzeitige Mutation von Lysin 5 und 7 der Na,K-ATPase β-Untereinheit verhindert die Hyperkapnie-induzierte Ubiquitinierung und Endozytose des Proteins. Die Mutation von Serin 11 der Na,K-ATPase β-Untereinheit zu Alanin verhindert die Hyperkapnie-induzierte Ubiquitinierung und Degradierung, wohingegen die Mutation von Serin 11 zu Aspartat, was eine Phosphorylierung imitiert, die Hyperkapnie-induzierten Effekte nicht verhindert. Koimmunopräzipitation und *in vitro* Experimente zur Interaktion der Protein belegen, dass die PKC-ζ Serin/Threonin-Kinase, die bekannterweise während der Hyperkapnie aktiviert wird, mit der Na,K-ATPase β-Untereinheit interagiert und diese Interaktion abhängig ist von Serin 11 der Na,K-ATPase

β-Untereinheit. Weiterhin verhindert die chemische Inhibition oder der knock-down von PKC-ζ die Hyperkapnie-induzierte Endozytose der Na,K-ATPase β-Untereinheit. In einem Protein-Microarray zur Identifikation von Bindungspartnern der Na,K-ATPase β-Untereinheit wurde die E3 Ligase TRAF2 gefunden, die auch in Koimmunopräzipitationsstudien und in *in vitro* Interaktionsstudien die Na,K-ATPase β-Untereinheit bindet. TRAF2 induziert die Ubiquitinierung der Na,K-ATPase β-Untereinheit *in vitro* und *in vivo*. Außerdem verhindert der Knock-down von TRAF2 die Hyperkapnie-induzierte Endocytose der Na,K-ATPase β-Untereinheit. Durch Zellaggregationsassays konnten wir zeigen, dass Hyperkapnie zu gestörten Zell-Zell-Adhäsionen führt und dieser Effekt durch Mutation der Lysine 5 und 7 der Na,K-ATPase β-Untereinheit verhindert werden konnte.

ERGEBNIS: In dieser Studie zeigen wir einen neuen Mechanismus auf, über den Hyperkapnie Einfluss auf die Funktion des alveolären Epitheliums nimmt. Wir belegen, dass Hyperkapnie unabhängig vom pH die Ubiquitinierung und infolgedessen die Endozytose der Na,K-ATPase β-Untereinheit induziert, wodurch die Fähigkeit alveolarer Zellen zur Ausbildung von Zell-Zell-Kontakten reduziert wird. Weiterhin demonstrieren wir, dass die Ubiquitinierung der Na,K-ATPase β-Untereinheit von der Aktivität von PKC-ζ abhängt, und dass TRAF2 die E3 Ligase ist, die die Hyperkapnie-induzierte Ubiquitinierung vermittelt. Demzufolge könnte Hyperkapnie die Wiederherstellung der alveolo-kapillaren Schranke in Patienten mit ARDS durch eine Herunterregulation der Na,K-ATPase β-Untereinheit behindern.

1. Introduction

1.1. Acute respiratory distress syndrome

The acute respiratory distress syndrome (ARDS) is the cause of 40% mortality in approximately 200000 patients per year in the United States [1]. ARDS is a syndrome of acute respiratory failure in which patients present progressive arterial hypoxemia, dyspnea, and a marked increase in the work of breathing. Arterial hypoxemia is caused by accumulation of edema fluid in the distal air spaces in the lung, which impairs blood gas exchange. ARDS occurs within hours to days of a predisposing event and most patients require endotracheal intubation and positive pressure ventilation [2]. In 1994, the American-European Consensus Conference proposed a definition, widely employed for more than 15 years as a diagnostic tool, in which ARDS is defined as a syndrome characterized by acute onset of bilateral pulmonary infiltrates with arterial hypoxemia, judged by the ratio of arterial partial pressure of oxygen to fraction of inspired oxygen (PaO_2/FiO_2 ratio), in the absence of left atrial hypertension. If PaO_2/FiO_2 ratio is less than 300 mmHg, patients are considered to present with acute lung injury (ALI) and if PaO_2/FiO_2 ratio is less than 200 mmHg, patients are considered to present with ARDS [3]. In 2012, with the aim to simplify diagnosis and improve mortality prediction, a revised version of ARDS definition, called Berlin Definition, was adopted. By this definition, ARDS is now classified into mild, moderate and severe according to PaO_2/FiO_2 ratios of <300, <200 or <100 mmHg respectively in patients with a PEEP of 5 cm H_2O or grater [4].

Different clinical disorders may lead to the development of ARDS. The most prevalent cause of ARDS is primary pneumonia, which can be bacterial, viral, or fungal [5, 6]. The second most common cause of lung injury is severe sepsis. Other causes include gastric contents aspiration and major trauma [6].

Pathogenic changes observed during the course of ARDS can be classified into three phases: (*i*) an early exudative phase evidenced by the presence of interstitial and alveolar edema with accumulation of neutrophils, macrophages and blood cells in the alveolar space and endothelial and epithelial injury; (ii) a proliferative phase with pneumocyte hyperplasia and proliferation of myofibroblasts; and (*iii*) a fibrotic phase with collagen deposition and fibroproliferation. In some patients with persistent inflammation, fibroproliferation continues leading to lung fibrosis [5, 7, 8].

ARDS is primarily driven by an increase in the permeability to protein-rich fluid across the endothelial and epithelial barriers of the lung [9]. Different events may trigger endothelial injury, although neutrophil-mediated lung injury is probably the best documented pathway. Neutrophils may accumulate in the lung microvasculature, become activated leading to degranulation and release of several mediators, including proteases, reactive oxygen species (ROS), proinflammatory cytokines and procoagulant molecules causing the increase in vascular permeability and the loss the normal endothelial barrier function [2, 10-12] (**Figure 1, Figure 2**). Increased pulmonary microvascular permeability can result in the accumulation of protein-rich edema [13, 14]. However, endothelial injury alone is insufficient to cause ARDS. Under normal conditions, the epithelial barrier is much tighter than the endothelial barrier and prevents cells and plasma from invading the air spaces. An injury to the alveolar epithelium is necessary for the accumulation of protein-rich fluid in the alveolar air spaces and the development of ARDS [15, 16]. It has been shown in animal models that endothelial injury by intravenous administration of endotoxin, in the absence of injury to the lung epithelium, was not sufficient to cause the development of alveolar edema. Only when the epithelial barrier function was also impaired by instillation of live bacteria, edema formation was evident [16, 17]. In line with these data, lung biopsies from patients dying from ARDS presented both endothelial and epithelial injury in the lungs [5].

The mechanisms responsible for epithelial injury during ARDS have not been fully elucidated. Experimental studies suggest that neutrophils and their products may initiate the damage to the alveolar epithelial barrier [2, 12, 17, 18]. Under pathologic conditions, large number of neutrophils may become activated and release toxic mediators such as proteases and ROS that may induce the disintegration of cell junctions and apoptosis and necrosis of alveolar epithelial cells [19] (**Figure 1, Figure 2**).

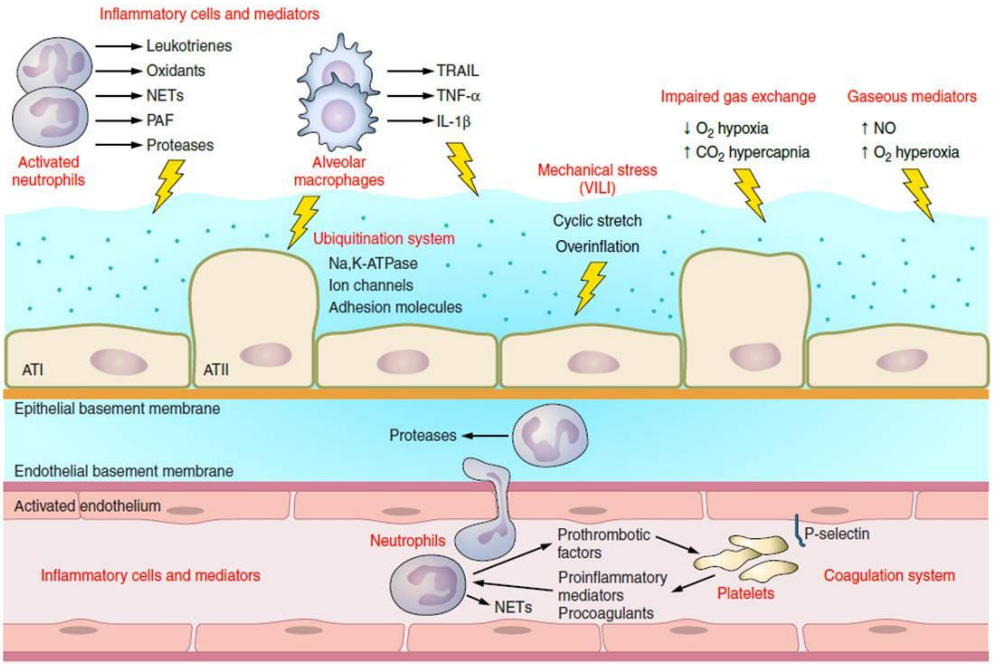

Figure 1: Schematic representation of inflammatory, non-inflammatory and mechanical stimuli and injures in the pathogenesis of ARDS [12].

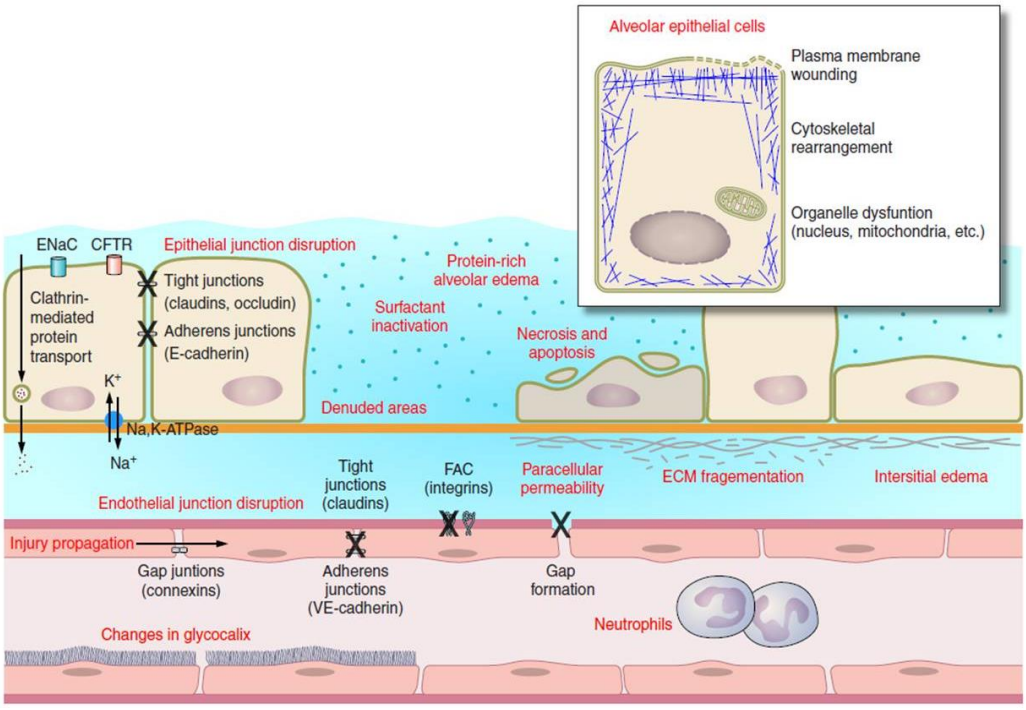

Figure 2: Schematic representation of impaired structures and functions of the alveolo-capillary barrier in ARDS [12].

1.2. Structural features of the alveolar epithelium

The alveolo-capillary barrier consists of an epithelial and endothelial monolayer, separated by a diminutive interstitial space. The close apposition between the alveolar epithelium and the vascular endothelium facilitates efficient gas exchange [20-22]. The alveolar epithelium contains equal numbers of thin, squamous alveolar type I (ATI) and cuboidal type II (ATII) cells, with the former accounting for approximately 95% of the surface area [23]. Both cell types contain well-organized adherens and tight junctions, and are polarized, displaying an asymmetric distribution of ion transporters, including the apical epithelial sodium channel (ENaC) and the basolaterally located Na,K-ATPase [24-26]. Thus, the intact alveolar epithelium regulates very tightly the permeability to proteins and solutes [24].

1.3. Clinical relevance of the repair of the alveolar epithelial injury

The alveolar epithelium, under physiological conditions, is much less permeable than the endothelium, and forms the primary barrier for solutes and electrolytes in the lung [15, 16, 27, 28]. The loss of integrity of the epithelial barrier, a hallmark in ARDS, leads to the accumulation of edema fluid in the alveolar air spaces [5]. Injured epithelial cells lose the capacity to remove fluid from the alveolar air spaces and produce less surfactant, causing further damage to the epithelium [6, 15, 16, 29-32]. The magnitude of the epithelial injury strongly affects the clinical course of patients with ARDS. Delayed or impaired epithelial resealing and alveolar fluid clearance are associated with worse prognosis [9, 15, 16, 29, 33, 34]. Severe injury to the alveolar epithelium, followed by inadequate repair, may lead to lung fibrosis [30].

1.4. Alveolar edema fluid clearance

Manifestation of alveolar edema causes severe impairment of gas exchange leading to local hypoxia and systemic hypoxemia the former of which causes further disruption of the alveolar epithelial barrier and fluid balance [35]. A critical step toward ARDS resolution involves the removal of the alveolar edema fluid to the lung interstitium, where clearance can occur through lung lymphatic vessels and pulmonary microcirculation [2]. The primary force driving fluid reabsorption from the alveolar space into the interstitium is the vectorial

transport of Na^+. Na^+ is taken up on the apical surface of the alveolar epithelium by amiloride-sensitive and -insensitive Na^+ channels and is subsequently "pumped" out of the cell by the Na,K-ATPase on the basolateral side [36, 37]. This process generates an osmotic gradient, which drives passive movement of water from the apical side of the epithelium (the alveolar space) to the basolateral side (the interstitium) paracellularly [12, 37] (**Figure 3**).

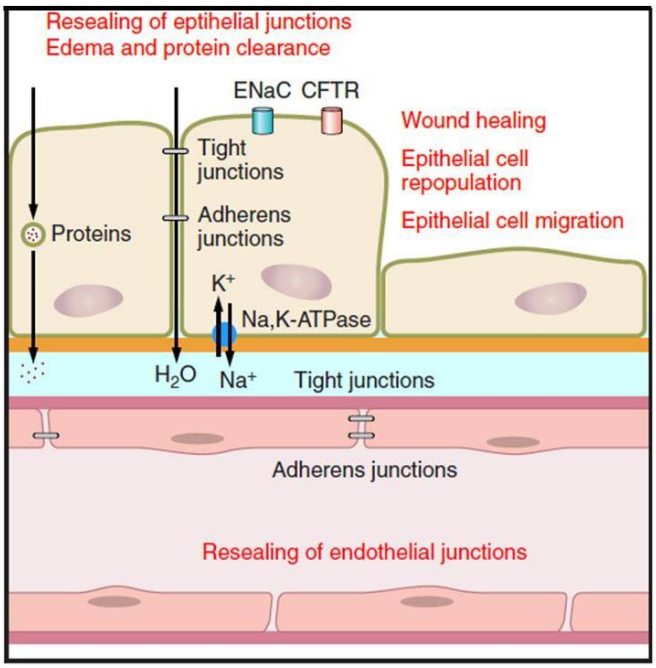

Figure 3: Key elements in ARDS resolution [12].

1.5. Alveolar epithelial barrier resealing

Only an intact alveolar epithelium can reabsorb fluid from the alveolar space and prevent further edema formation.. Therefore, a key factor in patients´ recovery from ARDS is the reconstitution of a normal alveolar structure. This involves spreading and migration of neighboring alveolar epithelial cells to cover denuded areas, migration and proliferation of progenitor cells to restore cell numbers, cell differentiation to restore function and cell junction organization to recover epithelium tightness and continuity [12, 15, 16, 38]. The major type of intercellular junctions responsible for re-establishing a tight epithelium are the tight junctions, adherens junctions and desmosomes [39, 40] (**Figure 3**).

1.6. Adherens junctions

Adherens junctions are a form of cell-cell adhesion structure found in several cell types [41]. Epithelial cadherin (E-cadherin), a member of the cadherin superfamily, is a transmembrane protein that mediates Ca^{+}-dependent homophilic cell-cell adhesion [42-44]. While the extracellular domain of E-cadherin establishes the interaction between adjacent cells, its cytoplasmic domain binds to intracellular adhesion molecules which link cell-cell adhesion to the actin cytoskeleton producing mature junctions [45-49]. Adherens junctions provide strong physical anchorage and participate in the generation of intracellular signaling [50]. These adherens junctions play a pivotal role in regulating the integrity and tightness of the epithelium and are involved in the formation of other cell-cell junctions [51, 52].

1.7. Tight junctions

The low paracellular permeability of the healthy pulmonary epithelium is due to the presence of tight junctions (TJ), belt-like interconnected junctional strands of proteins, connecting alveolar cells and separating the apical and basolateral surfaces of the epithelium [26, 53-55]. Tight junction proteins play a major role in regulating the lung barrier [24]. An emerging concept is that tight junction composition, as opposed to number of tight junction strands, determines the barrier properties [56]. ATI and ATII cells express occludin [57, 58], zonula occludens (ZO)-1 [55] and several members of the claudin family [59]. Claudins are a family of transmembrane proteins that are crucial structural and functional components of tight junctions, being claudin 3, 4 and 18 the most predominantly expressed in the alveolus [56]. Claudin 4 levels are positively correlated with an intact alveolar barrier function [60, 61] and it is up-regulated in response to ARDS [61]. Other stimuli such as oxidative stress, alcohol and NO_2 exposition, can also lead to changes in the composition, expression and localization of tight junctions, which in turn affect the integrity of the alveolar epithelial barrier [62-64].

1.8. The Na,K-ATPase

The Na,K-ATPase, a member of the P-type ATPase superfamily, is expressed in all animal tissues, establishing concentration gradients for Na^{+} and K^{+} within the cell by pumping

three Na^+ out of the cell and two K^+ into the cell per ATP molecule consumed [65, 66]. The Na,K-ATPase heterodimer, composed of a catalytic α- and a regulatory β-subunit, is assembled in the endoplasmic reticulum (ER) and delivered to the plasma membrane of epithelial cells (**Figure 4**) [67-69]. The α-subunit is a 112 kDa polytopic membrane protein with ten transmembrane segments. It contains the catalytic activity of the enzyme and the binding sites for Na^+, K^+ and ATP [67, 70, 71]. The β-subunit is a single membrane spanning polypeptide with a small cytoplasmic domain and a large extracellular portion, containing three disulphide bridges and three N-glycosylation sites. Depending on the degree of glycosylation, which differs within species and tissues, the mature β-subunit has a molecular weight between 40-60 kDa [72, 73]. The Na,K-ATPase β-subunit has been shown to be critical for translation, correct folding and membrane insertion of the α-subunit of the Na^+ pump [73]. To date, four α- and β-subunit isoforms have been identified in mammals, which are expressed in a tissue specific manner [74-76]. A third protein, termed the γ-subunit, can provide further tissue-specific regulation [77]. In the lung, the Na,K-ATPase localizes at the basolateral surface of ATI and ATII cells. Two isoforms of the Na,K-ATPase α-subunit (α1 and α2) and β-subunit are expressed in the alveolar epithelial cells, with the α1-subunit being expressed in both cell types, while the α2-subunit appears to be restricted to ATI cells [78-80].

The majority of the studies have been focused on the transport function of the Na,K-ATPase demonstrating its critical role in keeping alveoli free of edema [81]. However, growing evidence has demonstrated that the Na,K-ATPase is a multifunctional protein involved in the formation and maintenance of intercellular junctions, cell polarity, cell motility, cell signaling, actin dynamics and cancer [82, 83]. Thus, Na,K-ATPase could have physiological functions in the alveolar epithelium beyond ion transport.

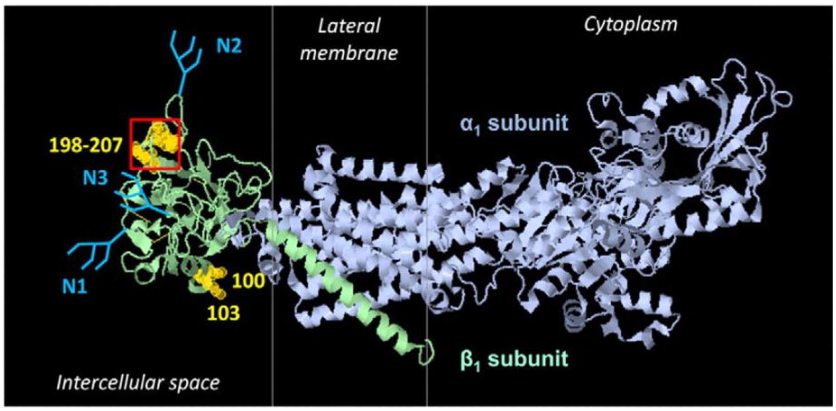

Figure 4: High-resolution structure of the Na,K-ATPase (2ZXE) [84, 85].

1.9. The Na,K-ATPase β-subunit as a cell adhesion molecule

The Na,K-ATPase is distributed in a highly polarized manner within epithelial cells. At the beginning of the formation of the epithelial monolayer, the major fraction of the Na,K-ATPase is present at the basal membrane. During the formation of cell-cell contacts the Na,K-ATPase starts to accumulate at the lateral border of adjacent cells [86]. Studies conducted in CHO fibroblast cell lines provided evidence that β-subunit expression in these cells induced the polarized expression of the Na,K-ATPase and conferred CHO cells adhesive properties [87]. On the other hand, inhibition of the Na,K-ATPase activity by ouabain disrupted Na,K-ATPase polarized expression and impaired cell-cell adhesion [51, 88, 89]. These results, together with the observation that β-subunit has a typical structure of an adhesion molecule [90, 91] are in line with a possible link between Na,K-ATPase and cell adhesion [87]. Studies conducted to examine the possibility that β-subunit is directly involved in cell-cell adhesion have consistently shown that the Na,K-ATPase β-subunit directly participates in the formation intercellular adhesion [85, 92, 93]. It has been reported that the Na,K-ATPase colocalizes with adherens junctions in all stages of the monolayer formation starting from the initiation of cell-cell contact [86] (**Figure 5**). In fact, the Na,K-ATPase β-subunit has been shown to act as a cell adhesion molecule in the adherens junctions. The cytoplasmic domain of the Na,K-ATPase is linked to E-cadherin via ankyrin/spectrin cytoskeleton while the extracellular domain of β-subunit interacts with the β-subunit of adjacent cells [92, 93]. The strength of β-β interactions has been proven to be dependent on its N-glycans and its amino acid sequence [85, 86]. The impairment of β-β binding by alterations in β-subunit N-glycans or amino acid sequence, or by the use of β-subunit blocking antibodies, caused instability of junctional complexes and increased paracellular permeability [85, 94-96]. These observations provide solid evidence that interactions between the Na,K-ATPase β-subunits of neighboring cells maintain the integrity of intercellular junctions. Taken together, these findings strongly support a major role of the Na,K-ATPase in the barrier function, separate from its role in the vectorial sodium transport.

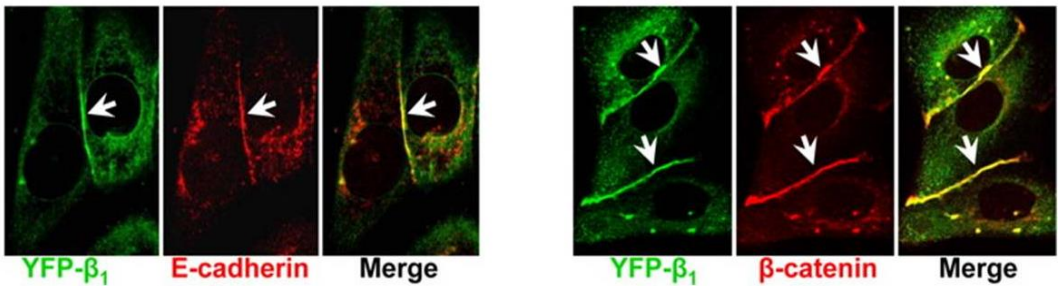

Figure 5: Immunostaining of MDCK cells shows that YFP-tagged Na,K-ATPase β.subunit colocalizes with E-cadherin and β-catenin in the sites of cell contacts [86].

1.10. Role of the Na,K-ATPase β-subunit in the organization and maintenance of tight junctions

The tightness of the healthy alveolar epithelium is due to the presence of tight junctions. It has been well-documented that E-cadherin and the β-subunit of the Na,K-ATPase play an essential role in the formation of tight junctions and establishment of epithelial polarity [46, 97-100]. Some of these studies were performed in Maloney sarcoma virus (MSV)-transformed Madin-Darby canine kidney (MDCK) cells, which express low levels of E-cadherin and Na,K-ATPase β-subunit and display a non-polarized phenotype. Experiments in which E-cadherin and Na,K-ATPase β-subunit were expressed, demonstrated that the simultaneous expression of both proteins is required for MSV-transformed MDCK to form functional tight junctions and display a polarized phenotype [97].

Additional evidence on the role of the Na,K-ATPase in tight junction formation has been provided by studies in mice embryos. These studies showed that Na,K-ATPase β-subunit is required for blastocyst formation and that the lack of β-subunit expression led to aberrant distribution of the Na,K-ATPase α-subunit and tight junction proteins during pre-implantation development [101].

The molecular mechanisms involved in the formation of tight junctions might differ from the mechanisms required to maintain tight junctions. In fact, although E-cadherin function is critical for the formation of tight junctions, its function appears to be dispensable once the cells have established the tight junctions. The Na, K-ATPase, on the other hand, has proven to be involved in both the establishment as well as the maintenance of functional tight junctions and epithelial polarity [97, 102]. Therefore, it is reasonable to propose that events leading to changes in Na,K-ATPase β-subunit expression, glycosylation pattern, distribution within the cell or stability may play a role in the

disruption of the alveolar epithelium and/or may cause delayed or impaired repair of the epithelial monolayer after injury.

1.11. Regulation of the Na,K-ATPase

In most polarized epithelial cells, the α- and β-subunit are expressed at an equimolar ratio, assembled as heterodimers, and delivered to the basolateral membrane where they contribute to active Na^+ transport and maintain epithelial integrity [65]. The abundance of Na^+ pump subunits and ATPase activity are tightly regulated by various stimuli. The pump is regulated by concentrations of its substrates as well as by changes in the molecular components of the surrounding environment (ions and non-ionic molecules). The Na,K-ATPase is modulated by membrane-associated components such as cytoskeletal elements and regulatory FXYD proteins, such as γ-subunit. The pump is also affected by variations in oxygen, carbon dioxide and nitrogen availability. As an important molecule in charge of various biological events, the Na,K-ATPase is regulated by a number of circulating endogenous inhibitors and hormones, such as aldosterone, thyroid hormone, glucocorticoid, catecholamines, insulin, carbachol, estrogen and androgen [34, 103-107]. All these stimuli can exert either short term or long term regulation of the Na, K-ATPase. Long term regulation of Na,K-ATPase usually involves changes in RNA and protein synthesis or degradation of the Na,K-ATPase isoforms [104, 107-111]. Short term modulation of the Na,K-ATPase function may be mediated by changes in the cellular distribution of pump units by reversible post-translational mechanisms such as phosphorylation or ubiquitination, or by changes in the intracellular Na^+ concentration which in turn modifies the pump kinetics [108, 111].

Functionality of the Na,K-ATPase is fundamental for edema clearance during ARDS and not only experimental models of acute lung injury (ALI), but also patients with ARDS, are characterized by an impairment of the Na,K-ATPase function leading to a decreased ability of the lungs to clear edema and worse outcomes [33, 34].

1.12. Hypercapnia

In mammals, CO_2 produced during aerobic cellular respiration is disposed by the lung. In patients with ARDS, the alveolar epithelium, the site of CO_2 elimination, is exposed to elevated CO_2 levels (hypercapnia), as a consequence of poor alveolar gas exchange.

Moreover, these patients often require mechanical ventilation with low tidal volumes which may result in a further increase in blood and tissue CO_2 levels [112, 113].

Whether hypercapnia brings any benefit or harm to patients remains controversial. Some clinicians argue that hypercapnia and its associated acidosis may enhance patients´ outcomes, particularly by reducing inflammation during the course of ARDS [114-116]. However, the fact that buffering hypercapnic acidosis worsen experimental ARDS [117] suggests that some of these effects might be due to acidosis rather than hypercapnia *per se* [112]. Other clinicians argue that hypercapnia might be detrimental in patients and often, various techniques including extracorporeal carbon dioxide elimination are employed to treat hypercapnia and acidosis [112, 118]. The latter theory is supported by preliminary observations of a prospective cohort of 3400 patients receiving mechanical ventilation for at least 48 hours. This study has shown that patients who developed hypercapnia in the first 48 hours had a higher incidence of new ARDS and required mechanical ventilation for longer periods [117]. High CO_2 levels have also been associated with increased mortality in hospitalized patients with community-acquired pneumonia [119] and have been found to be a marker of poor prognosis in COPD [120, 121] and a risk factor in patients with cystic fibrosis waiting for lung transplantation [122].

The notion of a sensor for CO_2 has been proposed in plants and insects [123, 124]. In Drosophila, a CO_2 sensitive receptor has been described in the olfactory neurons [123]. Recently, it has been reported that mice also can detect CO_2 through the olfactory system involving carbonic anhydrase [125]. The effects of hypercapnia on excitable cells are well characterized and include depolarization of glomus cells, which trigger an increase in alveolar ventilation to maintain normal CO_2 levels in the body [126]. In contrast, the effects of CO_2 on non-excitable mammalian cells are incompletely understood.

Our group has conducted studies to evaluate the hypothesis that elevated CO_2 levels have important deleterious effects on the alveolar epithelium, the site of CO_2 elimination in mammals. Results from these studies have shown that non-excitable alveolar epithelial cells sense and respond to elevated levels of CO_2, independently of extracellular and intracellular pH, by inhibiting Na,K-ATPase function. The decrease in Na^+ pump function results in impaired alveolar fluid reabsorption in rats exposed to hypercapnia [127]. Over the recent years, our group has contributed to the better understanding of the CO_2 signaling pathway. High CO_2 levels lead to the Ca^+-dependent activation of Ca^+/calmodulin-dependent kinase kinase-β. This kinase causes the activation of a well-recognized metabolic sensor, the AMP-activated protein kinase (AMPK), which promotes cell

adaptation to stress [128]. AMPK leads to activation of protein kinase C-ζ (PKC-ζ), which phosphorylates the Na,K-ATPase α-subunit, causing it to endocytose from the plasma membrane into intracellular pools, thus altering its function [127, 128]. These results have been also reconfirmed *in vivo* in animals exposed to elevated CO_2 levels for up to seven days [128].

These findings clearly demonstrate a deleterious effect of hypercapnia on Na,K-ATPase-mediated edema clearance. However, it remains unknown whether hypercapnia also affects Na,K-ATPase β-subunit stability. Once at the plasma membrane Na,K-ATPase subunits can be independently and differently regulated and Na,K-ATPase β-subunit emerges as a critical target of study, considering its key role in the formation and maintenance of tight and adherens junctions and therefore potential impact on the epithelial barrier integrity and repair after ARDS.

1.13. Ubiquitination

The canonical role of ubiquitination is to mediate the degradation of proteins that carry ubiquitin on specific lysine residues. However, increasing evidence shows that protein modification by ubiquitin has diverse functions and is involved in a broad variety of cellular processes. It has been well-documented that the attachment of ubiquitin can act as an internalization signal that sends the modified substrate to the endocytic/sorting compartments [129, 130]. The Na,K-ATPase α-subunit is one example of the several membrane proteins whose trafficking is regulated by the ubiquitin system [131]

Ubiquitin is a 76 amino acid peptide of 8.5 kDa. It is found in almost all tissues of all eukaryotic organisms and it is highly conserved among species, sharing 96% homology yeast and humans. Ubiquitin has a long half-life and is recyclable (**Figure 6**) [132-135].

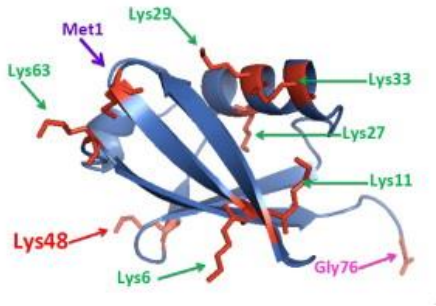

Figure 6: Ubiquitin structure. Key amino acid residues present in ubiquitin molecule are indicated [135].

Ubiquitination is an enzymatic, post-translational modification process in which a ubiquitin peptide is covalently attached to a protein substrate. The process is very complex involving several enzymes and accessory proteins. The reaction occurs via sequential action of three enzymes: a ubiquitin-activating enzyme E1, a ubiquitin-conjugating enzyme E2 and a ubiquitin ligase E3 (**Figure 7**). The first step involves ATP-dependent ubiquitin activation by the formation of a high-energy thioester linkage between the carboxyl group of ubiquitin´s glycine 76 and E1´s cysteine in the active-site. A second step involves the transfer of the high-energy thioester bond from the E1 to the active-site cysteine of one of ~40 E2s (in mammals). Finally, a third step consists of the transfer of the ubiquitin peptide from the E2 to the ε-amino group of a substrate´s lysine. This final step is mediated by one of the ~600 E3s (in mammals) [132, 136, 137].

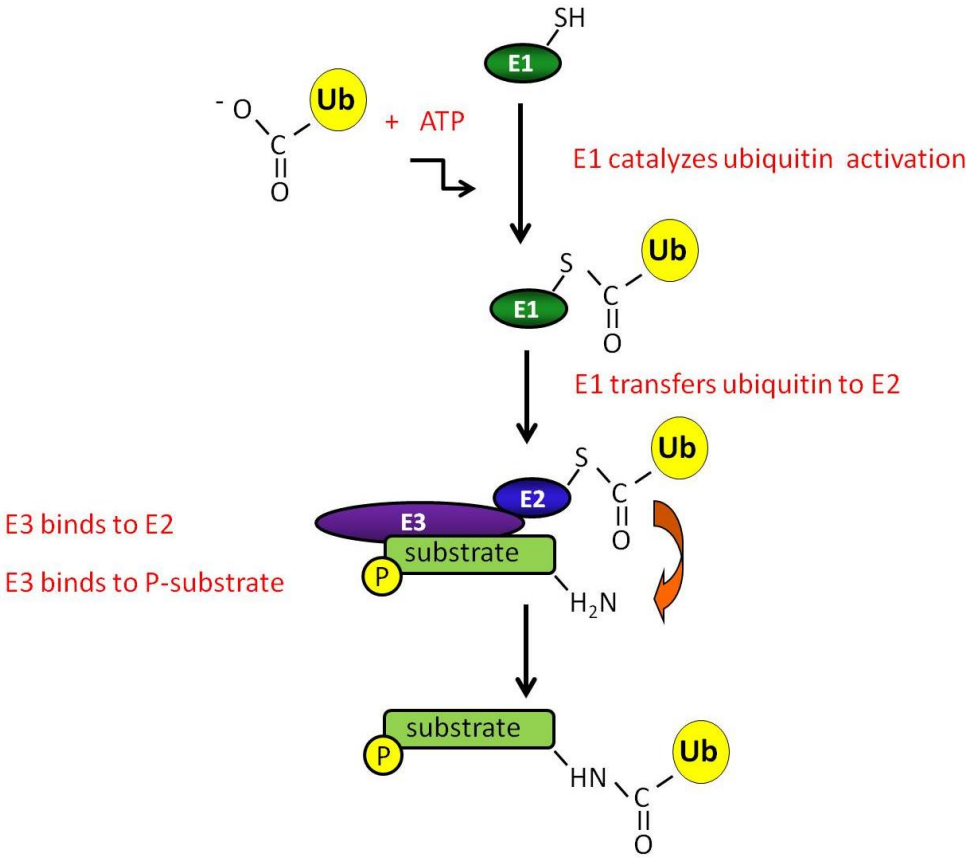

Figure 7: Schematic representation of the ubiquitination reaction. By the ATP-dependent sequential action of three enzymes: a ubiquitin-activating enzyme E1, a ubiquitin-conjugating enzyme E2 and a ubiquitin ligase E3, the ubiquitin molecule is covalently attached to a substrate which is often phosphorylated (P-substrate).

1.14. RING E3 ligases

The specificity and diversity of ubiquitination is a consequence of the hierarchical order of the ubiquitin enzymatic cascade. Although one or two E1s activate the ubiquitin conjugation machinery, a large number of E2 conjugating enzymes and E3 ligases have been identified [138] (**Figure 8**).

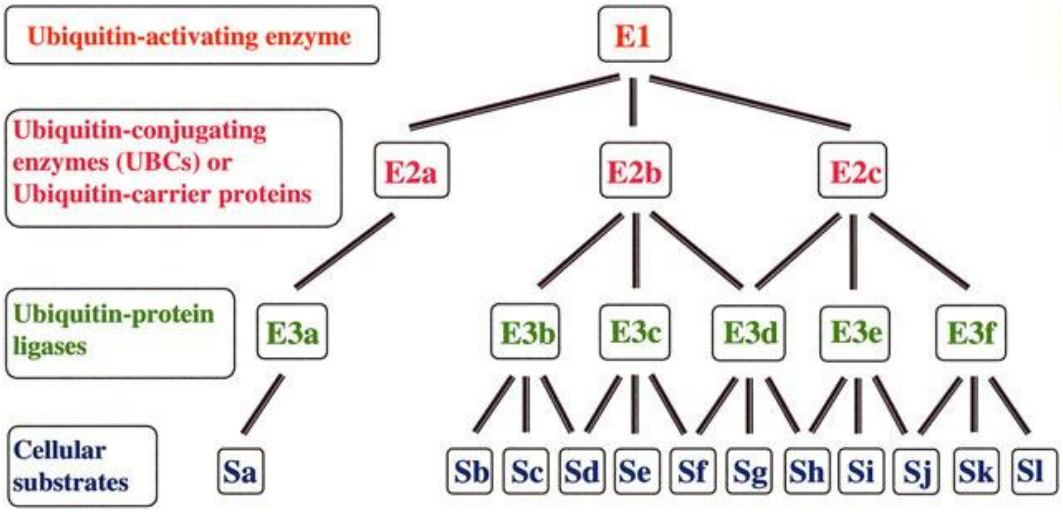

Figure 8: Schematic representation of the hierarchical structure of ubiquitin-conjugating machinery [138]. E1 can activate several E2s which act in turn on several E3s. E3s can be substrate-specific or can recognize some substrates via similar, but not identical, motifs. Some substrates may be recognized by different E3s via diverse motifs.

Ubiquitination has to occur with exquisite spatial, temporal and substrate specificity. E3 ligases determine the specificity of the ubiquitination reaction by specifically recognizing their substrates, by selecting the lysines to be modified by ubiquitin, and by catalyzing the formation of the same product (same size and chain topology) each time they act on their substrate [136]. Two primary classes of E3s have been described. The first is characterized by the presence of a homologous to E6-AP carboxyl terminus (HECT) domain [139]; the second by a really interesting new gene (RING)-finger domain [140, 141]. HECT E3 ligases participate in the catalytic reaction by forming a thioester bond between ubiquitin and the E3´s active-site cysteine, followed by the transfer of ubiquitin to the substrate. RING E3 ligases, on the other hand, mediate the direct transfer of ubiquitin from E2 to the substrate [130, 136].

RING-type E3 ligases are the most abundant in nature. The mammalian genome encodes more than 600 potential RING finger E3s [142]. RING E3s do not possess intrinsic catalytic activity. Its RING finger domain, containing series of spaced cysteine and histidine residues that coordinate Zn^{2+}, facilitates E2-dependent ubiquitination [143]. Based on the interpretation of E2-E3 complexes crystal structures, it is believed that RING E3 ligases contribute to catalysis by acting as scaffold proteins that bring together the active site of E2 and the acceptor lysine residue of the substrate. They may make an additional contribution by inducing allosteric activation of E2s [144]. RING E3 ligases can function as monomer, dimers or multiprotein complexes [136].

Substrate recognition by the appropriate E3 ligase can be influenced by the presence of accessory proteins, by subcellular compartmentalization of E3s and substrate, and by post-translational modifications, such as phosphorylation or neddylation of the substrate or the E3 ligase [136, 145-149]. The best studied regulatory mechanism of the ubiquitination process is phosphorylation. Phosphorylation of E3 ligases can regulate substrate ubiquitination either positively or negatively. RING E3 ligases are very often tightly regulated through phosphorylation which can promote or inhibit its binding to substrate proteins or E2 enzymes [149]. Substrate phosphorylation can also regulate E3 ligase-mediated substrate ubiquitination [149-151]. Phosphorylation itself can create a recognition signal or "phosphodegron" for binding of an E3 ligase. Phosphorylation can induce conformational changes in the substrate and result in exposure of degrons. Phosphorylation may also regulate substrate compartmentalization and therefore control the access of an E3 ligase to its target [149, 152].

It has been observed that the attachment of ubiquitin molecules to the substrate´s lysines take place on unstructured regions that are located near the degron elements bound by E3s. In most cases, there is no consensus sequence for ubiquitination. These observations suggest that ubiquitination may depend mainly on lysine accessibility and not primary sequence context. However, a factor that seems to enhance the reactivity of a lysine is the presence of near-by basic residues. Vicinal lysines could contribute to each other´s ubiquitination by depressing pKa and increasing reactivity [140, 153, 154].

The specific combination of E2 and E3 enzymes recruited to a substrate dictates the chain linkage type. Different ubiquitin modifications adopt diverse three dimensional structures which are recognized by specific ubiquitin receptors determining substrates´ fate [155-159].

Because E3s dictate the specificity of the ubiquitination process, they may be considered as therapeutic targets [160].

1.15. Types of ubiquitin modifications and substrate fate

The diversity of ubiquitination effects is further enhanced by the multiple ways in which ubiquitin can be attached to a protein. The addition of a single ubiquitin to a substrate is defined as monoubiquitination. Moreover, several lysine residues in the substrate can be tagged with single ubiquitin molecules, termed as multi-monoubiquitination. Finally, ubiquitin itself contains seven lysine residues (K6, K11, K27, K29, K33, K48 and K63) (**Figure 6**), which can also be targeted by another ubiquitin molecule in an interactive process, known as polyubiquitination, that leads to the formation of a ubiquitin chain attached to a single lysine. It is now clear that different types of ubiquitination are involved in the regulation of different cellular processes [155, 161-165]. Monoubiquitination has been implicated in the endocytosis of plasma membrane proteins [129]. In contrast, polyubiquitin chains formed via the C-terminal glycine and K48 or K11 of two ubiquitins have a well-characterized role in targeting proteins for degradation by the 26S proteasome [166, 167], whereas ubiquitin chains formed through K63 are involved in other cellular functions including DNA repair, cell signaling and endocytosis [168].

1.16. Ubiquitin-mediated degradation pathways

There are three major degradation pathways in mammalian cells: the proteasome, the lysosome and the autophagosome and it is now well demonstrated that ubiquitin is involved in all of them (**Figure 9**) [168]. Factors that may influence the route of degradation of a particular protein include chain length and linkage type, as well as the nature of the E2 and/or E3 enzymes involved [168].

The ubiquitin-proteasome degradation pathway is a major route for protein degradation. The proteasome is a multiprotein complex that participates in the degradation of cellular proteins. Its components are often referred to by the Svedberg sedimentation coefficient denoted S. The 2.5-MDa protein degradation machine 26S comprises a proteolytic core particle (CP) 20S and one or two regulatory particle(s) (RP) 19S. The CP consists of two outer α rings and two inner β rings, which are made up of seven structurally similar α- and β-subunits, respectively. The CP displays caspase-, trypsin-, and

chymotrypsin-like activities on the inner surface of the chamber. The RP serves to recognize polyubiquitinated proteins and plays a role in the deubiquitination, unfolding, and translocation of proteins into the interior of the CP for its destruction [169, 170]. Initial studies suggested that K48-linked ubiquitin chains consisting of at least 4 ubiquitin molecules were required for 19S recognition and proteasome-mediated degradation [166]. Recent studies, however, suggest that other types of chains may also lead to proteasomal degradation [165].

The lysosomal degradation pathway is prominent in the degradation of plasma membrane proteins. Lysosomes are cellular organelles that contain enzymes that mediate the degradation of proteins and other biological polymers. Lysosomal enzymes are acid hydrolases which require low pH, maintained by the v-ATPase, to be active [171]. Independently of the mode of entry, endocytosed proteins are usually delivered to the early endosome where sorting occurs. Proteins can be routed from the early endosome to late endosomes and lysosomes for degradation, to the *trans*-Golgi network (TGN), or recycled to the plasma membrane [172]. The role of ubiquitin in this degradation pathway consists of engaging the internalized protein with the endosomal sorting complexes required for transport (ESCRTs). Preferentially K63-linked polyubiqutintination is recognized by ubiquitin receptors present in the endocytosis machinery leading to protein internalization [168, 173].

Autophagy is generally thought to be a non-specific event in which cytosol and organelles are degraded. However, there are several cases in which selective autophagy take place and ubiquitin plays a role in these events. K27- and K63-linked poliubiquitination of autophagosomes can be recognized by specific ubiquitin receptors that may lead to regulated lysosome-mediated final degradation [174, 175].

Ubiquitin participates in the three major cellular degradation pathways, and the targeting of the substrate protein to a particular route is believed to rely on factors such as subcellular localization of the substrate, E2s and E3s enzymes, ubiquitin receptors, ubiquitin chain length and ubiquitin linkage type. Occasionally, non-canonical degradation occurs. For instance, ubiquitinated cytosolic proteins may be degraded by the lysosome and cytoplasm-exposed domains of membrane proteins may be degraded by the proteasome. Moreover, recent evidence suggests the existence of a proteasome pool associated with endosomes that influences protein sorting, highlighting an interplay between the proteasomal and lysosomal pathways.

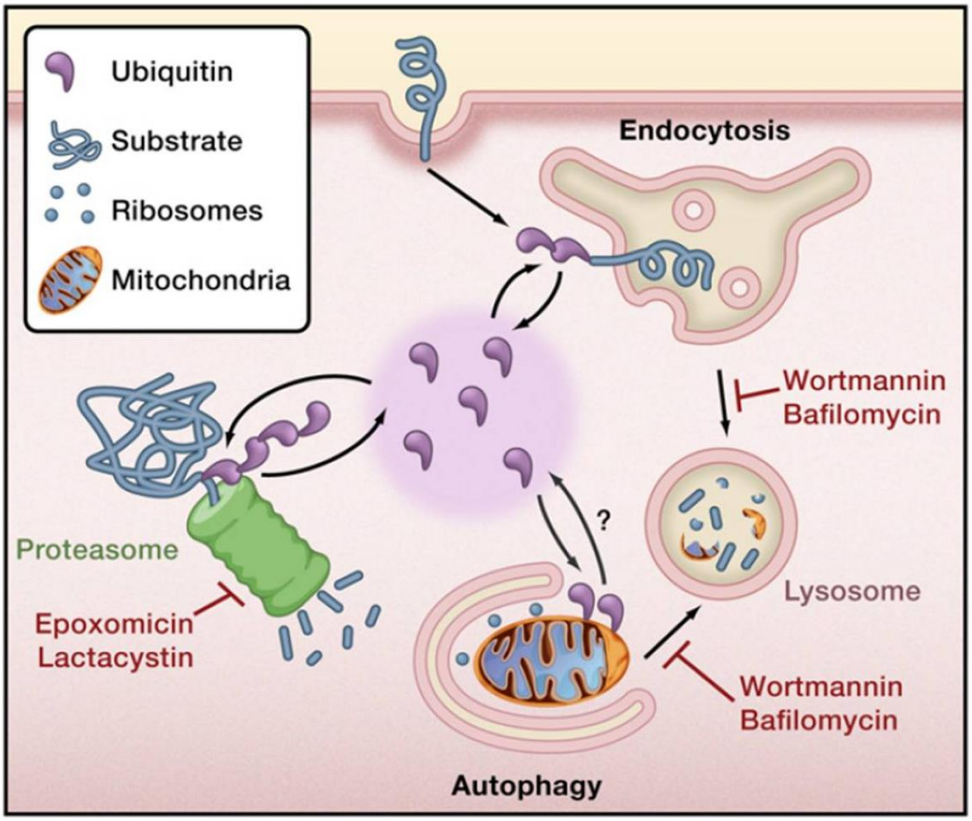

Figure 9: Schematic representation of the degradation pathways in which the ubiquitin molecule is implicated [168].

1.17. Work hypothesis and aims

We hypothesize that during ARDS, hypercapnia has negative effects on the re-establishment of an intact alveolar epithelium by inducing ubiquitin-mediated down-regulation of the Na,K-ATPase β-subunit.

In the present study we set out to answer the following questions:

What are the effects of hypercapnia on the mechanisms required for the re-establishment of an intact alveolar epithelium?

- Does hypercapnia negatively affect cell-cell adhesion?

Which is the molecular mechanism underlying the impaired cell adhesion observed in hypercapnia?

- Does hypercapnia induce instability of the Na,K-ATPase β-subunit located at the plasma membrane by promoting its endocytosis and/or degradation?
- Is ubiquitination implicated in Na,K-ATPase β-subunit endocytosis and/or degradation?
- If hypercapnia mediates ubiquitination of the Na,K-ATPase β-subunit, which are the molecular players involved?
- Is it possible to prevent the deleterious effects of hypercapnia on cell adhesion by inhibiting the ubiquitination of the Na,K-ATPase β-subunit ?

Understanding the mechanisms by which hypercapnia regulates the β-subunit of the Na,K-ATPase and epithelial barrier integrity may provide novel insights into hypercapnia-induced dysfunction of the alveolar epithelium, as well as the impaired repair of the alveolar epithelium associated with hypercapnia during ARDS. Identifying the E3 ligase responsible for the hypercapnia-induced ubiquitination of the Na,K-ATPase β-subunit may provide us with a highly specific tool that might be employed in therapies aiming to restore alveolar epithelial integrity.

2. Material and methods

2.1. General reagents

All chemicals used were of analytical grade purity. Detailed chemicals, reagents and consumables are specified along the methodology.

2.2. Alveolar epithelial type II cell lines

Hypercapnia-mediated effects on cell-adhesion and on Na,K-ATPase β-subunit regulation were mainly conducted in human A549 cells, an alveolar epithelial cell line in which the Na,K-ATPase expression, activity and regulation are characterized and similar to primary alveolar epithelial cells [127, 128, 176, 177]. This cell line transfects very efficiently, thus facilitating the mechanistic studies. In addition, key experiments on cell adhesion and mechanistic studies were validated in primary rat ATII cells which are known to polarize and form completely developed intercellular junctions, and are used to study alveolar epithelial cell adhesion and barrier properties [85, 178, 179].

A549 cells (American Type Culture Collection (ATCC), Manassas, VA; CCL 185) are human adenocarcinomic alveolar basal epithelial cells. This cell line was developed from cancerous lung tissue in an explanted tumor of a 58-year-old Caucasian male [180].

Primary rat ATII cells are ATII cells isolated from rat lung [181].

A549 cells stably expressing dog Na,K-ATPase β-subunit fused to yellow fluorescence protein (YFP) were employed in some experiments (A549-β1-YFP cells; a generous gift from Dr. Sznajder and Dr. Dada, Northwestern University, Chicago, IL, USA).

2.3. Drugs

Drug	Application	Concentration	Vehicle	Company
MG-132	proteasomal inhibitor	20 µM	DMSO	Calbiochem
Chloroquine	lysosomal inhibitor	100 µM	water	Sigma-Aldrich
E-64	lysosomal inhibitor	10 µM	water	Calbiochem
N-ethilmaneimide (NEM)	deubiquitination inhibitor	5 mM	ethanol	Sigma-Aldrich
Cycloheximide (CHX)	protein synthesis inhibitor	1.7 mM	water	Sigma-Aldrich
Bisindolylmaleimide I, Hydrochloride (BIS)	PKC inhibitor	10 µM	DMSO	Cell Signaling

Table I: Chemical agents applied in cellular experiments.

2.4. Primers

All primers were synthesized by METABION (Martinsried, Germany).

Construct	Primer
WT	Forward: 5´ATAGGATCCGTAATGGCCCGCGGGAAAGCCAAG3´ Reverse: 5´CTGGAATTCGCTCTTAACTTCAATTTTTACATC3´
K5R	5´GGATCCGTAATGGCCCGCGGGAGAGCCAAGGAGGAGGGCAGCTGG3´
K7R	5´GGATCCGTAATGGCCCGCGGGAAAGCCAGGGAGGAGGGCAGCTGG3´
K5RK7R	5´GGATCCGTAATGGCCCGCGGGAGAGCCAGGGAGGAGGGCAGCTGG3´
K13RK14R	5´GAGGAGGGCAGCTGGAGGAGATTCATCTGGAACTCAG3´
K21RK22R	5´CATCTGGAACTCAGAGAGGAGGGAGTTTCTGGGCAG3´
S11A	5´GCCCGCGGGAAAGCCAAGGAGGAGGGCGCCTGGAAGAAATTCATCTGG3´
S11D	5´GCCCGCGGGAAAGCCAAGGAGGAGGGCGACTGGAAGAAATTCATCTGG3´

Table II: Primers employed for cloning and site-directed mutagenesis.

2.5. Plasmids

Plasmid	Insert Description	Provider
pcDNA 3.1 V5-His	Na,K-ATPase β1-subunit, H. sapiens	Invitrogen
pRK5-HA-Ubiquitin-wt	Wild type (wt) ubiquitin, H. sapiens	Addgene (plasmid 17608) [182]
pEBG-TRAF2-GST	TRAF2, H. sapiens	Addgene (plasmid 21586) [183]

Table III: Plasmids employed in cell transfection experiments

2.6. siRNA

siRNA	Provider	pmols/transfection
siPKC-ζ	Cell Signaling	120
siTRAF2	Santa Cruz	120

Table IV: siRNAs employed for cell transfection experiments.

2.7. Synthetic peptides

All synthetic peptides were designed by our laboratory and synthesized by BIOMATIK (Delaware, USA). All peptides were labeled with biotin in the N-terminal.

Construct	Peptide
WT	Biotin-MARGKAKEEGSWKKFIWNSEKKEFLGRTGGSWFK
S11D	Biotin-MARGKAKEEGDWKKFIWNSEKKEFLGRTGGSWFK
S19D	Biotin-MARGKAKEEGSWKKFIWNDEKKEFLGRTGGSWFK
S31D	Biotin-MARGKAKEEGSWKKFIWNSEKKEFLGRTGGDWFK

Table V: N-terminal biotinylated synthetic peptides employed in *in vitro* studies.

2.8. Antibodies

Antibody	Dilution (application)	Company name
Anti-Na,K-ATPase β1-subunit mouse monoclonal IgG2a (Clone M17-P5-F11)	1:10000 (IB) 1:250 (IP) 1:40 (IF)	Thermo Scientific
Anti-E-cadherin rabbit polyclonal IgG (H-108)	1:200 (IB)	Santa Cruz Biotechnology
Anti-Actin rabbit polyclonal affinity purified antibody	1:10000 (IB)	Sigma-Aldrich
Anti-Ub mouse monoclonal IgG1 against mono and poliubiquitination (Clone P4D1)	1:10000 (IB)	Santa Cruz Biotechnology
Anti-V5 rabbit polyclonal IgG	1:250 (IP)	Sigma-Aldrich
Anti-V5 mouse monoclonal IgG	1:2000 (IB)	Invitrogen
Anti-HA.11 mouse monoclonal IgG1 (Clone 16B12)	1:5000 (IB)	Covance
Anti-GFP mouse IgG1 (clones 7.1 and 13.1)	1:1000 (IB) 1:50 (IP)	Roche Diagnostic
Anti-PKC-ζ mouse monoclonal IgG2 (H-1)	1:200 (IB) 1:40 (IF)	Santa Cruz Biotechnology
Anti-TRAF2 rabbit polyclonal IgG (C-20)	1:200 (IB)	Santa Cruz Biotechnology
Anti-mouse IgG (H+L) rabbit polyclonal IgG HRP-conjugated	1:5000 (IB)	Thermo Scientific
Anti-rabbit IgG goat polyclonal IgG HRP-conjugated	1:2500 (IB)	Cell Signaling
Anti-mouse IgG (H+L) rabbit polyclonal IgG FITC-conjugated	1:100 (IF)	Thermo Scientific

Table VI: Antibodies used for Western immunoblotting (IB), immunofluorescence (IF) and immunoprecipitation (IP) analysis.

2.9. Isolation of alveolar epithelial type II cells from rat lungs

The lungs from male Sprague Dawley rats (200–250 g) were perfused at 37°C with:

Solution A: 0.9% NaCl
0.1% glucose
30 mM HEPES
6 mM KCl
0.1 mg/ml streptomycin sulfate
0.2 mg/ml penicillin G
0.07 mg/ml EGTA
3 mM Na_2HPO_4
3 mM NaH_2PO_4, pH 7.4

Then, the lungs were lavaged 8-10 times at 37°C using:

Solution B: 3 mM $MgSO_4$
1.5 mM $CaCl_2$

Perfusion was followed by lung digestion by elastase (3 U/ml in solution A) at 37°C and incubating for 12-14 minutes. This step was repeated twice. After chopping with scissors for several times, the cell suspension was mixed with 100 mg/ml DNase I, incubated for 5 minutes at 37°C with gentle rotation, and filtered through 160 and 37 mm nylon mesh once, and 15 mm nylon mesh twice. The cells were incubated for 30 minutes at 37°C in rat IgG-coated polystyrene 100 mm Petri dishes (1.5mg rat IgG/dish). The unattached cells were centrifuged at 250 xg for 8 minutes and resuspended in:

Solution C: RPMI 1640 medium containing
25 mM HEPES
1% FBS
100 mg/ml DNase I

at a concentration of 10 ~ 20 $\times 10^6$ cells/ml. To remove the remaining macrophages, the cells were incubated with rat IgG (40 mg/ml) at room temperature for 15 minutes with

gentle rotation. After being washed twice with solution C, the cells were incubated with sheep anti-rat IgG magnetic beads (100 ml/rat) for 15 minutes at 41°C. The beads were removed by a magnetic device. To remove leukocyte and ATI contaminations, the cells were incubated with anti- LC (40 mg/ml) and rabbit anti-rat T1a (40 mg/ml) at 41°C for 40 minutes, followed by incubation with goat anti-mouse IgG Dynabeads (100 ml/rat) and goat anti-rabbit IgG BioMags beads (500 ml/rat). Finally, primary ATII cells were plated as needed and used in day 3.

2.10. Cell culture

Cells were incubated in a Haereus cell culture incubator (Haereus Instruments, Hanau, Germany) at a temperature of 37°C, 80-90% relative humidity and 5% carbon dioxide in air atmosphere. A549 cells were cultured in Dulbecco´s modified Eagle medium high glucose (DMEM High Glucose; PAA Laboratories, Egelsbach, Germany) containing 10% [vol/vol] fetal bovine serum (FBS; PAA Laboratories, Egelsbach, Germany), 100 U/ml penicillin, and 100 µg/ml streptomycin (both from PAN-Biotech, Aidenbach, Germany).

Cells were plated in 100 mm tissue culture dishes (Cellstar; Greiner Bio-One, Frickenhausen, Germany). For subculturing, cells were rinsed in Dulbecco´s Phosphate-Buffered Saline (DPBS; PAA Laboratories, Egelsbach, Germany) twice, incubated 5 minutes in 0.25% trypsin-EDTA (PAN-Biotech, Aidenbach, Germany) to allow cell detachment, resuspended in culture medium and seeded in a ratio 1:10 in 100 mm dishes for further subculturing. For experiments, cells from passage 3 to 15 were employed and plated on tissue culture dishes or cover slips.

2.11. DNA constructs generation

2.11.1. DNA construct strategy

For the development of the project we cloned the coding region of Na,K-ATPase β-subunit in a mammalian expression plasmid pcDNA 3.1 V5-His (**Figure 10**). This plasmid contains a strong promoter for high-level expression in mammalian cells (cytomegalovirus (CMV) promoter) and a V5 epitope tag for easy detection with a monoclonal antibody.

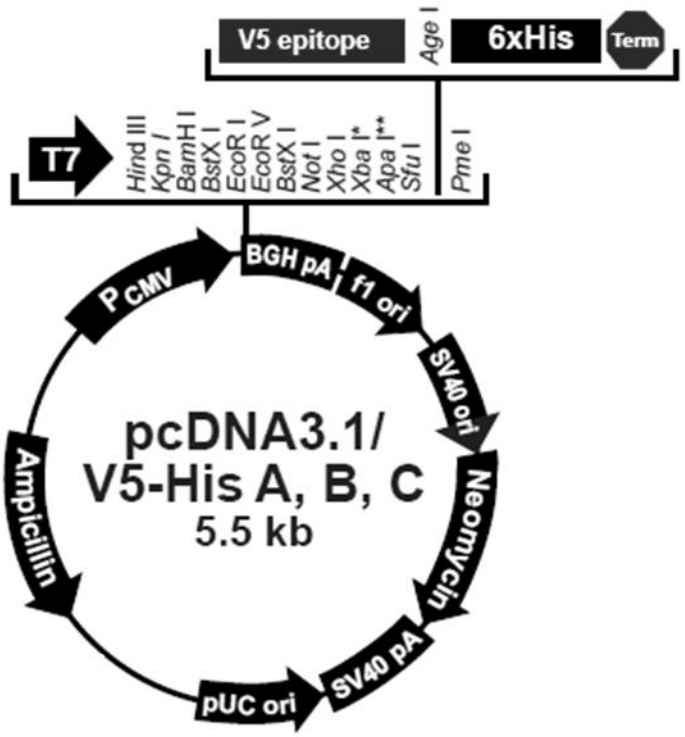

pcDNA3.1/V5-His® A Multiple Cloning Site

T7 promoter/priming site — *Hind* III — *Kpn* I — *Bam*H I

```
861  ATTAATACGA CTCACTATAG GGAGACCCAA GCTGGCTAGT TAA GCT TGG TAC CGA GCT CGG
                                                   Ala Trp Tyr Arg Ala Arg
```

BstX I* — *Eco*R I — *Eco*R V — *BstX* I* — *Not* I

```
922  ATC CAC TAG TCC AGT GTG GTG GAA TTC TGC AGA TAT CCA GCA CAG TGG CGG CCG
     Ile His *** Ser Ser Val Val Glu Phe Cys Arg Tyr Pro Ala Gln Trp Arg Pro
```

Xho I — *Xba* I — *Apa* I — *Sfu* I — V5 epitope

```
976  CTC GAG TCT AGA GGG CCC TTC GAA GGT AAG CCT ATC CCT AAC CCT CTC CTC GGT
     Leu Glu Ser Arg Gly Pro Phe Glu Gly Lys Pro Ile Pro Asn Pro Leu Leu Gly
```

Age I — Polyhistidine tag — *Pme* I

```
1030 CTC GAT TCT ACG CGT ACC GGT CAT CAT CAC CAT CAC CAT TGA GTTTAAACCC
     Leu Asp Ser Thr Arg Thr Gly His His His His His His ***
```

BGH Reverse priming site

```
1083 GCTGATCAGC CTCGACTGTG CCTTCTAGTT GCCAGCCAT
```

*Note that there are two *Bst*X I sites in the polylinker.

Figure 10: pcDNA3.1/V5-His A Multiple Cloning Site

The human Na,K-ATPase β-subunit mRNA sequence was obtained from the Genbank sequence database (Gene ATP1B1; NCBI Reference Sequence: NM_001677.3; GI: 49574487). In order to insert the complete human Na,K-ATPase β-subunit coding region into pcDNA 3.1 V5-His plasmid specific primers were designed containing restriction sites for BamHI and EcoRI to clone the protein unidirectionally:

Forward primer containing BamHI restriction site:
5´ ATAGGATCCGTAATGGCCCGCGGGAAAGCCAAG 3´

Reverse primer containing EcoRI restriction site:
5´ CTGGAATTCGCTCTTAACTTCAATTTTTACATC 3´

The underlined sequences show the position of the restriction sites for BamHI and EcoRI. The sequences in red correspond to β-subunit coding sequence. The stop codon was removed in order to add the fusion V5 tag in frame with the c-terminal domain of the protein.

Amplified fragment (122-1030 bp):
5´ATGGCCCGCGGGAAAGCCAAGGAGGAGGGCAGCTGGAAGAAATTCATCTGG
AACTCAGAGAAGAAGGAGTTTCTGGGCAGGACCGGTGGCAGTTGGTTTAAGAT
CCTTCTATTCTACGTAATATTTTATGGCTGCCTGGCTGGCATCTTCATCGGAAC
CATCCAAGTGATGCTGCTCACCATCAGTGAATTTAAGCCCACATATCAGGACC
GAGTGGCCCCGCCAGGATTAACACAGATTCCTCAGATCCAGAAGACTGAAATT
TCCTTTCGTCCTAATGATCCCAAGAGCTATGAGGCATATGTACTGAACATAGTT
AGGTTCCTGGAAAAGTACAAAGATTCAGCCCAGAGGGATGACATGATTTTTGA
AGATTGTGGCGATGTGCCCAGTGAACCGAAAGAACGAGGAGACTTTAATCATG
AACGAGGAGAGCGAAAGGTCTGCAGATTCAAGCTTGAATGGCTGGAAATTGCT
CTGGATTAAATGATGAAACTTATGGCTACAAAGAGGGCAAACCGTGCATTATT
ATAAAGCTCAACCGAGTTCTAGGCTTCAAACCTAAGCCTCCCAAGAATGAGTC
CTTGGAGACTTACCCAGTGATGAAGTATAACCCAAATGTCCTTCCCGTTCAGTG
CACTGGCAAGCGAGATGAAGATAAGGATAAAGTTGGAAATGTGGAGTATTTTG
GACTGGGCAACTCCCCTGGTTTTCCTCTGCAGTATTATCCGTACTATGGCAAAC
TCCTGCAGCCCAAATACCTGCAGCCCCTGCTGGCCGTACAGTTCACCAATCTTA
CCATGGACACTGAAATTCGCATAGAGTGTAAGGCGTACGGTGAGAACATTGGG
TACAGTGAGAAAGACCGTTTTCAGGGACGTTTTGATGTAAAAATTGAAGTTAA
GAGC 3´

One of the aims of the project consisted of studying hypercapnia effects on phosphorylation and ubiquitination of Na,K-ATPase β-subunit. In order to identify the amino acids involved in these phosphorylation and ubiquitination processes, we created

protein variants by adding point mutations to the original Na,K-ATPase β-subunit C-terminal V5-tagged (wt) construct with the Quick Change Mutagenesis Kit (Stratagene, La Jolla, California, USA). We only focused on the intracellular domain of Na,K-ATPase β-subunit because post-translational modifications would occur in that region. The strategy employed to study the amino acids involved in ubiquitination consisted of changing lysines (K) to arginines (R). In order to identify the amino acids involved in serine phosphorylation, serines (S) were changed to alanine (A) to prevent phosphorylation, or to aspartate (D) to mimic phosphorylation. Combination of multiple mutations was done by using plasmids already containing Na,K-ATPase β-subunit mutations as templates for additional desired point mutations. Forward primers employed in the mutagenesis are displayed in the **table II** (reverse primers consisting of the reverse complement of the forward primer sequence are not shown in the table). Variants employed in this work are: K5R, K7R, K5/7R, K13/14R, K21/22R, S11A and S11D.

2.11.2. RNA isolation

Total RNA was isolated from A549 cells with the use of the commercial RNAasy Minikit (QIAGEN, Hilden, Germany) and QIAshredder columns (QIAGEN, Hilden, Germany). Briefly, A549 cells were plated in 60 mm cell culture dishes and allow to reach confluency. Cells were rinsed with DPBS twice and lysed directly with RLT lysis buffer containing 1% β-mercaptoethanol. In order to reduce the viscosity of the cell lysate, homogenization was done by loading the cell lysate into a QIAshredder column. The homogenate was collected from the column by 2 minutes of centrifugation at 14000 xg and mixed with 70% ethanol in order to provide appropriate binding conditions to the RNeasy Mini spin column. Once in the column, RNA was preferentially bound to the silica column, whereas DNA and proteins were removed by sequential washes. Finally RNA was eluted from the column with RNAse free water. Samples were quantified with the Nanodrop (Thermo Fisher Scientific, Waltham, Massachusetts, USA) and approximately 30 µg of RNA per sample were recovered and stored at -70°C till use.

2.11.3. cDNA synthesis

In order to obtain copy DNA (cDNA), total RNA was reversed transcript employing iScript cDNA Synthesis Kit (Biorad, Hercules, California, USA). To conduct the cDNA synthesis we prepared a reaction mix as shown in **Table VII.**

Components	Volume per 20 µl Reaction
5x iScript reaction mix	4 µl
iScript reverse transcriptase	1 µl
nuclease-free water	14 µl
RNA template (1 µg/ul total RNA)	1 µl

Table VII: Reverse transcription reaction mix.

We conducted the reverse transcription reaction in a thermocycler (Thermo Fisher Scientific, Waltham, Massachusetts, USA). We employed a program that involved 5 minutes at 25°C, 30 minutes at 42°C and 5 minutes at 85°C. cDNA was stored at -20°C till use.

2.11.4. PCR

DNA amplification was done by the use of Q5 Hot Start High-Fidelity DNA Polymerase (Biolabs, Massachusetts, USA). The reaction mix is shown in **Table VIII**.

Components	Volume per 50 µl Reaction
5x Q5 Reaction Buffer (Biolabs)	10 µl
dNTP Mix, 10 mM each (Thermo Scientific)	1 µl
10 µM Forward Primer (Metabion)	2.5 µl
10 µM Reverse Primer (Metabion)	2.5 µl
template DNA (1µg/ul cDNA)	2 µl
Q5 Hot Start High-Fidelity DNA Polymerase (Biolab)	0.5 µl
nuclease-Free Water	31.5 µl

Table VIII: PCR reaction mix.

In order to obtain the DNA amplification we used the following thermocycling conditions in a thermocycler (Thermo Fisher Scientific, Waltham, Massachusetts, USA):

Initial Denaturation	5 minutes	25°C	
Denaturation	30 seconds	95°C	35 cycles
Annealing	1 minute	60°C	
Extension	1 minute	72°C	
Final extension	7 minutes	72°C	

PCR products were purified as described below and stored at -20°C till use.

2.11.5. DNA purification

PCR products as well as plasmids and DNA fragments digested by restriction enzymes were all purified by the use of Wizard SV Gel and PCR Clean-Up System (Promega, Fitchburg, Wisconsin, USA). Briefly, equal volume of membrane binding solution was added to the DNA solution and loaded into the SV Minicolumn and centrifuged 1 minute at 16000 xg. DNA fragments from 100 bp to 10 kb were preferentially bound to this column, whereas nucleotides, primers, enzymes were washed away from the DNA mixtures by sequential washes with washing buffers provided by the kit. Finally DNA was eluted with 30 µl nuclease-free water with approximately 98% efficiency. DNA was quantified with Nanodrop and stored at -20°C till use.

2.11.6. DNA digestion

Our aim was to clone the complete human Na,K-ATPase β-subunit coding region into pcDNA 3.1 V5-His plasmid unidirectionally and in frame with V5 tag. As stated before, specific primers containing BamHI and EcoRI restriction enzyme sites were used to amplify Na,K-ATPase β-subunit coding region by PCR, obtaining a DNA fragment flanked by BamHI on 5´and by EcoRI on 3´. Then, DNA fragment and plasmid were digested with these enzymes and ligated. This strategy allowed us to control the appropriate direction of the insert required for Na,K-ATPase β-subunit protein expression.

For the restriction enzyme digestion FastDigest BamHI and EcoRI (Thermo Fisher Scientific, Waltham, Massachusetts, USA) were employed. These enzymes were suitable for double digestions as they were fully functional in equal buffer conditions. For the DNA insert, 100 µl of PCR products were purified as described before, eluted in 30 µl of nuclease-free water and used in the digestion reaction. 1 µg of plasmid was used in the digestion reaction. The reaction mixture, prepared according to the manual instructions, was incubated 30 minutes at 37°C in water bath and inactivated 5 minutes at 80°C in a heating block. Digestion products were purified as described before and stored at -20°C till use.

2.11.7. DNA ligation

In order to insert complete human Na,K-ATPase β-subunit coding region into pcDNA 3.1 V5-His plasmid digested and purified DNA insert and plasmid were ligated employing T4 DNA Ligase (Promega, Fitchburg, Wisconsin, USA). For the ligation reaction we used an insert/vector ratio of 3/1 and followed the provider recommendations. The reaction was allowed to proceed overnight at 4°C. Negative controls were included in order to assess the proportion of uncutted plasmid (T4 DNA Ligase was omitted) and plasmid cutted only with one of the restriction enzymes (insert was omitted).

2.11.8. Transformation of competent bacteria

JM109 competent bacteria (Promega, Fitchburg, Wisconsin, USA) were thawn on ice for 5-10 minutes. For transformation, 50 µl of JM109 cells suspension was added to 10 µl of the ligation reaction and incubated during 30 minutes on ice. Then a heat shock (90 seconds at 42°C in water bath) was applied to the cells and immediately after cells were placed on ice for 5 minutes. After adding 100 µl of LB Broth medium (Luria-Bertani Broth Medium, Invitrogen, Karlsruhe, Germany), bacteria were allowed to recover during 30 minutes at 37°C with 250 rpm agitation. Transformation reaction was plated onto selective bacterial LB agar (Luria-Bertani Agar Medium, GIBCO, Invitrogen, Karlsruhe, Germany) containing 100 µg/ml ampicillin (Sigma, St.Luis, USA).

2.11.9. Colony PCR

In order to screen for positive clones, PCRs from liquid cultures were performed. Minor modifications were done to the PCR protocol described before. 2 µl of bacteria liquid culture were used as a template and the initial denaturalization step was done for 10 minutes in order to completely lyse bacteria.

2.11.10. Agarose gel electrophoresis

PCR reactions were analyzed on 1% agarose gels (Invitrogen, Karlsruhe, Germany) in

1x TAE Buffer:	40 mM Tris
	20 mM acetic acid
	1 mM EDTA (pH 8.0)

containing 1% (v/v) SYBRSafe (Invitrogen, Karlsruhe, Germany). Samples were mixed with loading buffer 6x (Thermo Fisher Scientific, Waltham, Massachusetts, USA). The gel was run in 1x TAE buffer for 30 minutes at 100 V. Gene Ruler High Range DNA Ladder (Thermo Fisher Scientific, Waltham, Massachusetts, USA) was included. DNA bands were visualized under UV Transilluminator (Biorad, Hercules, California, USA).

2.11.11. Small scale plasmidic DNA isolation

Plasmid DNA was prepared at a small scale using PeqGOLD Plasmid Mini Kit (Peqlab, Erlangen, Germany). Briefly, a single colony was picked using a sterile tip and used to inoculate 7 ml of selective LB medium containing 100 µg/ml ampicillin. Bacteria cultures were incubated overnight at 37°C with constant agitation at 250 rpm. Bacteria pellet was collected by centrifugation at 5000 xg for 10 minutes. Cell pellet was resuspended in 250 µl buffer P1 (containing RNase A). Then bacteria were lysed by adding 250 µl buffer P2 SDS/alkaline solution. Genomic DNA was precipitated when 350 µl of buffer P3 was added, and separated from the solution by 10 minutes centrifugation at 10000 xg. Supernatant was loaded into the PerfectBind DNA Column which consist of a silica column that specifically binds DNA. By sequential washes protein and RNA were

removed. Finally, plasmidic DNA was eluted from the column with 30 µl Nuclease-Free water, quantified with Nanodrop and stored at -20°C till use.

2.11.12. Large scale plasmidic DNA isolation

Plasmid DNA was prepared at a big scale using EndoFree Plasmid Purification Maxi Kit (Qiagen, Hilden, Germany) which has the advantage of giving high yields of plasmidic DNA and free of bacteria toxins that may result toxic for mammalian cells in cell transfection protocols.

Briefly, 100 ml of selective LB medium containing 100 µg/ml ampicillin were inoculated with 200 µl of bacteria culture containing the plasmid of interest. Bacteria cultures were incubated overnight at 37°C with constant agitation at 250 rpm. Bacteria pellet was collected by centrifugation of 50 ml centrifuge tubes at 6000 xg for 15 minutes. Cell pellet was resuspended in 10 ml buffer P1 (containing RNase A). Then bacteria were lysed by adding 10 ml buffer P2 SDS/alkaline solution. Genomic DNA was precipitated when 10 ml of buffer P3 was added, and separated from the solution by filtering in QIAfilter Maxi Cartridge. The filtered lysate was loaded into a QIAGEN-Tip Column which consist of a silica column that specifically binds DNA. The lysate was allowed to enter the resin by gravity flow. By sequential washes protein and RNA were removed and plasmidic DNA was eluted from the column with 15 ml of elution buffer. Then, DNA was precipitated by centrifugation at 15000 xg for 30 minutes at 4°C after the addition of 10.5 ml isopropanol. DNA pellet was washed once with 5 ml of 70% ethanol and the pellet was redissolved in 100-200 µl of TE (Tris-EDTA solution). Plasmidic DNA was quantified with Nanodrop and stored at -20°C till use.

2.11.13. Site-directed mutagenesis

In vitro site-directed mutagenesis is a useful technique for studing protein structure-function relationship. In order to identify Na,K-ATPase β-subunit amino acids involved in ubiquitination and phosphorylation processes we performed point mutations and changed intracellular lysines to arginines, and intracellular serines to alanines or aspartates. For this purpose, we employed QuickChange Site-Directed Mutagenesis Kit (Stratagene, La Jolla, California, USA). The basic procedure involves the employment of a plasmid, insert and two synthetic primers containing the desired mutation. The oligonucleotide primers, each

complementary to opposite strands of the vector, are extended during temperature cycling by PfuTurbo DNA polymerase which replicates both plasmid strands with high fidelity and without displacing the mutant olginonucleotide primers. Incorporation of the primers generates a mutated plasmid. The product is treated with Dpn I endonuclease which is specific for methylated and hemimethylated DNA and is used to digest the parental DNA template (which is methylated when grown in *dam*$^{+}$ strains) and therefore to select for mutation-containing DNA. Then, the mutated DNA is transformed into XL1-Blue supercompetent cells and positive colonies are picked, DNA plasmid isolated and sequenced to confirm the presence of the desired mutations.

The design of mutagenesis primers was done following kit considerations. The nucleotides codifying for the amino acids of interested were identified in Na,K-ATPase β-subunit coding sequence and changed accordingly with the use of the genetic code.
DNA amplification was done by the use of PfuTurbo DNA polymerase provided by the kit. The reaction mix is shown in **Table IX**.

Components	Volume per 25 µl Reaction
10x Q5 Reaction Buffer	2.5 µl
dNTP Mix	0.5 µl
Forward Primer (100 ng/µl, Metabion, HPLC quality)	0.75 µl
Reverse Primer (100 ng/µl, Metabion, HPLC quality)	0.75 µl
Template DNA (50 ng/µl cDNA)	0.5 µl
PfuTurbo DNA Polymerase	0.5 µl
Nuclease-Free Water	19.5 µl

Table IX: Site-directed mutagenesis PCR reaction mix.

In order to obtain the DNA amplification we used the following thermocycling conditions in a thermocycler (Thermo Fisher Scientific, Waltham, Massachusetts, USA):

Initial Denaturation	1 minute	95°C	
Denaturation	30 seconds	95°C	16 cycles
Annealing	1 minute	55°C	
Extension	6 minutes 30 seconds	68°C	
Hold		4°C	

PCR products were immediately incubated with 0.5 µl of DpnI during 1 hour at 37 °C in an incubator, order to digest unmutated parental plasmid DNA.

DpnI-treated DNA was used to transform XL1-Blue supercompetent cells. Briefly, 0.5 µl of DpnI-treated DNA was added to 25 µl of bacteria suspension and incubated during 30 minutes on ice. Then a heat shock (45 seconds at 42 °C in water bath) was applied to the cells and immediately after cells were placed on ice for 5 minutes. After adding 250 µl of NZY^+ broth medium containing:

NZY^+ broth: 40 mM NZ amine pH 7.5 (Roth; Karlsruhe, Germany)
5g/L yeast extract
85 mM NaCl (Sigma, St. Luis, USA)
12.5 mM $MgCl_2$ $6H_2O$ (Sigma, St. Luis, USA)
12.5 mM $MgSO_4$ (1M) (Sigma, St. Luis, USA)
20 mM Glucose (Sigma, St. Luis, USA)

Bacteria were allowed to recover during 1 hour at 37°C with 250 rpm agitation. Transformation reaction was plated onto selective bacterial LB agar (Luria-Bertani Agar Medium, Invitrogen, Karlsruhe, Germany) containing 100 µg/ml ampicillin (Sigma-Aldrich, St. Luis, USA). Usually, two positive colonies per mutagenesis reaction were picked, grown in selective liquid media and used to isolate DNA. Plasmidic DNA was sent to sequence in order to confirm the presence of the desired mutations**.**

2.11.14. DNA sequencing

Incorporation of the complete human Na,K-ATPase β-subunit coding region into pcDNA 3.1 V5-His plasmid in frame with V5 tag as well as nucleotide sequence accuracy were both confirmed by DNA sequencing. With this purpose, 2 µg of plasmid DNA previously isolated with PeqGOLD Plasmid Mini Kit were sent to sequence to Seqlab Company (Göttingen, Germany). Clones were sequenced using T7 promoter and BHG reverse universal primers. Sequences obtained were aligned with a reference sequence (Genbank Database) employing BLAST (Basic Local Alignment Search Tool) bioinformatic program.

2.11.15. Glycerol stock

For storage of recombinant clones, 500 µl overnight bacterial culture were mixed with 500 µl of 80% glycerol and frozen at -80°C freezer.

2.12. DNA transfection of A549 cells

For DNA transfection with V5-Na,K-ATPase β1-subunit wt (V5-β1 wt) and V5-β1 variants, A549 cells were plated on 60 mm tissue culture dishes at 60% confluency. On the day of transfection, 12 µl of lipofectamine 2000 (Invitrogen, Karlsruhe, Germany) were diluted in 500 µl of DMEM media and preincubated 5 minutes before adding 4 µg of plasmid DNA. After 30 minutes incubation, the mix was added onto the cells containing 2 ml of growing media. Experiments were performed 18 hours later. For DNA cotransfection with V5-β1 wt and V5-β1 variants and HA-Ubiquitin wt and variants, A549 cells were plated on 100 mm tissue culture dishes at 60% confluency. On the day of transfection, 42 µl of lypofectamine 2000 (Invitrogen, Karlsruhe, Germany) were diluted in 2.7 ml of optiMEM media and preincubated 5 minutes before adding 4 µg of V5-β1 plasmid DNA and 10 µg of HA-ubiquitin plasmid DNA. After 30 minutes incubation, the mix was added onto the cells. 4 hours later transfection solution was removed and fresh complete media was added to cells. Experiments were performed 18 hours later. Controls with empty vector were included.

2.13. siRNA transfection of A549 cells

A549 cells were plated on 60 mm tissue culture dishes at 60% confluency. On the day of transfection, 17 µl of lipofectamine RNAiMax Reagent (Invitrogen, Karlsruhe, Germany) were diluted in 250 µl of optiMEM media and 17 µl of siRNA (10 µM stock) were diluted in 250 µl of optiMEM media. After 5 minutes preincubation, solutions were mixed and incubated for additional 30 minutes, after which the mix was added onto the cells containg 2 ml of growing media. For the knock-down of TRAF2, experiments were performed 48 hours later and for the knock-down of PKC-ζ, experiments were performed 72 hours later. Controls with scramble siRNA were included.

2.14. Plasmidic DNA nucleofection of A549 cells and rat primary ATII cells

For DNA transfection with V5-β1 wt and variants, immediately after isolation, ATII cells were plated on 60 mm tissue culture dishes at 40% confluency. The next day, cells were harvested as usual. $1x10^6$ cells were resuspended in 100 µl of the Nucleofector solution indicated for primary cultures and 4 µg of DNA was added. Immediately cells were placed in the cuvette and pulsed with the indicated cell-type specific Nucleofector program (Lonza Company). After 10 minutes incubation cells were plated in complete DMEM media. Experiments were conducted 2 days after transfection. A549 nucleofection was conducted similarly, but employing the indicated cell-line solution and program.

2.15. Protocols of cellular experiments

2.15.1. Hypercapnia treatments

In order to study hypercapnia effects on cells different solution were employed, in which the buffering capacity of the medium was modified by changing the initial pH with Tris to obtain a pH of 7.4 at 40 mmHg (Control, "Ctrl") and 110 mmHg (Hypercapnia, "CO_2").

Normocapnia Media (Ctrl): 3 ml DMEM High Glucose with FCS 10% [vol/vol]
1 ml Ham´s F-12 medium (GIBCO, Invitrogen, Karlsruhe, Germany)
0.5 ml Tris base solution 0.5 M (pH 7.4)

Hypercapnia Media (CO_2): 3 ml DMEM High Glucose FCS 10% [vol/vol]
1 ml Ham´s F-12 medium
0.5 ml Tris base solution 0.5 M (pH 10)

The desired CO_2 and pH levels were achieved by equilibrating medium overnight in a humidified chamber (C-Chamber, BioSpherix Ltd., NY, USA). The atmosphere of the C-Chamber was controlled with a PROCO2 carbon dioxide controller (BioSpherix Ltd. NY, USA). In this chamber, cells were exposed to the desired pCO_2 while maintaining 21% O_2, balanced with N_2. Prior CO_2 exposure, pH, pCO_2, and pO_2 levels in the media were measured with a blood gas analyzer (Rapidlab, Siemens, Erlangen, Germany).

2.15.2. Na,K-ATPase β-subunit endocytosis studies

A549 cells transfected with V5-β1 wt and variants were exposed to normocapnia or hypercapnia media for 30 minutes at 37°C in the humidified C-Chamber. Cells were washed three times with PBS Ca^+ Mg^+ (PAA Laboratories, Egelsbach, Germany) and cell surface proteins were labeled for 20 minutes using 1 mg/ml cell-impermeable EZ-link NHS-SS-biotin (Thermo Fisher Scientific, Waltham, Massachusetts, USA) in PBS Ca^+ Mg^+. Cells were rinsed for 10 minutes three times with PBS Ca^+ Mg^+ containing 100 mM glycine to quench unreacted biotin. Cells were lysed in modified radioimmunoprecipitation buffer:

mRIPA	50 mM Tris-HCl, pH 8
	150 mM NaCl
	1% NP-40
	1% sodium deoxycholate
	protease inhibitor cocktail

Protein extract were quantified by Bradford technique (see **Section 2.17.**) and 150-400 µg of protein were rotated overnight at 4°C with in the presence of streptavidin-agarose beads. (Thermo Fisher Scientific, Waltham, Massachusetts, USA). The beads were thoroughly washed as indicated:

Solution 1 (1x):	150 mM NaCl
	50 mM Tris, pH 7.4
	5 mM EDTA
Solution 2 (2x):	500 mM NaCl
	50 mM Tris, pH 7.4
	5 mM EDTA
Solution 3 (3x):	500 mM NaCl
	20 mM Tris, pH 7.4
	0.2% BSA

Tris 10 mM pH 7.4 (1x)

and then resuspended in 30 µl of:

Laemmli Sample Buffer 2x [184]:	100 mM Tris, 6.8 pH
	4% SDS
	0.02% bromophenol blue
	20% glycerol

containing 10% β-mercaptoethanol. Samples were incubated for 30 minutes at 37°C in the heating block. Proteins were analyzed by SDS-PAGE and IB (See **Section 2.18.**).

2.15.3. Cell surface Na,K-ATPase β-subunit degradation studies

Cell surface proteins from A549 cells were labeled for 10 minutes using 1 mg/ml cell-impermeable EZ-link NHS-SS-biotin in PBS Ca^+ Mg^+ ("pulse" with cell impermeable biotin). Cells were rinsed for 10 minutes three times with PBS Ca^+ Mg^+ containing 100 mM glycine to quench unreacted biotin. Cells were exposed to normocapnia or hypercapnia media for different time points at 37°C in the humidified C-Chamber ("chase" under normocapnic or hypercapnic conditions). Cells were washed three times with PBS Ca^+ Mg^+ and lysed in mRIPA buffer. Protein extracts were quantified by Bradford technique and 400 µg of protein were rotated overnight at 4°C in the presence of streptavidin-agarose beads. The beads were thoroughly washed as indicated before and then resuspended in 30 µl of Laemmli sample buffer solution 2x containing 10% β-mercaptoethanol. Samples were incubated for 30 minutes at 37°C in heating block. Proteins were analyzed by SDS-PAGE and IB.

2.15.4. Total Na,K-ATPase β-subunit degradation studies

A549 cells were incubated with cycloheximide (CHX), an inhibitor of protein synthesis, for different time points at 37°C in the humidified C-Chamber, after which cells were rinsed three times with PBS Ca^+ Mg^+ and lysed in mRIPA buffer. Protein extract were quantified by Bradford technique and 40 µg of protein resuspended in 1x Laemmli sample

buffer solution containing 5% β-mercaptoethanol. Samples were incubated for 30 minutes at 37°C in a heating block. Proteins were analyzed by SDS-PAGE and IB.

2.15.5. Cell surface Na,K-ATPase β-Subunit ubiquitination studies

Cell surface proteins from A549 cells were labeled for 20 minutes using 1 mg/ml cell-impermeable EZ-link NHS-SS-biotin in PBS Ca^+ Mg^+. Cells were rinsed for 10 minutes three times with PBS Ca^+ Mg^+ containing 100 mM glycine to quench unreacted biotin. Cells were exposed to normocapnia or hypercapnia media for different time points at 37°C in the humidified C-Chamber. Cells were washed three times with PBS Ca^+ Mg^+ and lysed in mRIPA buffer. Then 1% Triton x100 and 0.1% SDS were added to 800-1000 µg of protein in 500 µl final volume and precleared with protein A/G PLUS agarose (Santa Cruz Biotechnology, California, USA). Precleared lysates were rotated with the indicated antibodies for 1 hour at 4°C. Then antigen-antibody complexes were immunoprecipitated by adding 50 µl of protein A/G and rotated overnight at 4°C. Immunoprecipitates were washed 5 times with mRIPA buffer containing protease inhibitors. Agarose beads were resuspended in 30 µl of the following buffer:

Resuspension Buffer:	25 mM Tris HCl pH 6.8
	NEM
	Protease Inhibitor cocktail
	1% SDS

and boiled for 5 minutes. Beads were pelleted by centrifuging 1 minute at 14000 xg and supernatant was adjusted to 300 µl final volume with mRIPA buffer containing protease inhibitors and NEM. Then, 60 µl of streptavidin-agarose beads were rotated overnight at 4°C. The beads were thoroughly washed as indicated before and then resuspended in 30 µl of Laemmli sample buffer solution 2x containing 20% β-mercaptoethanol. Samples were boiled for 10 minutes in heating block. Proteins were analyzed by SDS-PAGE and IB.

2.15.6. Total Na,K-ATPase β-Subunit ubiquitination studies

A549 cells were exposed to normocapnia or hypercapnia media for 15 minutes at 37°C in the humidified C-Chamber. Cells were washed three times with PBS Ca^+ Mg^+ and lysed in

mRIPA buffer. Then 1% Triton x100 and 0.1% SDS were added to 800-1000 µg of protein in 500 µl final volume and precleared with protein A/G PLUS Agarose. Precleared lysates were rotated with the indicated antibodies for 1 hour at 4°C. Then antigen-antibody complexes were immunoprecipitated by adding 50 µl of protein A/G and rotated overnight at 4°C. Immunoprecipitates were washed 5 times with mRIPA buffer containing protease inhibitors. Agarose beads were resuspended in 2x Laemmli sample buffer solution containing 20% β-mercaptoethanol. Samples were boiled for 10 minutes in the heating block. Proteins were analyzed by SDS-PAGE and IB.

2.15.7. *In vitro* protein interaction studies

A549 cells were exposed to normocapnia or hypercapnia media for 15 minutes at 37°C in the humidified C-Chamber. Cells were washed three times with PBS Ca^{+} Mg^{+} and lysed in:

Co-IP buffer: 20 mM HEPES pH 7.4
150 mM NaCl
0.5% NP-40
2 mM EDTA
2 mM EGTA
5% glycerol
Phosphatase/protease inhibitor cocktail

The interaction mixture was prepared with 500 µg of protein total lysate and 2.5 nmol of a biotinylated synthetic peptide containing Na,K-ATPase β-Subunit intracellular domain wt or mutated (cyt-β1 peptide wt, S11D, S19D, S31D; see **Table V**) in a 500 µl volume. After overnight incubation, 100 µl streptavidin-agarose beads was added and allowed to interact during 2 hours. Biotin-streptavidin complexes were washed 5 times with co-IP buffer. Agarose beads were resuspended in 2x Laemmli sample buffer solution containing 10% β-mercaptoethanol and 20 mM DTT. Samples were boiled for 10 minutes in a heating block. Proteins were analyzed by SDS-PAGE and IB.

2.15.8. Coimmunoprecipitation studies

A549 cells were exposed to normocapnia or hypercapnia media for 15 minutes at 37°C in the humidified C-Chamber. Cells were washed three times with PBS Ca^{+} Mg^{+}. Cells were lysed by incubating 15 minutes in the presence of co-IP buffer. After pre-clearing, equal amounts of proteins (700-1200 µg) were incubated with the indicated antibodies for 1 hour. 30 µl protein A/G Plus-agarose beads (Santa Cruz Biotechnology) were added and incubated overnight at 4°C. The beads were washed 5 times with co-IP buffer and resuspended in 2x Laemmli buffer containing 10% β-mercaptoethanol and 20 mM DTT. Samples were boiled for 10 minutes in a heating block. Proteins were analyzed by SDS-PAGE and IB.

2.16. Na,K-ATPase β-subunit *in vitro* ubiquitination

Endogenous TRAF2 was purified from A549 cells (2 plates of 100 mm per reaction) by immunoprecipitation in co-IP buffer containing 2 mM DTT, 0.5% Triton X100, 1 mg/ml NEM (Sigma, St. Luis, USA), 5 µM ubiquitin aldehyde (Boston Biochem, Cambridge, MA, USA) and 2x protease/phosphatase inhibitor cocktail with anti-TRAF2 antibody. A/G-agarose beads were washed 5 times with co-IP buffer and employed as a source of ubiquitin E3 ligase. Ubiquitination reactions were carried out at 37°C for 2 hours in 1x reaction buffer (Boston Biochem, Cambridge, MA, USA), 1x ATP/ Mg^{+} (Boston Biochem, Cambridge, MA, USA), 100 nM sphingosine-1-phosphate (S1P) (Avati Polar Lipids), 50 nM E1 UBE1 (Boston Biochem, Cambridge, MA, USA), 150 nM E2 canonical UbcH13 (in an heterocomplex with Uev1a which lacks E2 active site) (Boston Biochem, Cambridge, MA, USA), 100 µg/ml human recombinant ubiquitin (Boston Biochem, Cambridge, MA, USA), A/G-agarose beads containing immunoprecipitated TRAF2 and biotinylated cyt-β1 wt peptide (see **Table V**). Reactions were conducted in 100 µl final volume with gentle agitation every 10 minutes. Supernatants were recovered and resuspended in:

Pull-down Buffer: 20 mM Tris/HCl pH8
100 mM NaCl
1 mM EDTA
0.5% NP-40
5 µM ubiquitin aldehyde
2x protease/phosphatase inhibitor cocktail

60 µl of streptavidin-agarose beads were employed to pull-down ubiquitinated biotinylated cyt-β1 peptides. After ON rotation at 4°C, beads were washed 3 times in pull-down buffer and samples were boiled in 2x Laemmli sample buffer solution containing 10% β-mercaptoethanol for 10 minutes in a heating block. Proteins were analyzed by SDS-PAGE and IB.

2.17. Protein quantification

Protein concentration was quantified by Bradford assay (Bio-Rad, Hercules, CA, USA) according to the manufacturer instructions.

2.18. SDS-PAGE and Western immunoblotting

Proteins were resolved in 10% polyacrylamide gels (unless stated) and transferred to nitrocellulose membranes (Optitran; Schleider & Schuell) using a semi-dry transfer apparatus (Bio-Rad, Hercules, CA, USA). Membranes were blocked in 5% fat-free dried milk powder (Sigma, St. Luis, USA) in:

T-TBS Buffer: 50 mM Tris
150 mM NaCl
0.05% Tween-20

and incubated with the indicated antibodies overnight at 4°C. The blots were washed 3 times with T-TBS and incubated for another hour with second antibodies. Blots were developed with SuperSignal West Pico Chemiluminescent Substrate detection kit (Thermo Scientific, Waltham, MA, USA), as recommended by the manufacturer. ImageJ was used for densitometric analysis.

2.19. Membrane fractioning

A549 cells in 100 mm plates were transfected with V5-β1 S11D. 18 hours later cells were washed three times with PBS Ca^{+} Mg^{+} and resuspended in:

Membrane Fractioning Buffer 1:	3 mM Imidazole (pH 7.2)
	250 mM Sucrose
	1 mM EDTA
	Protease inhibitor cocktail

Cell monolayer was scraped and homogenized with a syringe. Cell debris was removed by 10 minutes centrifugation at 2000 rpm. Then, supernatant was ultracentrifuged for 1 hour at 35000 rpm (rotor T120). Membrane pellet was resuspended in:

Membrane Fractioning Buffer 2:	3 mM Imidazole (pH 7.5)
	250 mM Sucrose
	1 mM EDTA
	1 mg/ml $C_{12}E_{10}$
	Protease inhibitor cocktail

homogenized with a syringe and incubated during 30 minutes in the dark. Then, supernatant was ultracentrifuged for 1 hour at 35000 rpm (rotor T120). The supernatant contained membrane proteins soluble in $C_{12}E_{10}$. Samples were used in the ubiquitin protein microarray.

2.20. Ubiquitin protein microarray

The membrane fraction isolated from A549 transfected with V5-β1 S11D was used in an ubiquitin protein microarray (LifeSensors, Catalog # MA101). V5-β1 S11D was detected by the use of anti-V5 antibody conjugated with Alexa Fluor 647 (Invitrogen, Karlsruhe, Germany).

2.21. Immunofluorescence microscopy

Cells were plated on cover slips and prepared for fluorescence microscopy at day three. A549 cells were exposed to normocapnia or hypercapnia media for the indicated times at 37°C in the humidified C-Chamber. Cells were washed three times with PBS Ca^{+} Mg^{+} and fixed by adding 3.7% formaldehyde for 4 minutes at 4°C.

After washing the cover slips three times they were blocked in PBS Ca^+ Mg^+ containing 2% BSA for 30 min at room temperature. Cover slips were then incubated overnight at 4°C in the indicated antibody in blocking solution. The next day cover slips were washed with PBS Ca^+ Mg^+ and incubated with FITC-conjugated secondary antibody. Cover slips were placed on glass slides with fluorescent Vectashield mounting medium (Vector Laboratories, Cambridgeshrie, UK). Analysis was undertaken by using a fluorescence microscope (Leica DMLA Q550/W; Leica Microsystems), a digital camera (DC 300 FX; Leica Microsystems) and software (Q-Win; Leica Microsystems).

To study the kinetics of the movement of the Na,K-ATPase β-subunit, A549-β1-YFP cells were incubated in normocapnia or hypercapnia β1-YFP was followed by time-lapse microscopy under a confocal microscope (Leica SP5 inverted; Leica Microsystems).

2.22. Cell aggregation assay

A549 cells or rat primary ATII cells (40000 cells/drop; 4 drops/experiment) were incubated in presence of vehicle (DMSO) or MG-132 (20μM) or transfected with V5-β1 wt and variants and exposed to normocapnia or hypercapnia during 4 or 8 hours (indicated for each experiment in **Section 3**), after which the whole drop was fixed with 3.7% formaldehyde and mounted. Pictures were taken and the number of cells per aggregate was determined. ImageJ was used for the analysis of the pictures. A scale was set in which the area corresponding to one average-size cell was call 1 unit, thus area units were equivalent to number of cells.

2.23. Statistical analysis of data

Values are expressed as mean ± standard error of the media (SEM). Comparisons between two groups were made using a paired, two tailed Student's t-test. Comparisons between more than two groups were done using One-Way ANOVA test and Tukey multiple comparisons. Statistical significance was defined as *$p<0.05$, **$p<0.005$, ***$p<0.0005$. GraphPad Prism 5 for Windows software (GraphPad Software; San Diego, USA) was used for data plotting and statistical analysis.

3. Results

Most of the mechanistic studies oriented to determine hypercapnia effects on Na,K-ATPase β-subunit required the expression of Na,K-ATPase β-subunit wild type (wt) and mutant proteins as well as the down-regulation of specific targets via siRNA transfections. Since efficient lipid-mediated DNA transfection into A549 cells is possible, most of our experiments were conducted in this alveolar epithelial cell line, in which the function and expression of the Na,K-ATPase are fully characterized and similar to primary ATII cells [127, 128, 176, 177]. However, cell-adhesion experiments were validated in primary rat ATII cells, known to form mature cellular junctions and a tight and polarized monolayer [85, 178, 179, 185].

The effects of elevated CO_2 on the alveolar epithelium were evaluated by exposing cells to 110 mmHg of CO_2, which is considered to be clinically-relevant since CO_2 levels may rise up to 100 mmHg in mechanically-ventilated ARDS patients [114, 115, 186-189] and up to 250 mmHg in patients with uncontrolled asthma [190, 191]. Importantly, since a constant extracellular pH (pH_e) of 7.4 was employed in all our studies, the observed effects of elevated CO_2 on alveolar cells were not due to hypercapnia-associated acidosis. Intracellular pH (pH_i) was not particularly controlled in these experiments, since previous studies demonstrated that exposure of cells to elevated CO_2 at a pHe of 7.4 led only to a mild and transient decrease in pH_i, which rapidly returned to basal levels [127].

3.1. Elevated CO_2 levels impair alveolar epithelial cell-cell junction formation

During ARDS, disruption of the alveolar-capillary barrier integrity and formation of edema leads to impaired gas exchange. Restoration of the physical integrity of the alveolar epithelial monolayer is critical for the removal of liquid from the alveolar space and re-establishment of a functional respiratory epithelium [6]. However, elevated CO_2 levels due to impaired gas exchange could have negative effects on the mechanisms of repair of the alveolar epithelium. Particularly, the impact of hypercapnia on the organization of cell-cell contacts has not been addressed before. Therefore, to evaluate whether elevated CO_2 levels affect the ability of epithelial cells to interact with each other we conducted a cell aggregation assay, also termed “hanging drop”, in which a single-cell suspension of A549 cells was incubated in normocapnic (40 mmHg CO_2, pH 7.4) or hypercapnic (110 mmHg

CO_2, pH 7.4) conditions at normal pH for 8 hours. Data analysis showed that the number of large aggregates, defined as aggregates containing more than 10 cells, was significantly reduced in hypercapnia compared to normocapnia, suggesting that elevated CO_2 levels were impairing the ability of cells to interact with their neighbors. Interestingly, the deleterious effects of hypercapnia on cell-cell contact formation were partially prevented when A549 cells were incubated with the proteasome inhibitor, MG-132, suggesting that the negative impact of elevated CO_2 on cell adhesion may involve a proteasome-dependent event, perhaps by inducing degradation of one or more adhesion molecules (**Figure 11**).

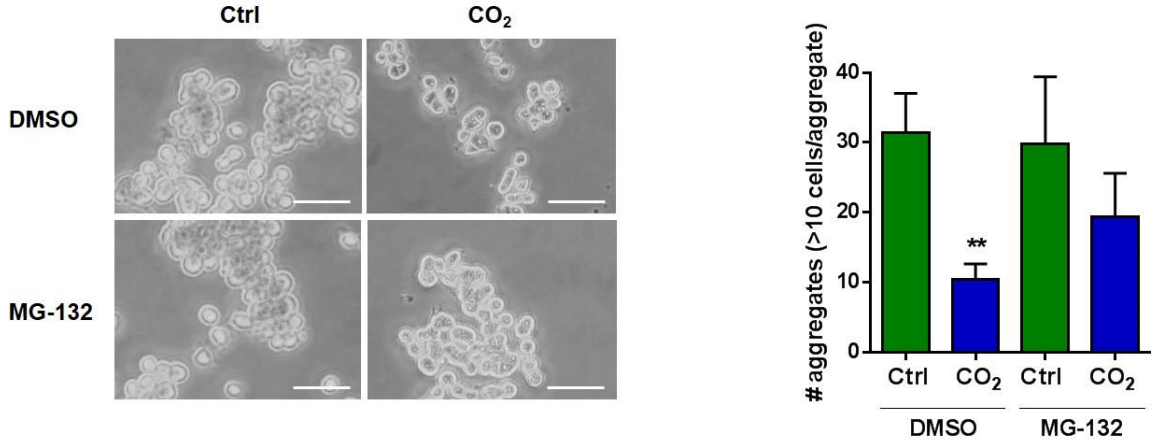

Figure 11: Elevated CO_2 levels impair cell-cell contact formation in A549 cells. A549 cells were incubated in normocapnia (40 mmHg CO_2, pH 7.4) or hypercapnia (110 mmHg CO_2, pH 7.4) in the presence of vehicle (DMSO) or MG-132 proteasome inhibitor for 8 hours. The number of aggregates containing more than 10 cells was determined. Mean ± SEM, n = 4, unpaired t-test, **p < 0.005. Scale bar = 50 µM.

The above-mentioned results were confirmed in a second set of experiments conducted in rat primary ATII cells. Due to its highly-adhesive phenotype, primary ATII cells formed larger aggregates than A549 cells. However, similarly to A549 cells, the adhesive properties were impaired in cells exposed to hypercapnia (110 mmHg CO_2, pH 7.4), thus demonstrating the adverse effects of elevated CO_2 levels on the ability of cells to establish cell-cell contacts (**Figure 12**).

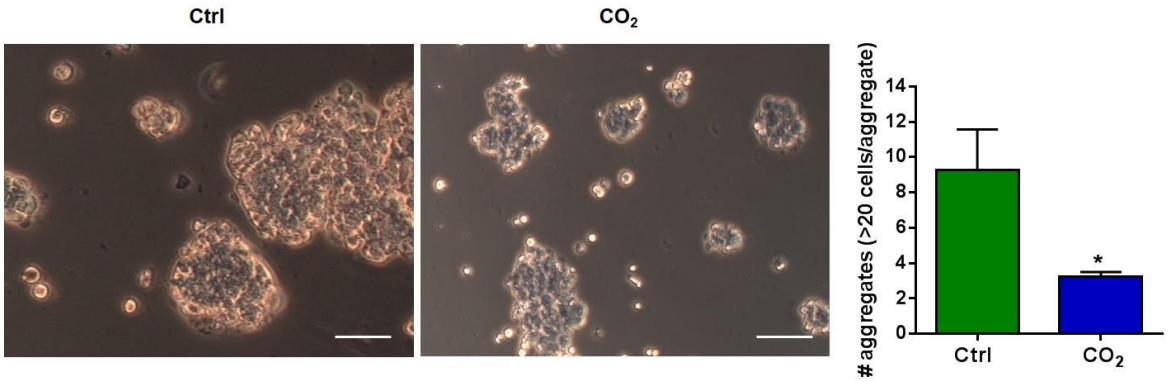

Figure 12: Elevated CO_2 levels impair cell-cell contact formation in ATII cells. Primary rat ATII cells were incubated in normocapnia (40 mmHg CO_2, pH 7.4) or hypercapnia (110 mmHg CO_2, pH 7.4) for 4 hours. The number of aggregates containing more than 20 cells was determined. Mean ± SEM, n = 3, unpaired t-test, *p < 0.05. Scale bar = 50 µM.

3.2. Elevated CO_2 levels induce the endocytosis of the Na,K-ATPase β-subunit in alveolar epithelial cells

Na,K-ATPase β-subunit consists of 2 N-glycosylated isoforms that are detected as a broad band at 45-55 kDa and a sharper band at ~40 kDa. Only the fully-glycosylated band is found at the plasma membrane where it participates in homophilic cell-cell adhesion [93, 192]. To test the hypothesis that elevated CO_2 levels impair alveolar cell-cell adhesion by affecting the localization of the Na,K-ATPase β-subunit at the cell surface, we conducted immunofluorescence experiments in which A549 cells were exposed to normocapnia (40 mmHg CO_2, pH 7.4) or hypercapnia (110 mmHg CO_2, pH 7.4) for 30 minutes and Na,K-ATPase β-subunit localization was observed under confocal microscopy. Cells exposed to elevated CO_2 levels showed a decrease in Na,K-ATPase β-subunit abundance at the plasma membrane, accompanied by a translocation of the protein into the intracellular compartments (**Figure 13**).

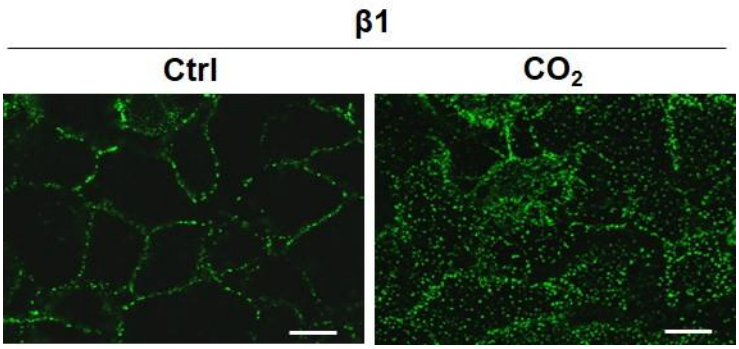

Figure 13: Elevated CO_2 levels alter Na,K-ATPase β-subunit subcellular localization in A549 cells. A549 cells were incubated in normocapnia (40 mmHg CO_2, pH 7.4) or hypercapnia (110 mmHg CO_2, pH 7.4) for 30 minutes. Na,K-ATPase β-subunit was detected by the use of anti-Na,K-ATPase β1-subunit antibody followed by FITC-conjugated secondary antibody. Fluorescence was observed at a confocal microscope. Scale bar = 10 µM.

To further characterize the kinetics of the movement of the Na,K-ATPase β-subunit in cells exposed to elevated CO_2 levels, we employed time-lapse confocal microscopy. A549 cells stably expressing dog Na,K-ATPase β-subunit fused to yellow fluorescence protein (A549-β1-YFP) were incubated in normocapnia (40 mmHg CO_2, pH 7.4) or hypercapnia (110 mmHg CO_2, pH 7.4) for 12 minutes, collecting pictures every minute. Whereas in normocapnia, Na,K-ATPase β-subunit was located at the borders of adjacent cells, in hypercapnia a redistribution of Na,K-ATPase β-subunit was evident already 6 minutes after elevated CO_2 exposure. After exposing cells to hypercapnic media for 12 minutes, most of the Na,K-ATPase β-subunit was endocytosed from the plasma membrane into intracellular compartments (**Figure 14**).

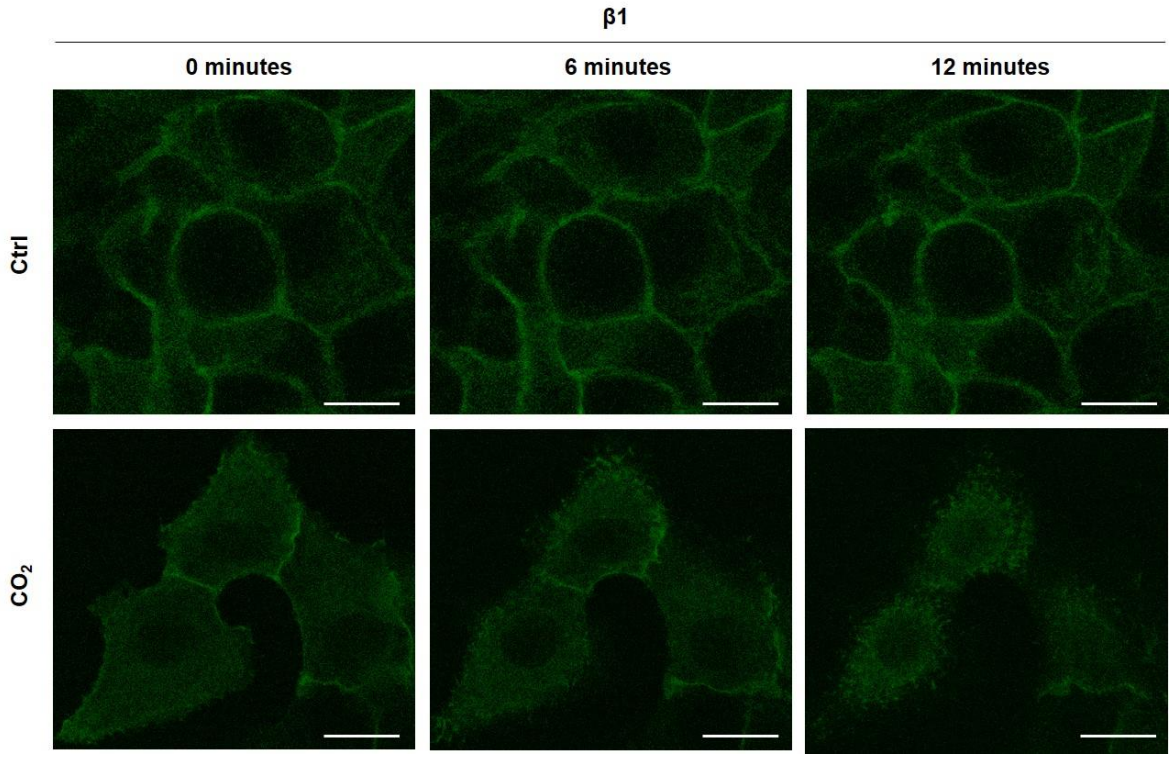

Figure 14: Elevated CO_2 levels lead to a decrease in Na,K-ATPase β-subunit surface abundance within minutes. Using time-lapse confocal microscopy, we analyzed the kinetics of Na,K-ATPase β-subunit in A549-β1-YFP cells over 0-12 minutes of exposure to normocapnia (40 mmHg CO_2, pH 7.4) or hypercapnia (110 mmHg CO_2, pH 7.4). Images were collected every 1 minute. Representative pictures at 0, 6 and 12 minutes are shown here. Scale bar = 10 µM.

To quantitatively evaluate the hypercapnia-induced endocytosis of the Na,K-ATPase β-subunit , cells were exposed to normocapnia (40 mmHg CO_2, pH 7.4) or hypercapnia (110 mmHg CO_2, pH 7.4) for 30 minutes after which biotin-streptavidin pull-downs were performed to determine Na,K-ATPase β-subunit protein levels at the plasma membrane. The results of these experiments showed a 30% reduction of Na,K-ATPase β-subunit at the membrane of cells exposed to elevated CO_2 levels compared to cells exposed to normocapnia. In contrast, total levels of the Na,K-ATPase β-subunit did not show significant changes after treatment with elevated CO_2 concentrations (**Figure 15**). The specific detection of plasma membrane proteins, due to cell impermeability to biotin, was confirmed by the fact that only the ~50-kDa mature form of Na,K-ATPase β-subunit was detected in the pull-downs.

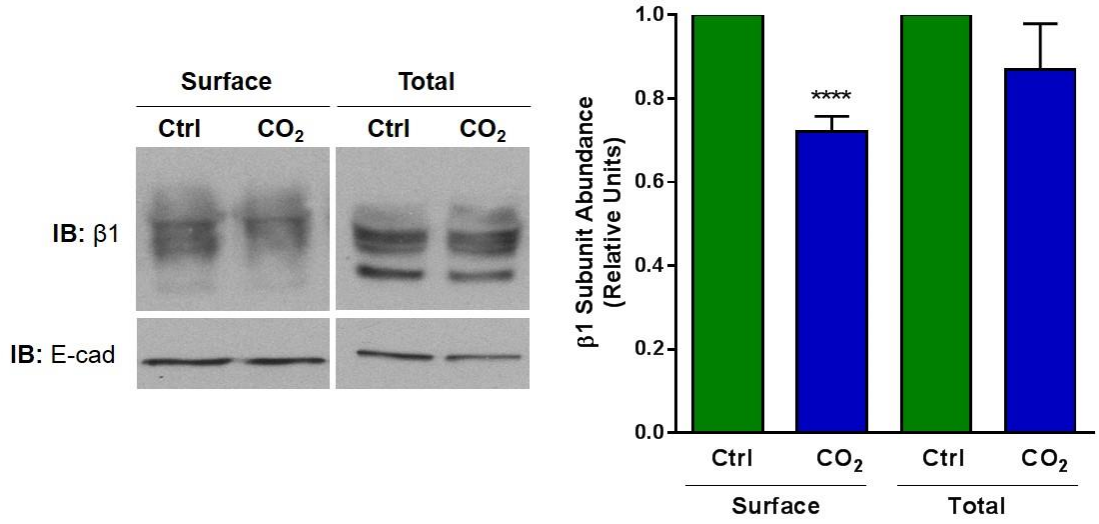

Figure 15: Elevated CO_2 levels promote the endocytosis of the Na,K-ATPase β-subunit. A549 cells were exposed to normocapnia (40 mmHg CO_2, pH 7.4) or hypercapnia (110 mmHg CO_2, pH 7.4) for 30 minutes. Na,K-ATPase β-subunit at the surface was determined by biotin-streptavidin pull-down and IB. Representative Western blots of Na,K-ATPase β-subunit at the surface and total protein abundance are shown. Mean ± SEM, n = 5, paired t-test, ****p < 0.0001.

3.3. Na,K-ATPase β-subunit turnover under steady-state conditions is proteasome-dependent

Understanding the timing and mechanism of Na,K-ATPase β-subunit degradation under steady-state conditions was important for our future studies on Na,K-ATPase β-subunit stability under hypercapnic conditions.

To determine the half-life of endogenous Na,K-ATPase β-subunit under steady-state conditions in our system, we labeled membrane proteins with cell-impermeable biotin, incubated A549 cells in normal conditions (40 mmHg CO_2, pH 7.4) for 4 and 6 hours and did protein pull-downs with streptavidin. We found that after 4 hours approximately 50% of cell surface Na,K-ATPase β-subunit was degraded (**Figure 16**). This observation was in agreement with previous studies done by other groups in HeLa and A549 cells which have shown that cell surface Na,K-ATPase β-subunit has a half-life of approximately 4 hours in steady-state conditions [193, 194].

As protein degradation can be proteasome- or lysosome-mediated, we set out to determine the mechanism involved in the degradation of the Na,K-ATPase β-subunit under

steady-state conditions in the alveolar epithelium. Biotin-labeled proteins were chased in the presence of the proteasome inhibitor, MG-132 or the lysosome inhibitor, chloroquine. Normal turnover of the Na,K-ATPase β-subunit was prevented in the presence of the proteasome inhibitor but not when the lysosomal function was inhibited (**Figure 16**). These studies suggest that degradation of the Na,K-ATPase β-subunit located at the plasma membrane is primarily mediated by the proteasome system under steady state conditions. These findings are in line with published data in which inhibition of the proteasome system prevented Na,K-ATPase β-subunit degradation under steady-state conditions in HeLa cells [193].

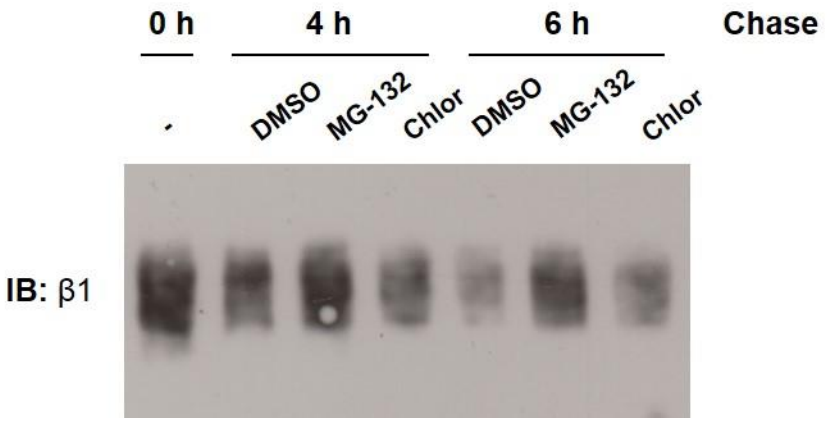

Figure 16: Plasma membrane Na,K-ATPase β-subunit has a half-life of 4 hours and its turnover requires the proteasome function. Surface proteins of A549 cells were labeled with biotin and chased in normocapniaconditions (40 mmHg CO_2, pH 7.4) for 4 and 6 hours in the presence of vehicle (DMSO), proteasome inhibitor (MG-132, MG) or lysosome inhibitor (chloroquine, Chlor) . Afterwards, streptavidin pull-down was performed and Na,K-ATPase β-subunit abundance was analyzed by IB. Representative Western blot of Na,K-ATPase β-subunit protein abundance is shown.

Although our studies mainly focused on the plasma membrane Na,K-ATPase β-subunit, to further characterize Na,K-ATPase β-subunit degradation mechanism under steady state conditions, we set out to examine Na,K-ATPase β-subunit degradation, not only at the plasma membrane but in total cell lysates. It has been previously reported that isoforms of the Na,K-ATPase β-subunit are degraded differently in MDCK cells, the immature Na,K-ATPase β-subunit being degraded faster than the mature isoform, levels of which decreased only slightly after 5 hours [192]. However, the mechanism of degradation of the different isoforms has not been addressed in these studies.

To assess the mechanism of Na,K-ATPase β-subunit degradation in total cell lysates under steady-state conditions, A549 cells were incubated in the presence of the

protein-synthesis inhibitor, cycloheximide (CHX). Indeed, these studies showed that immature Na,K-ATPase β-subunit is degraded faster than total mature Na,K-ATPase β-subunit in A549 cells. After 4 hours incubation with CHX, approximately 50% of immature Na,K-ATPase β-subunit was degraded, whereas no significant changes were observed in the amount of total mature Na,K-ATPase β-subunit (**Figure 17**).

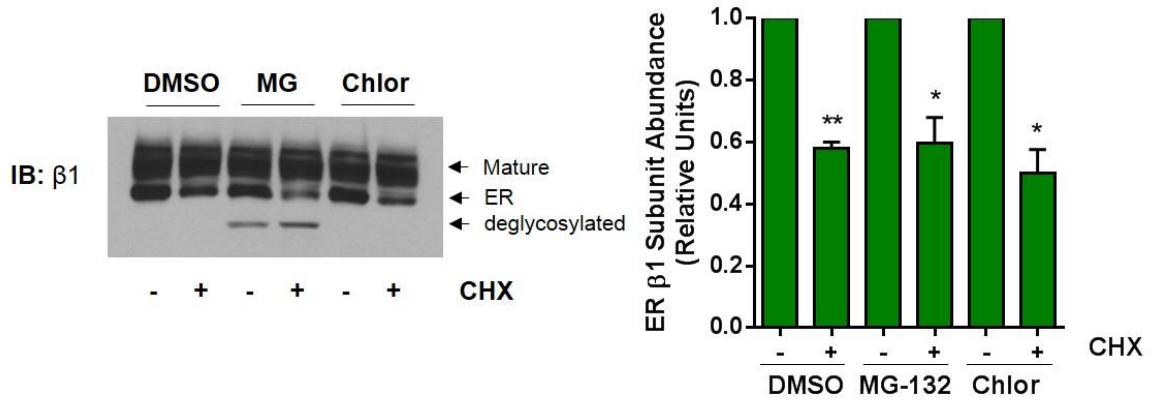

Figure 17: Endoplasmic reticulum Na,K-ATPase β-subunit has higher turnover than mature β-subunit and the proteasome pathway is involved. A549 cells were incubated with the protein synthesis inhibitor, cycloheximide (CHX), for 4 hours in the presence of vehicle (DMSO), proteasome inhibitor (MG-132, MG) or lysosome inhibitor (chloroquine, Chlor) in normal (40 mmHg CO_2, pH 7.4) conditions. Afterwards, Na,K-ATPase β-subunit abundance in total cell lysates was analyzed by IB. Representative Western blot shows mature Na,K-ATPase β1-subunit, endoplasmic reticulum-associated Na,K-ATPase β1-subunit (ER) and deglycosylated Na,K-ATPase β1-subunit. Mean ± SEM, n = 3, paired t-test, *p < 0.05, **p<0.005.

It has been previously described that some glycoproteins may be retro-translocated from the endoplasmic reticulum into the cytosol, subsequently deglycosylated and degraded via the proteasomal pathway [195, 196]. However, it remained unknown whether the intracellular immature Na,K-ATPase β-subunit form undergoes this pathway. Importantly, in our experiments we observed that proteasome inhibition with MG-132, but not lysosome inhibition, led to the accumulation of a ~35 kDa form of the Na,K-ATPase β-subunit (**Figure 17**), which comigrated with PNGaseF-degycosylated Na,K-ATPase β-subunit forms in SDS-PAGE (data not shown). This result suggests that immature Na,K-ATPase β-subunit gets deglycosylated before being degraded and that, similarly to plasma membrane Na,K-ATPase β-subunit, immature Na,K-ATPase β-subunit is also degraded by the proteasome.

Taken together, these results strongly imply that the Na,K-ATPase β-subunit is degraded by the proteasome irrespective of its location or maturations status.

3.4. Elevated CO_2 levels promote the degradation of the plasma membrane Na,K-ATPase β-subunit

In the previous experiments we demonstrated that elevated CO_2 levels induced Na,K-ATPase β-subunit internalization from the plasma membrane. Since internalized proteins may be recycled or degraded, we set out to study whether hypercapnia-induced endocytosis of the Na,K-ATPase β-subunit was followed by its degradation. To this end, we conducted pulse-chase experiments with cell-impermeable biotin in normocapnia (40 mmHg CO_2, pH 7.4) or hypercapnia (110 mmHg CO_2, pH 7.4). After 1 hour of exposure to hypercapnia, 44% of the Na,K-ATPase β-subunit was degraded, as opposed to a markedly slower degradation rate under normocapnia (**Figure 18**).

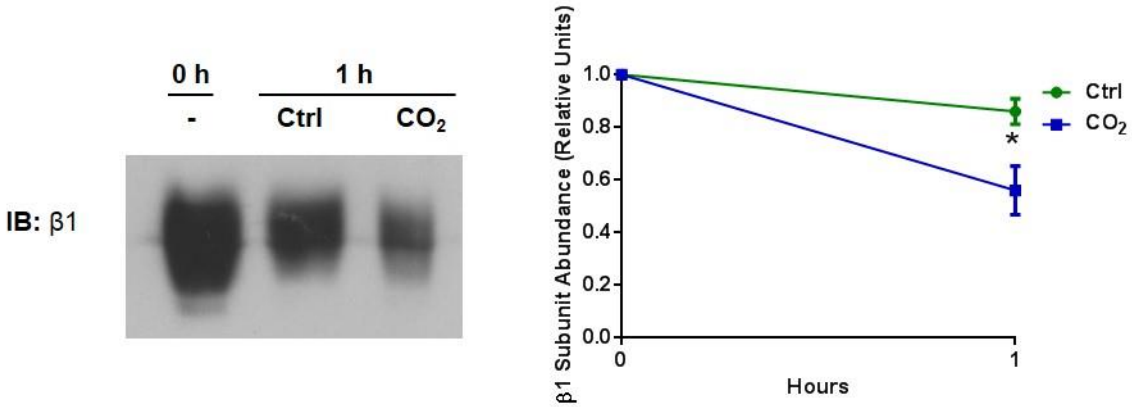

Figure 18: Elevated CO_2 levels promote the degradation of the plasma membrane Na,K-ATPase β-subunit. Surface proteins of A549 cells were labeled with biotin and chased in normocapnia (40 mmHg CO_2, pH 7.4) or hypercapnia (110 mmHg CO_2, pH 7.4) for 1 hour. Afterwards, streptavidin pull-down was performed and Na,K-ATPase β-subunit abundance was analyzed by IB. Representative Western blot of surface Na,K-ATPase β-subunit total protein abundance is shown. Mean ± SEM, n = 3, paired t-test, *$p<0.05$.

In a second set of experiments, we transfected A549 cells with a C-terminal V5-tagged Na,K-ATPase β-subunit wild-type (V5-β1 wt) construct and performed pulse-chase experiments with cell-impermeable biotin in normocapnia (40 mmHg CO_2, pH 7.4) or

hypercapnia (110 mmHg CO_2, pH 7.4) for different time points. These studies clearly showed that hypercapnia promoted the fast degradation of plasma membrane V5-β1 wt, having a strong impact on the protein half-life which was reduced to 1 hour.

In summary, our data show that elevated CO_2 levels lead to the endocytosis and degradation of the plasma membrane Na,K-ATPase β-subunit (**Figure 19**).

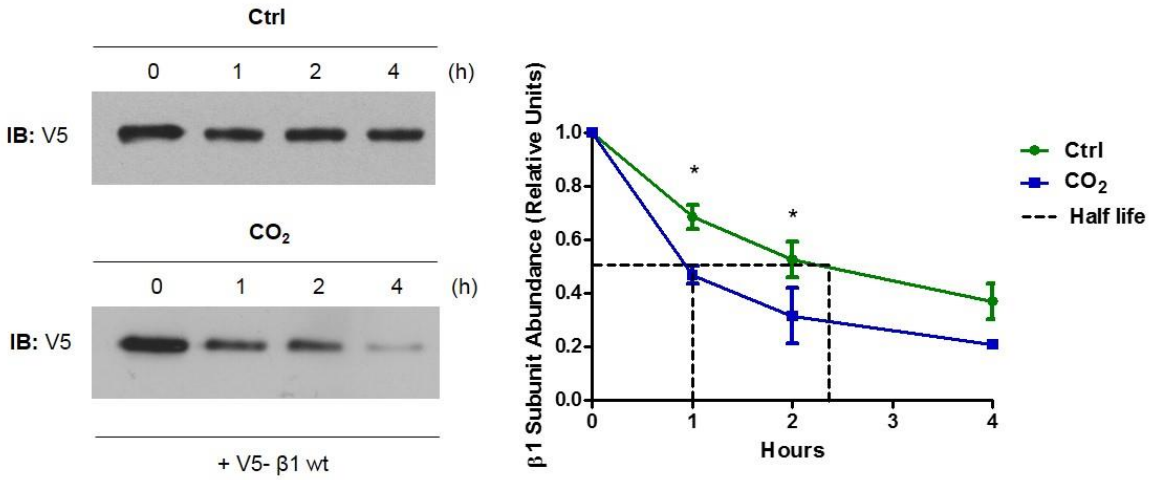

Figure 19: Elevated CO_2 levels promote the rapid degradation of the plasma membrane V5-β1 wt. A549 cells were transfected with V5-β1 wt and surface proteins were labeled with biotin and chased in normocapnia (40 mmHg CO_2, pH 7.4) or hypercapnia (110 mmHg CO_2, pH 7.4) for different time points. Afterwards, streptavidin pull-down was performed and Na,K-ATPase β-subunit abundance was analyzed by IB. Representative Western blot of surface Na,K-ATPase β-subunit total protein abundance is shown. Mean ± SEM, n = 3, paired t-test, *p<0.05.

3.5. Hypercapnia-induced Na,K-ATPase β-subunit degradation is mediated by the proteasome

To elucidate the pathway implicated in hypercapnia-induced endocytosis and degradation of the Na,K-ATPase β-subunit, we assessed plasma membrane Na,K-ATPase β-subunit protein abundance in A549 cells exposed to high CO_2 in the presence of inhibitors of the lysosome, chloroquine and E64, and of the proteasome, MG-132. Exposure of cells to hypercapnia in the absence of inhibitors decreased the plasma membrane Na,K-ATPase β-subunit protein abundance by approximately 25%. This effect was completely prevented by pretreatment of cells with the proteasome inhibitor. In contrast, pretreatment of cells with lysosome inhibitors did not prevent the hypercapnia-induced effect on the plasma membrane of the Na,K-ATPase β-subunit (**Figure 20**).

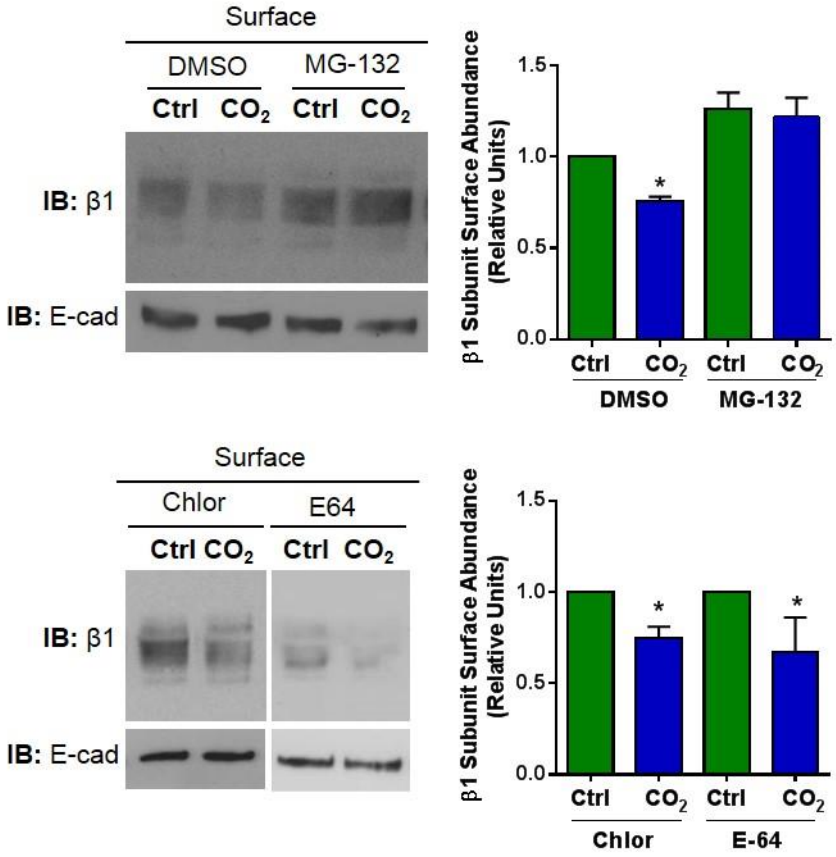

Figure 20: Inhibition of the proteasome prevents CO_2-induced Na,K-ATPase β-subunit endocytosis. A549 cells were preincubated with vehicle (DMSO), proteasome inhibitor (MG-132) or lysosome inhibitors (chloroquine, Chlor, and E64) for 4 hours and then exposed to normocapnia (40 mmHg CO_2, pH 7.4) or hypercapnia (110 mmHg CO_2, pH 7.4) for 30 minutes. Biotin-streptavidin pull-down of cell surface proteins was performed and Na,K-ATPase β-subunit abundance was analyzed by IB. Representative Western blots of surface Na,K-ATPase β-subunit abundance are shown. Mean ± SEM, n = 3, paired t-test, *p<0.05.

In a second set of experiments, we further examined hypercapnia-mediated pathway of Na,K-ATPase β-subunit degradation by conducting pulse-chase experiments with impermeable-biotin in the presence of lysosome and proteasome inhibitors. Exposure of cells to elevated CO_2 levels in the presence of lysosome inhibitor increased degradation of the plasma membrane Na,K-ATPase β-subunit protein by approximately 35% compared to control cells, whereas the same experiment in the presence of the proteasome inhibitor, MG-132 did not significantly increased plasma membrane Na,K-ATPase β-subunit protein degradation (**Figure 21**).

Altogether, these studies suggest that the hypercapnia-induced degradation of the Na,K-ATPase β-subunit located at the plasma membrane involves a proteasome-mediated event.

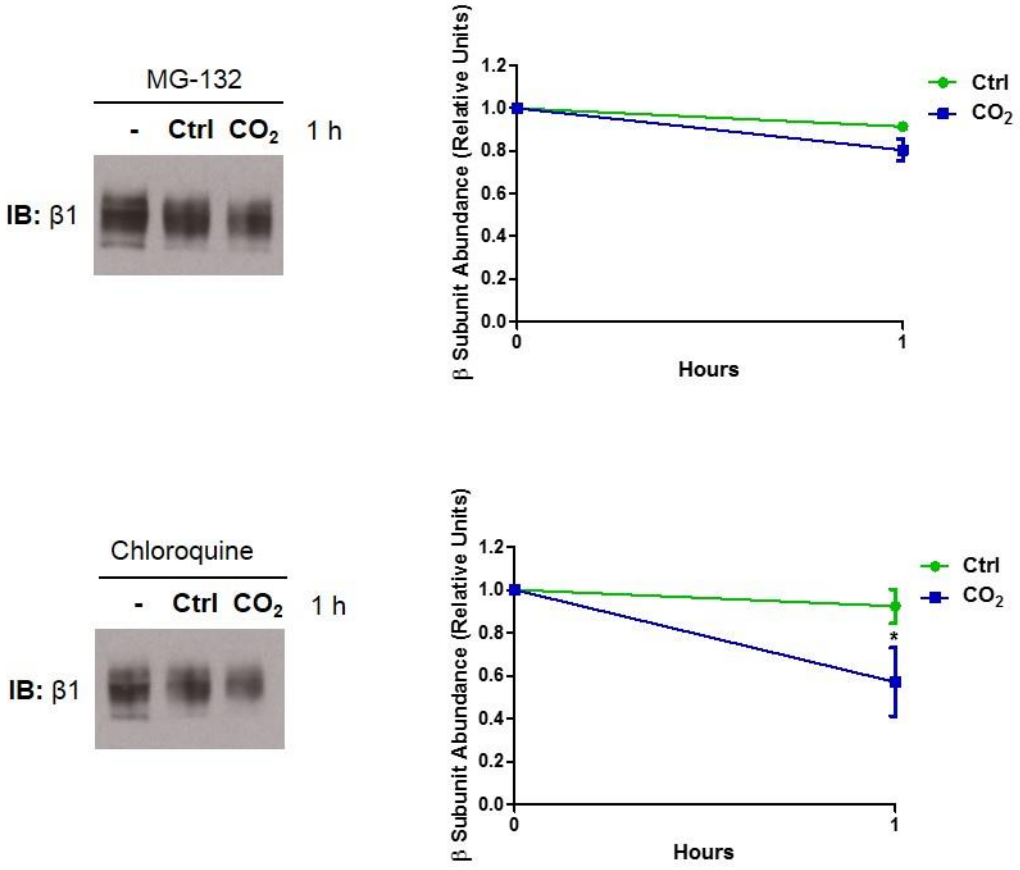

Figure 21: Inhibition of the proteasome prevents CO_2-induced Na,K-ATPase β-subunit degradation. A549 cells were preincubated with vehicle (DMSO), proteasome inhibitor (MG-132) or lysosomal inhibitor (chloroquine) for 4 hours. Surface proteins of A549 cells were labeled with biotin and chased in normocapnia (40 mmHg CO_2, pH 7.4) or hypercapnia (110 mmHg CO_2, pH 7.4) for 1 hour. Afterwards, streptavidin pull-down was performed and Na,K-ATPase β-subunit abundance was analyzed by IB. Representative Western blots of surface Na,K-ATPase β-subunit abundance are shown. Mean ± SEM, n = 3, paired t-test, *p<0.05.

3.6. Hypercapnia induces the ubiquitination of the Na,K-ATPase β-subunit at the plasma membrane

In the last decades, the endocytosis of multiple classes of proteins has been found to be regulated by the ubiquitin system [129, 197]. Therefore, the next step was to evaluate

whether ubiquitination played a role in the hypercapnia-induced endocytosis of the Na,K-ATPase β-subunit .

First, we evaluated whether hypercapnia induces ubiquitination of the Na,K-ATPase β-subunit. To this end, we transfected A549 cells with HA-ubiquitin and V5-β1 wt and exposed the cells to normocapnia (40 mmHg CO_2, pH 7.4) or hypercapnia (110 mmHg CO_2, pH 7.4). V5-β1 wt subunit was immunoprecipitated and ubiquitinated Na,K-ATPase β-subunit isoforms were detected with anti-HA antibody. Exposure of cells to hypercapnia for 15 minutes led to the ubiquitination of Na,K-ATPase β-subunit, detected as a typical smeared pattern over 50 kDa characteristic of polyubiquitinated proteins, due to the presence of polyubiquitin chains of various lengths (**Figure 22**).

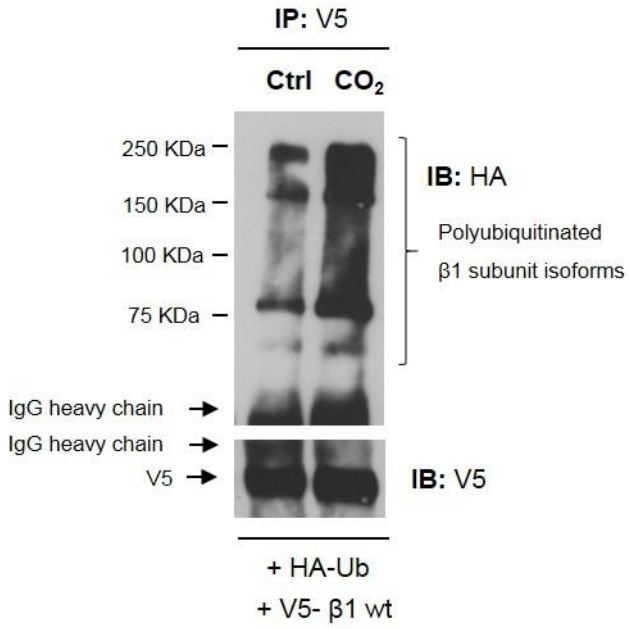

Figure 22: Elevated CO_2 levels promote ubiquitination of the Na,K-ATPase β-subunit. A549 cells were cotransfected with HA-Ubiquitin (Ha-Ub) and V5- β1 wt. After 18 hours transfection, cells were exposed to normocapnia (40 mmHg CO_2, pH 7.4) or hypercapnia (110 mmHg CO_2, pH 7.4) for 15 minutes in the presence of MG-132. V5-β1 wt was immunoprecipitated with anti-V5 polyclonal rabbit antibody and ubiquitinated forms were detected with anti-HA monoclonal mouse antibody by IB. Loading was done with anti-V5 monoclonal mouse antibody. Representative Western blots are shown.

Furthermore, an increase in ubiquitination of Na,K-ATPase β-subunit after cell-treatment with elevated CO_2 could also be detected in total protein lysates when blotting against V5 (**Figure 23**). This is an alternative accepted method to detect ubiquitinated

proteins [198]; however it may require overexposure of x-ray films because ubiquitinated proteins often represent a small fraction of the total pool of a protein.

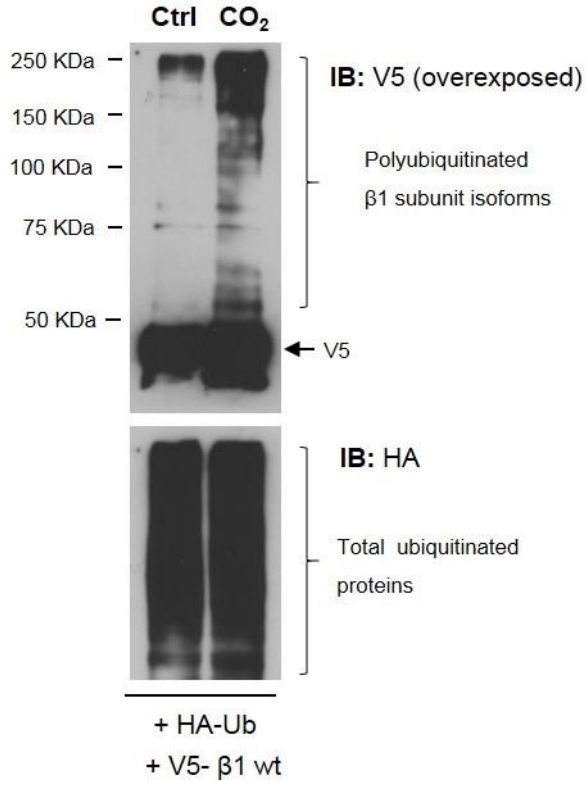

Figure 23: Elevated CO_2 levels promote ubiquitination of the Na,K-ATPase β-subunit. A549 cells were cotransfected with HA-Ubiquitin (Ha-Ub) and V5-β1 wt. After 18 hours transfection, cells were exposed to normocapnia (40 mmHg CO_2, pH 7.4) or hypercapnia (110 mmHg CO_2, pH 7.4) for 15 minutes. V5-β1 wt was detected with anti-V5 monoclonal mouse antibody by IB. Films were overexposed to detect Na,K-ATPase β-subunit polyubiquitinated isoforms. Total proteins with HA-ubiquitin modifications were detected with anti-HA antibody. Representative Western blots are shown.

These experiments confirmed that elevated CO_2 levels indeed triggered Na,K-ATPase β-subunit polyubiquitination. We hypothesized that if the hypercapnia-induced ubiquitination of the Na,K-ATPase β-subunit plays a role in the endocytosis signaling, the most likely site of ubiquitination is at the plasma membrane. To test this hypothesis, we assessed the levels of ubiquitinated Na,K-ATPase β-subunit isoforms at the plasma membrane of A549 cells exposed to normocapnia (40 mmHg CO_2, pH 7.4) or hypercapnia (110 mmHg CO_2, pH 7.4) for 15 minutes. Membrane proteins were labeled with cell-impermeable biotin and streptavidin pull-downs were performed in order to isolate surface proteins. Immunoprecipatation of Na,K-ATPase β-subunit from the pool of membrane proteins was done to detect ubiquitinated β-subunit isoforms. A specific antibody against

ubiquitin was used to detect the endogenous ubiquitinated Na,K-ATPase β-subunit isoforms. The experiments showed a significant increase in ubiquitinated forms in cells exposed to elevated CO_2 levels compared to cells exposed to normal CO_2 levels, suggesting that hypercapnia promotes ubiquitination of Na,K-ATPase β-subunit at the plasma membrane (**Figure 24**).

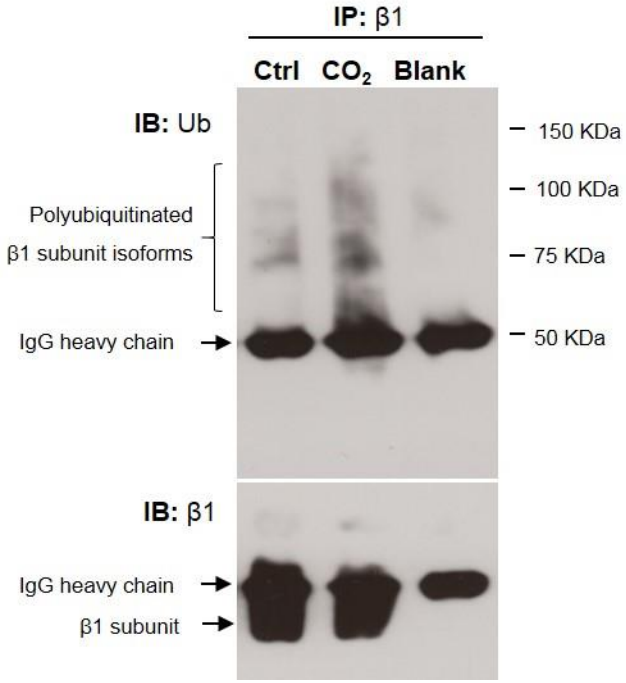

Figure 24: Elevated CO_2 levels promote ubiquitination of the Na,K-ATPase β-subunit at the plasma membrane. A549 cells were incubated in normocapnia (40 mmHg CO_2, pH 7.4) or hypercapnia (110 mmHg CO_2, pH 7.4) for 15 minutes. Biotin-streptavidin pull-down was performed to enrich in surface proteins. Na,K-ATPase β-subunit was immunoprecipitated with anti-β1-subunit mouse monoclonal antibody and Na,K-ATPase β-subunit polyubiquitinated isoforms were detected with anti-ubiquitin mouse monoclonal antibody by IB. Representative Western blots are shown.

3.7. Hypercapnia-induced endocytosis of the Na,K-ATPase β-subunit requires ubiquitination of the protein at lysine residues 5 and 7

Previous observations suggested that the hypercapnia-induced ubiquitination of the Na,K-ATPase β-subunit at the plasma membrane may act as a trafficking signal responsible for Na,K-ATPase β-subunit endocytosis. To identify the specific lysine residues in Na,K-ATPase β-subunit that serve as ubiquitin acceptors, we used site-directed mutagenesis to introduce lysine to arginine substitutions at each intracellular lysine in the intracellular

domain of V5-β1 wt. This is a widely-used method to identify the ubiquitination site as this conservative substitution preserves the positive charge and does not significantly alter the protein conformation [131, 199]. Moreover; considering the possibility of functional redundancy, mutants containing simultaneous replacements were produced.

To perform the analysis, A549 cells were transfected with the different mutants. After exposure of cells to hypercapnia (110 mmHg CO_2, pH 7.4) for 15 minutes, V5-β1 wt or mutants were immunoprecipitated and ubiquitinated Na,K-ATPase β-subunit isoforms were detected. Replacement of both lysines 5 and 7 with arginines (V5-β1 K5/7R), led to a significant prevention of hypercapnia-induced Na,K-ATPase β-subunit ubiquitination (**Figure 25**).

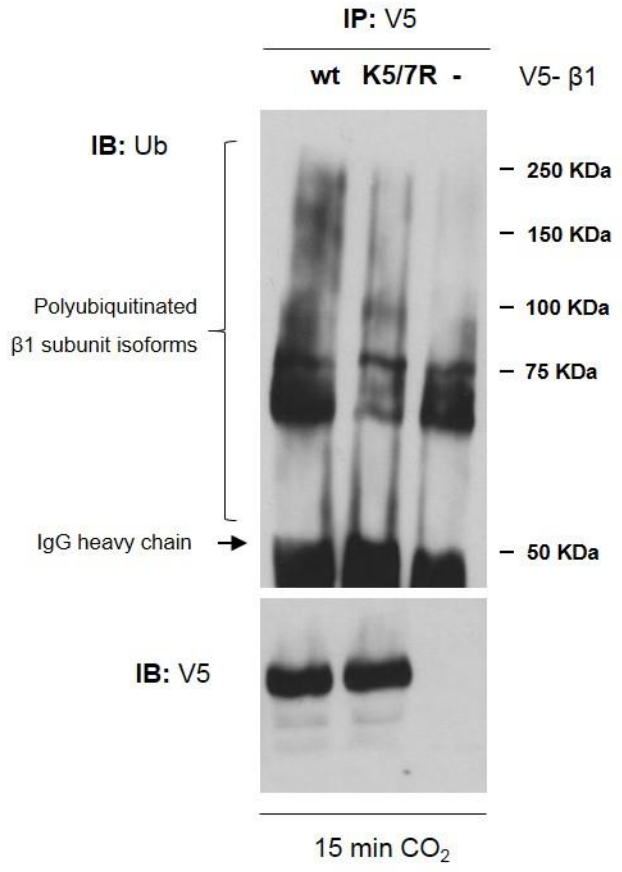

Figure 25: Replacement of both lysines 5 and 7 with arginines prevent the hypercapnia–induced ubiquitination of the Na,K-ATPase β-subunit. A549 cells were transfected with V5-β1 wt, V5-β1 K5/7R or empty plasmid. After 18 hours transfection, cells were exposed to hypercapnia (110 mmHg CO_2, pH 7.4) for 15 minutes. V5-β1 wt or K5/7R were immunoprecipitated with anti-V5 polyclonal rabbit antibody and ubiquitinated forms were detected with anti-ubiquitin monoclonal mouse antibody by IB. As loading control V5-β1 wt or K5/7R were detected with anti-V5 mouse antibody. Representative Western blots are shown.

To address the role of ubiquitination in the internalization of the Na,K-ATPase β-subunit , we set out to examine the effect of elevated CO_2 on the endocytosis of the V5-β1 K5/7R mutant protein. A549 cells were transfected with V5-β1 wt or K5/7R contructs, exposed to normocapnia (40 mmHg CO_2, pH 7.4) or hypercapnia (110 mmHg CO_2, pH 7.4) for 30 minutes and biotin-streptavidin pull-downs were performed. Importantly, when lysines 5 and 7 were replaced with arginine the hypercapnia-induced endocytosis of the Na,K-ATPase β-subunit was prevented. These findings provide strong evidence that ubiquitin may function as an endocytosis signal that mediates the hypercapnia-induced Na,K-ATPase β-subunit endocytosis (**Figure 26**).

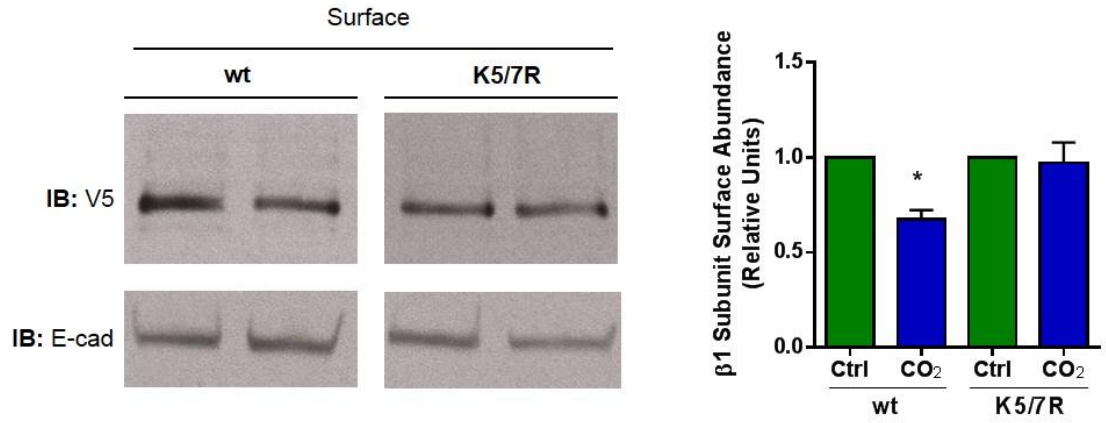

Figure 26: Replacement of lysines 5 and 7 with arginines prevents the hypercapnia–induced endocytosis of the Na,K-ATPase β-subunit. A549 cells were transfected with V5-β1 wt or V5-β1 K5/7R. After 18 hours transfection, cells were exposed to normocapnia (40 mmHg CO_2, pH 7.4) or hypercapnia (110 mmHg CO_2, pH 7.4) for 30 minutes. Afterwards, biotin-streptavidin pull-downs were performed and V5-β1 wt or V5-β1 K5/7R abundance was analyzed by IB. Representative Western blots are shown. Mean ± SEM, n = 3, paired t-test, *$p<0.05$.

In contrast, the substitution of other intracellular lysine residues of the Na,K-ATPase β-subunit (mutants K13/14R and K21/22R) did not prevent hypercapnia-induced endocytosis (**Figure 27**).

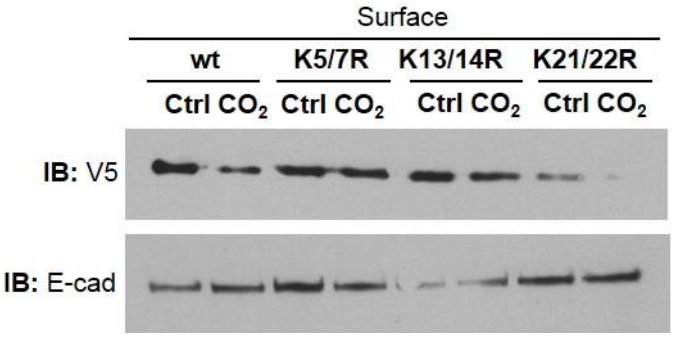

Figure 27: Only replacement of lysines 5 and 7 with arginines prevents hypercapnia–induced Na,K-ATPase β-subunit endocytosis. A549 cells were transfected with V5-β1 wt, V5-β1 K5/7R, V5-β1 K13/14R or V5- β1 K21/22R. After 18 hours transfection, cells were exposed to normocapnia (40 mmHg CO_2, pH 7.4) or hypercapnia (110 mmHg CO_2, pH 7.4) for 30 minutes. Afterwards, biotin-streptavidin pull-downs were performed and V5-β1 abundance was analyzed by IB. Representative Western blots are shown.

The above-mentioned observations demonstrated that only lysines 5 and 7 act as ubiquitin acceptors in hypercapnia-induced Na,K-ATPase β-subunit ubiquitination and is required as a signal for the endocytosis of the protein.

3.8. Mutations in lysine residues 5 and 7 restore hypercapnia-impaired cell-cell junction formation

To determine whether there is a causal link between CO_2-mediated effects on plasma membrane Na,K-ATPase β-subunit stability and cell-cell adhesion, we expressed V5-β1 K5/7R mutant which remains at the cell surface under hypercapnic conditions, and look for its capacity to restore cell-cell junctions formation in cells exposed to elevated CO_2 levels. For that, we conducted cell aggregation assays in A549 cells transfected with V5-β1 wt or K5/7R mutant. Importantly, since we found that cell adhesion was affected by lipid-mediated transfection procedures, we employed nuclofection, as an alternative method to express V5-β1 constructs. Results from these experiments showed that whereas hypercapnia inhibited the formation of larger aggregates in cells expressing V5-β1 wt, this phenotype was prevented in cells expressing V5-β1 K5/7R, in which no differences in the aggregate sizes were found between normocapniaand CO_2 treated cells (**Figure 28**).

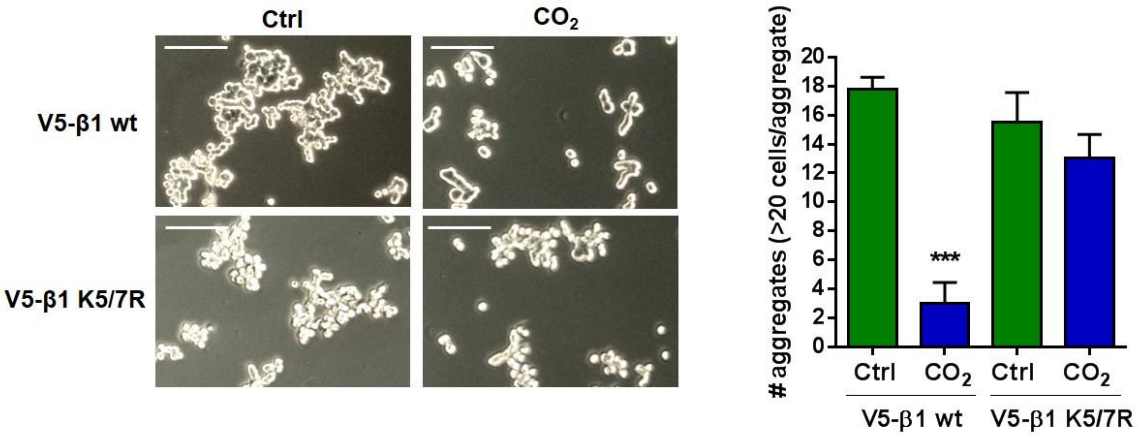

Figure 28: Replacement of lysines 5 and 7 with arginines prevents hypercapnia-mediated inhibition of cell-cell contact formation in A549 cells. A549 nucleofected with V5-β1 wt or V5-β1 K5/7R were incubated in normocapnia (40 mmHg CO_2, pH 7.4) or hypercapnia (110 mmHg CO_2, pH 7.4) for 4 hours. The number of aggregates containing more than 20 cells was determined. Mean ± SEM, n = 3, unpaired t-test, ***p<0.0005. Scale bar = 50 µM.

The above-mentioned results were confirmed in a second set of experiments conducted in rat primary ATII cells transfected with V5-β1 wt or K5/7R mutant. It is well-known that primary ATII cells do not uptake DNA efficiently by lipid-mediated procedures. However, our group have recently demonstrated that ATII nucleofection results in highly-efficient DNA delivery into the cells [200], and we employed this method to express V5-β1 constructs in this cell type. Similarly to A549 cells, cell junctions formation was impaired in cells exposed to hypercapnia (110 mmHg CO_2, pH 7.4), thus demonstrating the deleterious effects of elevated CO_2 levels on the ability of cells to establish cell-cell contacts (**Figure 29**).

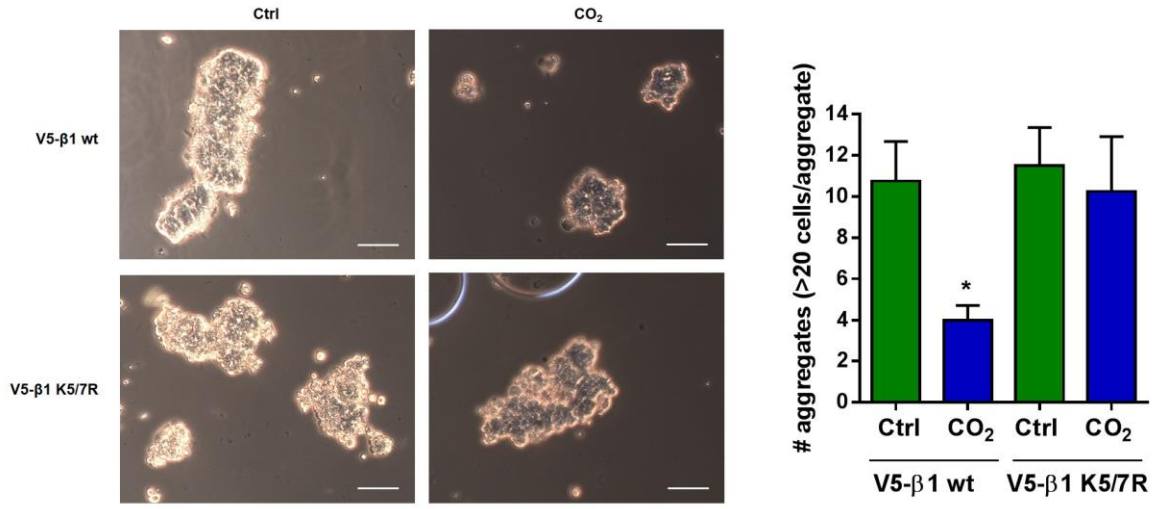

Figure 29: Replacement of lysines 5 and 7 with arginines prevents hypercapnia-mediated inhibition of cell-cell contact formation in rat primary ATII cells. Rat primary ATII cells nucleofected with V5-β1 wt or V5-β1 K5/7R were incubated in normocapnia (40 mmHg CO_2, pH 7.4) or hypercapnia (110 mmHg CO_2, pH 7.4) for 4 hours. The number of aggregates containing more than 20 cells was determined. Mean ± SEM, n = 3, unpaired t-test, *p<0.05. Scale bar = 10 µM.

3.9. Hypercapnia-induced ubiquitination and degradation of the Na,K-ATPase β-subunit requires its serine 11.

Protein phosphorylation at amino acid residues which are in near proximity to the sites of ubiquitination often serves as a phosphodegron which is recognized by the E3 ubiquitin ligase that mediates the ubiquitination reaction [151, 152][131, 201]. We set to evaluate if this was the case for Na,K-ATPase β-subunit, and based on proximity, the serine 11 residue of the Na,K-ATPase β-subunit was a probable candidate.

A widely-used method to identify potential phosphorylation sites consists of the substitution of phosphoacceptor residues to alanine, which prevents the covalent attachment of a phosphate group to the protein; or to aspartate or glutamate, which on the other hand, by adding a negative charge to the protein mimics phosphorylation [202]. Therefore, we used site-directed mutagenesis to introduce serine to alanine and serine to aspartate substitutions in the intracellular domain of V5-β1 wt (mutants S11A and S11D, respectively). A549 cells transfected with V5-β1 constructs were exposed to normocapnia (40 mmHg CO_2, pH 7.4) or hypercapnia (110 mmHg CO_2, pH 7.4) for 30 minutes and Na,K-ATPase β-subunit ubiquitinated isoforms were detected. Serine 11 to alanine substitution led to a significant prevention of hypercapnia-induced Na,K-ATPase β-subunit

ubiquitination whereas serine 11 to aspartate substitution did not it, suggesting that hypercapnia-mediated ubiquitination probably requires Na,K-ATPase β-subunit phosphorylation at serine 11 (**Figure 30**).

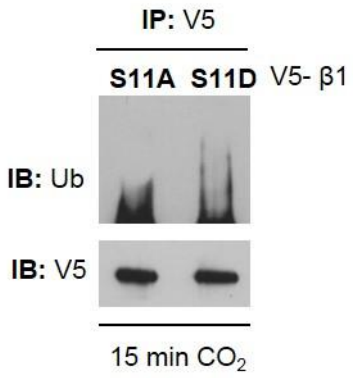

Figure 30: Replacement of serine 11 with alanine prevents hypercapnia-induced ubiquitination. A549 cells were transfected with V5-β1 S11A or V5-β1 S11D. After 18 hours transfection, cells were exposed to hypercapnia (110 mmHg CO_2, pH 7.4) for 15 minutes. V5-β1 S11A or V5-β1 S11D were immunoprecipitated with anti-V5 polyclonal rabbit antibody and ubiquitinated forms were detected with anti-ubiquitin monoclonal mouse antibody by IB. Representative Western blots are shown.

Based on our previous results, we hypothesized that prevention of ubiquitination of the Na,K-ATPase β-subunit by mutating its serine 11 residue to alanine may block the hypercapnia-induced endocytosis and degradation of the protein. Thus, we evaluated the effect of S11A and S11D mutations on hypercapnia-induced degradation. To this end, we conducted pulse-chase experiments with impermeable biotin in A549 cells were transfected with V5-β1 constructs. As anticipated, hypercapnia-induced Na,K-ATPase β-subunit degradation was prevented in the S11A mutant but not in the S11D mutant (**Figure 31**).

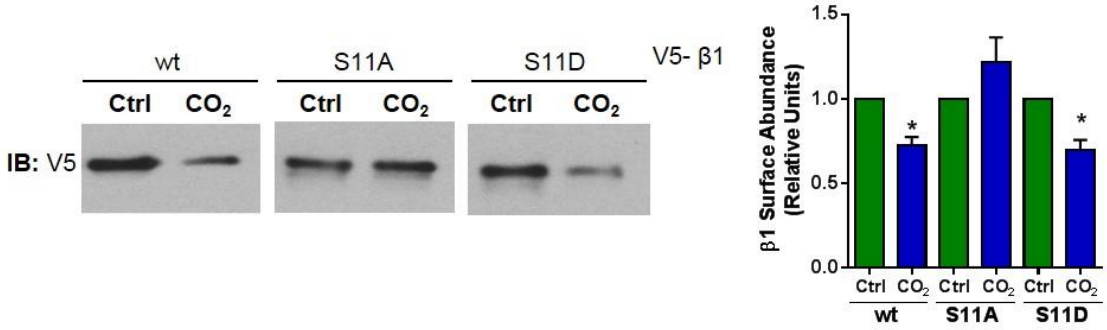

Figure 31: Replacement of serine 11 with alanine prevents hypercapnia-induced degradation of the Na,K-ATPase β-subunit. A549 cells were transfected with V5- β1 wt, V5- β1 S11A or V5- β1 S11D. After 18 hours transfection, surface proteins were labeled with cell-impermeable biotin and chase in normocapnia (40 mmHg CO_2, pH 7.4) or hypercapnia (110 mmHg CO_2, pH 7.4) for 1 hour. Afterwards, streptavidin pull-down was performed and Na,K-ATPase β-subunit abundance was analyzed by IB. Representative Western blots are shown. Mean ± SEM, n = 3, paired t-test, *$p<0.05$.

Mutations of the other intracellular serine residues did not affect hypercapnia-induced effects on the Na,K-ATPase β-subunit (data not shown).

Taken together, these experiments prove that the hypercapnia-induced ubiquitination and subsequent degradation of the Na,K-ATPase β-subunit requires the serine 11 residue of the protein. Though not directly addressed in these experiments, it is reasonable to speculate that probably hypercapnia induces Na,K-ATPase β-subunit serine 11 phosphorylation, which is probably required as a docking site for the ubiquitination machinery. Additional evidence supporting this notion, is the fact that when serine 11 is mutated to aspartate, which adds a negative charge and mimics phosphorylation, the hypercapnia-induced endocytosis and degradation of the Na,K-ATPase β-subunit are not prevented. The fact that this phosphomimic mutant alone is not sufficient to replicate the hypercapnia-induced effects on the Na,K-ATPase β-subunit suggests that other stimuli, apart from phosphorylation, are required.

3.10. Hypercapnia induces the interaction of PKC-ζ with the serine 11 of the Na,K-ATPase β-subunit

Our above-mentioned data suggest that elevated CO_2 levels may lead to activation of a kinase that specifically recognizes, binds and phosphorylates the Na,K-ATPase β-subunit at serine 11. Previous studies from our group conducted in alveolar epithelial cells, have provided strong evidence that protein kinase C ζ (PKC-ζ) becomes activated in response to elevated CO_2 levels and translocates from the cytosol to the plasma membrane where it adds phosphate groups to specific membrane targets [127, 128].

If Na,K-ATPase β-subunit is a substrate of PKC-ζ, it is expected that the proteins interact with each other. To test this hypothesis, A549 cells stably expressing the Na,K-ATPase β-subunit fused to an N-terminal YFP tag (A549-β1-YFP).were used in coimmunoprecipitation studies. Since the YFP tag adds 35 kDa to Na,K-ATPase β-subunit, β1-YFP protein does not comigrate with the immunoprecipitating IgG heavy chain, as opposed to endogenous Na,K-ATPase β-subunit. Cells were exposed to normocapnia (40 mmHg CO_2, pH 7.4) or hypercapnia (110 mmHg CO_2, pH 7.4) for 10 minutes and β1-YFP protein was immunoprecipitated from total protein lysates. These experiments revealed that PKC-ζ coimmunoprecipitated with Na,K-ATPase β-subunit in both normocapnica and hypercapnic conditions (**Figure 32**).

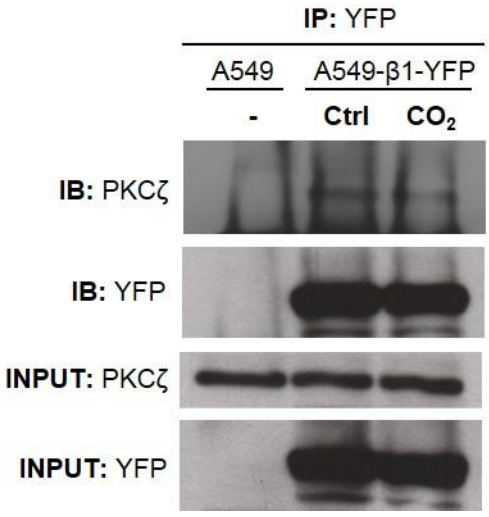

Figure 32: PKC-ζ interacts with Na,K-ATPase β-subunit in A549 cells. A549-β1-YFP cells were exposed to normocapnia (40 mmHg CO_2, pH 7.4) or hypercapnia (110 mmHg CO_2, pH 7.4) for 10 minutes. β1-YFP protein was immunoprecipitated from total lysates with anti-GFP monoclonal mouse antibody and PKC-ζ was detected with anti-PKC-ζ monoclonal mouse antibody by IB. Representative Western blot is shown.

To confirm the binding of PKC-ζ to Na,K-ATPase β-subunit, *in vitro* experiments were conducted, for which we designed synthetic peptides containing the entire intracellular domain of the Na,K-ATPase β-subunit (cyt-β1 wt peptide) where we expected PKC-ζ to bind (**Figure 33**). Protein extracts from A549 cells exposed to normocapnia (40 mmHg CO_2, pH 7.4) or hypercapnia (110 mmHg CO_2, pH 7.4) for 10 minutes were incubated with biotinylated cyt-β1 wt peptide, followed by streptavidin pull-downs. These experiments showed that PKC-ζ was bound to the intracellular portion of Na,K-ATPase β-subunit and revealed that elevated CO_2 levels led to an increase in PKC-ζ interaction with the Na,K-ATPase β-subunit (**Figure 33**).

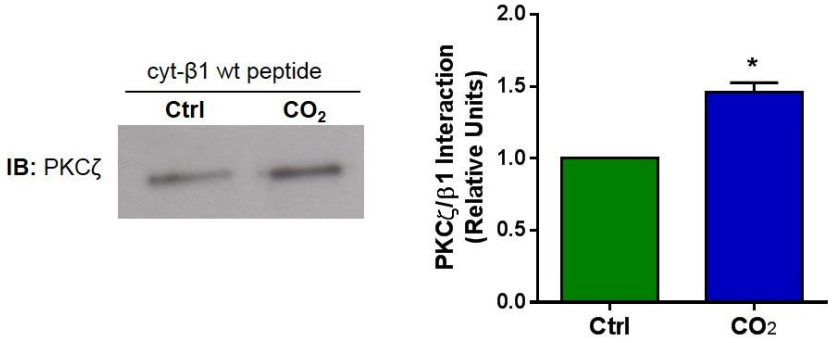

Figure 33: PKC-ζ interacts with Na,K-ATPase β-subunit intracellular domain *in vitro*. A549 cells were exposed to normocapnia (40 mmHg CO_2, pH 7.4) or hypercapnia (110 mmHg CO_2, pH 7.4) for 10 minutes. Total lysates were incubated with biotinylated synthetic peptides containing the whole β-subunit intracellular domain (cyt-β1 wt peptide) overnight and streptavidin pull-downs were performed. PKC-ζ was detected with anti-PKC-ζ monoclonal mouse antibody by IB. Representative Western blots are shown. Mean ± SEM, n = 3, paired t-test, *p<0.05.

To further verify the phosphorylation site in Na,K-ATPase β-subunit, we designed peptides containing mutations for each intracellular serine. We reasoned that once Na,K-ATPase β-subunit is phosphorylated by PKC-ζ, the affinity of the kinase to the Na,K-ATPase may decrease. Therefore, we mutated each serine residue of the Na,K-ATPase β-subunit to aspartate to mimic phosphorylation, and identified which mutation affected PKC-ζ interaction with β-subunit. In line with our previous findings, only when serine 11 was mutated to aspartate, PKC-ζ binding to Na,K-ATPase β-subunit was prevented (**Figure 34**).

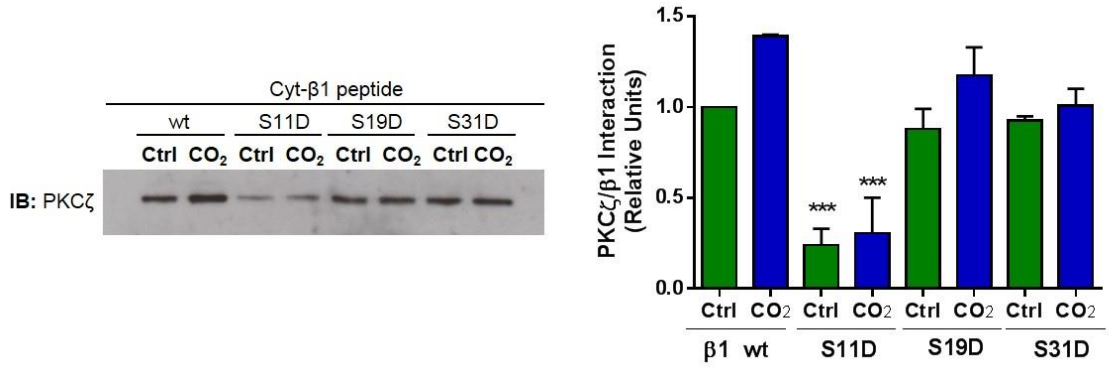

Figure 34: Only the mutation of serine 11 to aspartate prevents PKC-ζ interaction with β-subunit intracellular domain. A549 cells were exposed to normocapnia (40 mmHg CO_2, pH 7.4) or hypercapnia (110 mmHg CO_2, pH 7.4) for 10 minutes. Total lysates were incubated with biotinylated synthetic peptides containing the whole Na,K-ATPase β-subunit intracellular domain wt or mutated (cyt-β1 peptide wt, S11D, S19D, S31D) overnight and streptavidin pull-downs were performed. PKC-ζ was detected with anti-PKC-ζ monoclonal mouse antibody by IB. Representative Western blots are shown. Mean ± SEM, n = 3, one-way ANOVA and Tukey´s multiple comparisons, ***p<0.0005 vs β1-wt.

Altogether, these experiments provided strong evidence of the interaction between PKC-ζ and Na,K-ATPase β-subunit, in which the serine 11 residue of the Na,K-ATPase is involved. Moreover, our data suggest that elevated CO_2 levels might facilitate this interaction, which is expected given that hypercapnia activates PKC-ζ [128].

3.11. Hypercapnia-induced endocytosis of the Na,K-ATPase β-subunit requires the activity of PKC-ζ

To determine whether the activity of PKC-ζ was required for the hypercapnia-induced endocytosis of the Na,K-ATPase β-subunit, we assessed plasma membrane Na,K-ATPase β-subunit protein abundance in A549 cells exposed to elevated CO_2 in the presence of PKC inhibitor bisindolmaleimide I (Bis). These experiments showed that inhibition of PKC activity prevented hypercapnia-induced endocytosis of Na,K-ATPase β-subunit (**Figure 35**).

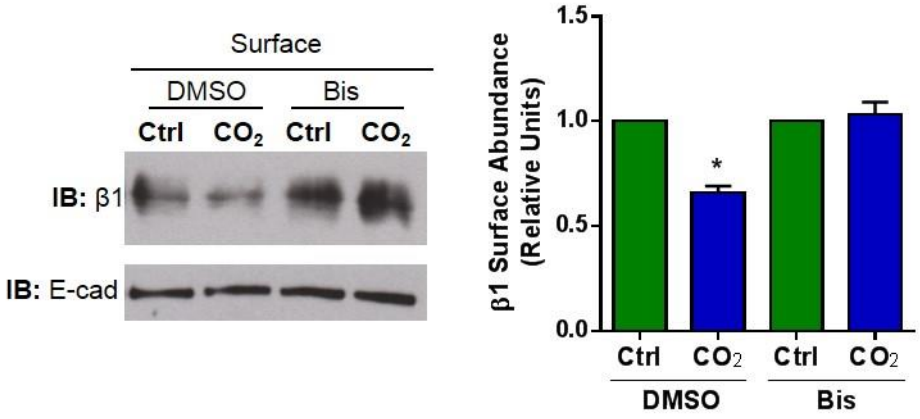

Figure 35: Inhibition of PKC activity prevents hypercapnia-induced endocytosis of the Na,K-ATPase β-subunit. A549 cells were pre-incubated with vehicle (DMSO) or PKC inhibitor (bisindolmaleimide I, Bis) for 30 minutes and exposed to normocapnia (40 mmHg CO_2, pH 7.4) or hypercapnia (110 mmHg CO_2, pH 7.4) for 30 minutes. Biotin-streptavidin pull-down of cell surface proteins was performed and analyzed by IB. Representative Western blots are shown. Mean ± SEM, n = 3, paired t-test, *p<0.05.

Considering that Bis inhibits the activity of several members of the PKC family, we further examined the requirement of PKC-ζ in the hypercapnia-induced effects on β-subunit endocytosis by knocking down PKC-ζ expression with the use of a specific siRNA. A549 cells transfected with siRNA against PKC-ζ or a scrambled siRNA as a control, were exposed to normocapnia (40 mmHg CO_2, pH 7.4) or hypercapnia (110 mmHg CO_2, pH 7.4) for 30 minutes and plasma membrane Na,K-ATPase β-subunit abundance was determined by biotin-streptavidin pull-downs. These experiments showed that when PKC-ζ expression was significantly downregulated, hypercapnia-induced β-subunit endocytosis was completely prevented (**Figure 36**).

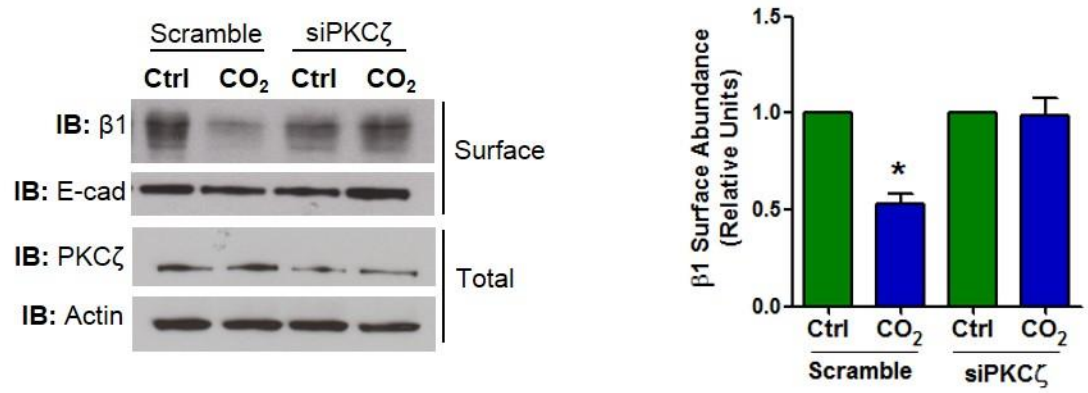

Figure 36: Knock-down of PKC-ζ by siRNA prevents hypercapnia-induced endocytosis of the Na,K-ATPase β-subunit. A549 cells were transfected with siRNA against PKC-ζ or scramble siRNA. After 72 hours transfection, cells were exposed to normocapnia (40 mmHg CO_2, pH 7.4) or hypercapnia (110 mmHg CO_2, pH 7.4) for 30 minutes. Biotin-streptavidin pull-down of cell surface proteins was performed and Na,K-ATPase β-subunit abundance was analyzed by IB. Representative Western blots are shown. Mean ± SEM, n = 3, paired t-test, *$p<0.05$.

These results provide strong evidence that PKC-ζ activity is required for the hypercapnia-induced ubiquitination and endocytosis of Na,K-ATPase β-subunit.

3.12. TRAF2 E3 ligase interacts with the Na,K-ATPase β-subunit

So far our data support the hypothesis that elevated CO_2 levels lead to Na,K-ATPase β-subunit polyubiquitination at lysines 5 and 7, which act as a signal for the endocytosis of the protein. In the ubiquitination process, the substrate specificity is conferred by the E3 ubiquitin ligases [136]. Therefore, we set out to identify the E3 ligase involved in the hypercapnia-induced Na,K-ATPase β-subunit ubiquitination. To this end, we used a protein microarray to screen for proteins that interact with human Na,K-ATPase β-subunit. Based on our previous results suggesting that the phosphorylation of Na,K-ATPase β-subunit at serine 11 might be required for hypercapnia-induced ubiquitination, a protein lysate from cells expressing Na,K-ATPase β-subunit phosphomimic (V5-β1 S11D) was applied to a microarray of more than 9000 human proteins, among which 239 were ubiquitin E3 ligases. After a hypothesis-driven analysis of the 47 E3 ligases that were found to significantly interact with Na,K-ATPase β-subunit *in vitro*, we identified tumor necrosis factor (TNF) receptor-associated factor 2 (TRAF2) as a likely candidate.

It has been recently described that TRAF2 can act as a RING E3 ubiquitin ligase when bound to intracellularly-produced sphingosine-1-phosphate (S1P), which acts as a cofactor of the enzyme [198].

We first set out to confirm the interaction of TRAF2 with Na,K-ATPase β-subunit by performing coimmunoprecipitation experiments. Na,K-ATPase β-subunit was immunoprecipitated from protein lysates of A549 cells exposed to normocapnia (40 mmHg CO_2, pH 7.4) or hypercapnia (110 mmHg CO_2, pH 7.4) for 10 minutes. TRAF2 coimmunoprecipited with Na,K-ATPase β-subunit in both normocapnic and hypercapnic conditions, indicating that indeed TRAF2 is interacting with Na,K-ATPase β-subunit. Importantly, we were also able to detect PKC-ζ in these coimmunoprecipitation studies (**Figure 37**).

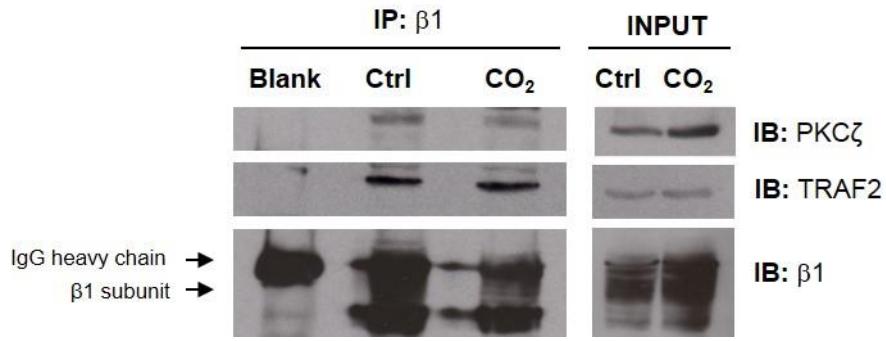

Figure 37: TRAF2 interacts with the Na,K-ATPase β-subunit in A549 cells. A549 were exposed to normocapnia (40 mmHg CO_2, pH 7.4) or hypercapnia (110 mmHg CO_2, pH 7.4) for 10 minutes. Na,K-ATPase β-subunit was immunoprecipitated from total lysates with anti-Na,K-ATPase β1-subunit monoclonal mouse antibody and TRAF2 and PKC-ζ were detected with their respective antibodies by IB. Representative Western blots are shown.

We were able to further confirm the binding of TRAF2 to Na,K-ATPase β-subunit by performing a reverse coimmunoprecipitation in which we immunprecipitated TRAF2 and detected Na,K-ATPase β-subunit (**Figure 38**).

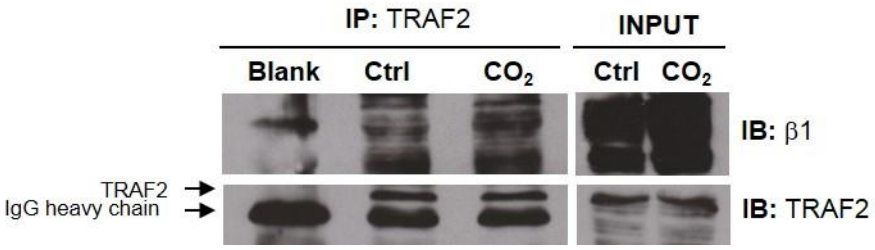

Figure 38: TRAF2 interacts with the Na,K-ATPase β-subunit in A549 cells. A549 were exposed to normocapnia (40 mmHg CO_2, pH 7.4) or hypercapnia (110 mmHg CO_2, pH 7.4) for 10 minutes. TRAF2 was immunoprecipitated from total lysates with anti-TRAF2 polyclonal rabbit antibody and Na,K-ATPase β-subunit was detected anti-Na,K-ATPase β1-subunit antibody by IB. Representative Western blots are shown.

To further validate TRAF2 interaction with Na,K-ATPase β-subunit we conducted *in vitro* experiments, for which total lysates from A549 cells exposed to normocapnia (40 mmHg CO_2, pH 7.4) or hypercapnia (110 mmHg CO_2, pH 7.4) for 10 minutes were incubated with biotinylated cyt-β1 wt peptides. In line with our previous results, we detected TRAF2 in the streptavidin pull-downs, confirming that TRAF2 binds to the intracellular domain of Na,K-ATPase β-subunit (**Figure 39**).

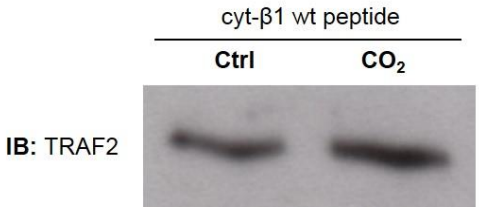

Figure 39: TRAF2 interacts with the intracellular domain of the Na,K-ATPase β-subunit *in vitro*. A549 cells were exposed to normocapnia (40 mmHg CO_2, pH 7.4) or hypercapnia (110 mmHg CO_2, pH 7.4) for 10 minutes. Total lysates were incubated with biotinylated cyt-β1 wt peptide overnight and streptavidin pull-downs were performed. TRAF2 was detected with anti-TRAF2 monoclonal mouse antibody by IB. Representative Western blots are shown.

3.13. TRAF2 ubiquitinates the Na,K-ATPase β-subunit

We also conducted experiments to assess the potential effect of TRAF2 overexpression on the ubiquitination of the Na,K-ATPase β-subunit. For that, we transfected A549 cells with a TRAF2-GST construct, and detected Na,K-ATPase β-subunit ubiquitinated forms in the total lysates by overexposing films. TRAF2 overexpression caused a substantial

accumulation of the ubiquitinated Na,K-ATPase β-subunit isoforms, as opposed to untransfected cells (**Figure 40**).

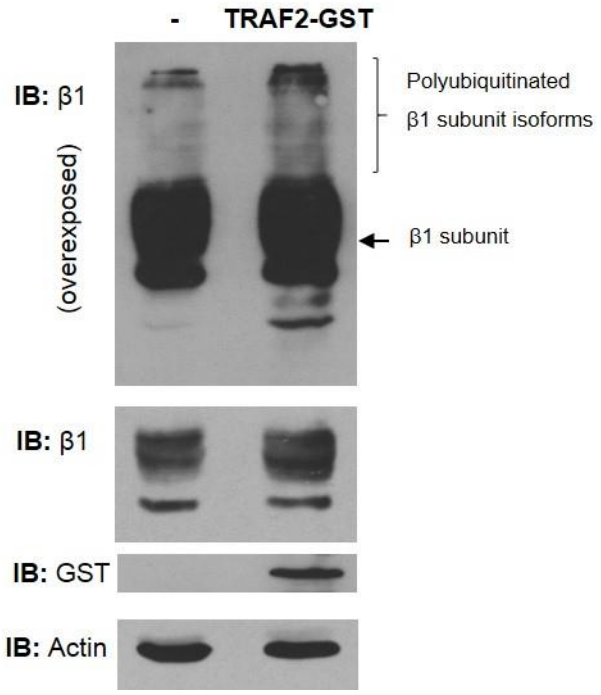

Figure 40: TRAF2 overexpression increases the ubiquitination of the Na,K-ATPase β-subunit. Ubiquitinated Na,K-ATPase β-subunit isoforms were detected in total lysates from A549 cells transfected with TRAF2-GST construct or untransfected, by anti Na,K-ATPase β-subunit antibodies. Overexposition of the films shows Na,K-ATPase β-subunit polyubiquitinated isoforms. Representative Western blots are shown.

To evaluate whether TRAF2 directly mediates Na,K-ATPase β-subunit ubiquitination, we conducted *in vitro* ubiquitination experiments, in which immunoprecipitated TRAF2 supplemented with its cofactor, S1P, were employed as a source of E3 ubiquitin ligase to ubiquitinate the cyt-β1 wt peptide. Following the ubiquitination reaction, biotinylated cyt-β1 wt peptides were isolated with streptavidin pull-downs and the ubiquitinated Na,K-ATPase β-subunit isoforms were detected with anti-ubiquitin antibodies. In these studies, we observed a significant accumulation of ubiquitinated Na,K-ATPase β-subunit isoforms (**Figure 41**).

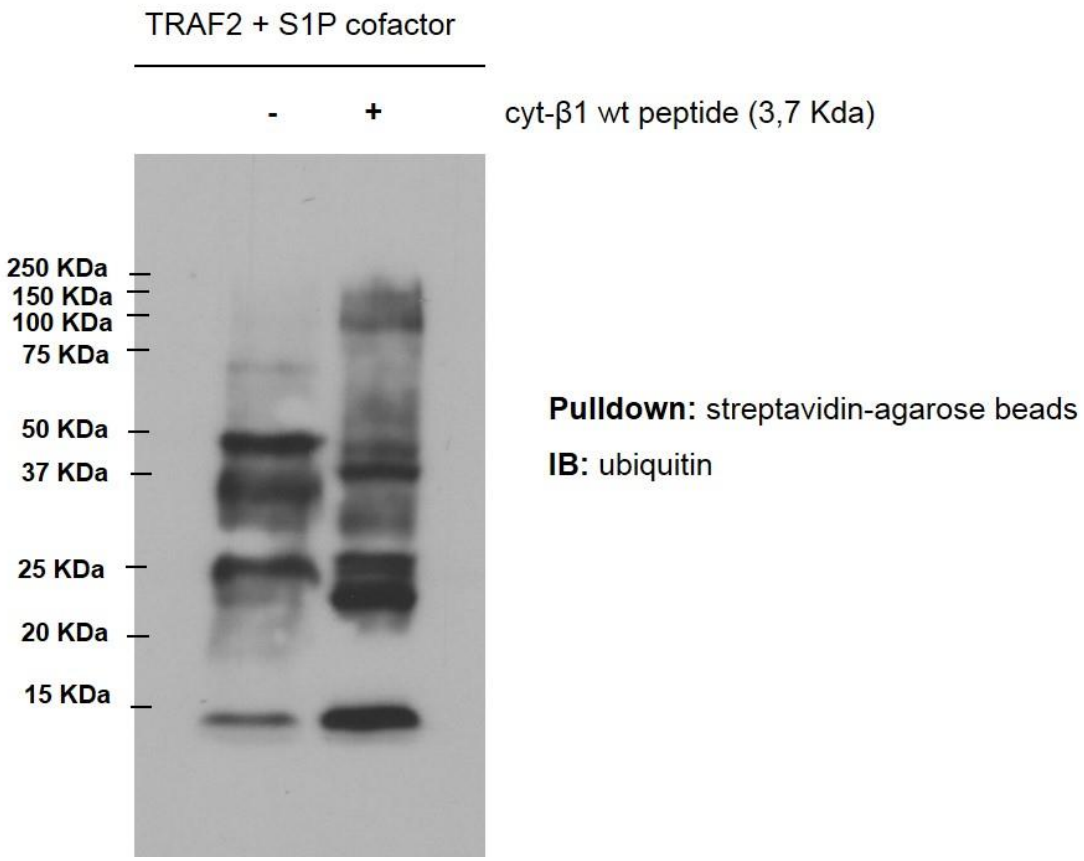

Figure 41: TRAF2 E3 ubiquitin ligase ubiquitinates the intracellular domain of the Na,K-ATPase β-subunit *in vitro*. TRAF2 immunoprecipitated from A549 cells was used to ubiquitinate cyt-β1 wt peptide in an *in vitro* ubiquitination reaction. As a negative control the cyt-β1 wt peptide was omitted. Biotinylated cyt-β1 wt peptides were purified by streptavidin pull-downs and the Na,K-ATPase β-subunit ubiquitinated isoforms were detected with anti-ubiquitin antibody by IB. A representative Western blot is shown.

These results suggest that TRAF2 has the capacity to ubiquitinate the Na,K-ATPase β-subunit.

3.14. TRAF2 is required for hypercapnia-induced endocytosis of the Na,K-ATPase β-subunit

Since our findings suggest that TRAF2 E3 ligase is able to interact with the Na,K-ATPase β-subunit and mediate its ubiquitination, we aimed to evaluate whether TRAF2 mediates hypercapnia-induced effects on Na,K-ATPase stability. For that, we evaluated the hypercapnia-induced endocytosis of Na,K-ATPase β-subunit in A549 cells in which TRAF2 was depleted by the use of specific siRNA against the protein. Results from these

experiments showed that TRAF2 depletion was sufficient to prevent the hypercapnia-induced endocytosis of the Na,K-ATPase β-subunit (**Figure 42**).

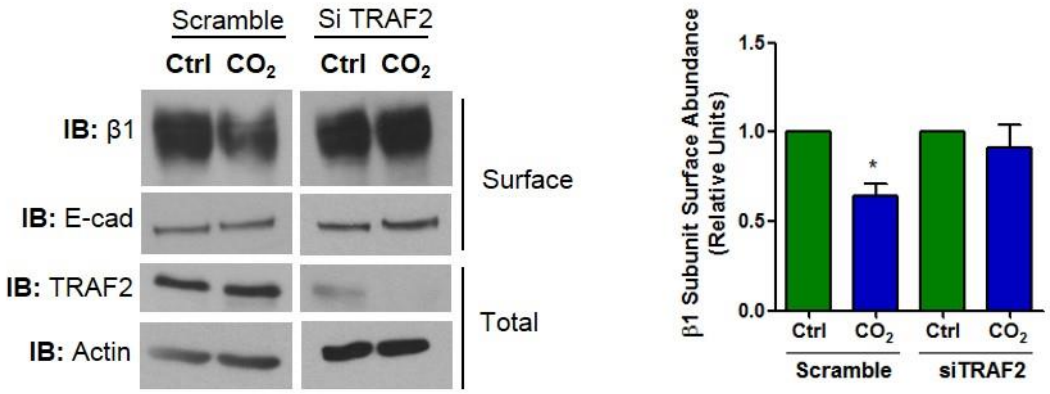

Figure 42: Knockdown of TRAF2 by siRNA prevents hypercapnia-induced endocytosis of the Na,K-ATPase β-subunit. A549 cells were transfected with siRNA against TRAF2 or scramble siRNA. After 48 hours transfection, cells were exposed to normocapnia (40 mmHg CO_2, pH 7.4) or hypercapnia (110 mmHg CO_2, pH 7.4) for 30 minutes. Biotin-streptavidin pull-down of cell surface proteins was performed and Na,K-ATPase β-subunit abundance was analyzed by IB. Mean ± SEM, n = 3, paired t-test, *$p<0.05$.

Altogether, these results provide evidence that TRAF2 acts as the E3 ligase for the Na,K-ATPase β-subunit, mediating the effects of hypercapnia on the protein.

4. Discussion

Here we report a novel mechanism by which hypercapnia affects the function of the alveolar epithelium. We provide new evidence that elevated CO_2 levels lead to the endocytosis and degradation of the Na,K-ATPase β-subunit which results in reduced ability of alveolar cells to form intercellular junctions. Our data show that ubiquitin chains covalently-attached to lysines 5 and 7 of the Na,K-ATPase β-subunit during hypercapnia are the primary signal leading to the endocytosis of the protein. Moreover, our results show that ubiquitination depends on PKC-ζ activity and involves the serine 11 residue of the Na,K-ATPase β-subunit. Most importantly, we identify TRAF2 as the E3 ligase that mediates the hypercapnia-induced ubiquitination of the Na,K-ATPase β-subunit. Our results are consistent with a key role of Na,K-ATPase β-subunit as a cell-adhesion molecule in the alveolar epithelium.

4.1. Hypercapnia inhibits the formation of cell-cell contacts between alveolar epithelial cells by promoting endocytosis of the Na,K-ATPase β-subunit

Hypercapnia is often observed in patients with ARDS and has been associated with worse patient prognosis [112, 117]. Several experimental studies support the existence of a causal link between hypercapnia and poor clinical outcomes [112, 127, 128, 203].

Though the CO_2 sensor remains unknown, it has been well-demonstrated that elevated CO_2 is sensed by cells in the lung leading to deleterious effects on cell function, independently of intra- or extracellular pH. Indeed, elevated CO_2 has been reported to activate AMPK, a master regulator of cellular adaptation to stressful conditions [128]. Under hypercapnic conditions, AMPK activation has been shown to promote PKC-ζ-mediated phosphorylation of the Na,K-ATPase α-subunit and subsequent endocytosis of the protein, which results in impaired alveolar fluid clearance [127, 128].

Here we report that elevated CO_2 levels impair the formation of new cellular junctions between alveolar epithelial cells. This CO_2-associated adverse effect can particularly affect patients with ARDS, in which the alveolar epithelium is injured, and the organization of new cell contacts is required in order to re-establish the integrity of the alveolar epithelial barrier.

We hypothesized that CO_2-mediated down-regulation of one or more cell adhesion molecules may account for the CO_2-associated inhibitory effects on cell adhesion. One

attractive candidate appeared to be the Na,K-ATPase β-subunit, which apart from its auxiliary role in the pump functionality, it is also a cell adhesion molecule that is involved in the organization and stability of cellular junctions [96]. The Na,K-ATPase β-subunit is normally located at the basolateral surface of epithelial cells where it mediates homophilic cell-cell adhesion [85, 86, 93]. Consistent with our hypothesis, the studies demonstrated that elevated CO_2 levels lead to the endocytosis of the Na,K-ATPase β-subunit from the plasma membrane of alveolar epithelial cells. By biochemical studies in which we labeled plasma membrane proteins with impermeable biotin and by immunofluorescence microscopy, we were able to solidly demonstrate that elevated CO_2 levels lead to a time-dependent endocytosis of the Na,K-ATPase β-subunit, which is already evident after 6 minutes of cell exposure to hypercapnia.

Plasma membrane Na,K-ATPase β-subunit has a fundamental role in the organization and stability of tight and adherens junctions in epithelia [96]. In the light of our findings showing that elevated CO_2 levels promote the ubiquitination-driven Na,K-ATPase β-subunit endocytosis, we hypothesize that hypercapnia-associated impaired cell-adhesion is a consequence of the reduced abundance of the Na,K-ATPase β-subunit protein at the plasma membrane of alveolar epithelial cells. To test the hypothesis, we conducted cell aggregation experiments in which we employed Na,K-ATPase β-subunit mutants containing lysine 5 and 7 replaced with arginines to prevent hypercapnia-induced Na,K-ATPase β-subunit endocytosis. Results from these experiments show that Na,K-ATPase β-subunit mutants which do not get ubiquitinated at lysines 5 and 7 are capable of restoring cell junctions formation in alveolar epithelial cells exposed to elevated CO_2 levels. These findings solidly demonstrate that hypercapnia-triggered impaired cell-cell adhesion is mediated by the plasma membrane Na,K-ATPase β-subunit down-regulation. This is in agreement with our initial data in which we observed that MG-132, which prevents the endocytosis of the Na,K-ATPase β-subunit, also prevents the detrimental effects of hypercapnia on cell-cell contacts formation.

4.2. Ubiquitination of the Na,K-ATPase β-subunit acts as a signal for the endocytosis of the protein

Ubiquitin is a key player in the regulation of the endocytosis of several membrane proteins [129, 197]. It has been proposed that ubiquitinated proteins are recognized by ubiquitin-binding motifs present in various proteins that belong to the endocytic machinery,

coordinating protein internalization [197, 201]. Ubiquitination of the Na,K-ATPase β-subunit during the normal turnover of the protein has been recently reported [193], but whether this process is required for the endocytosis or the degradation of the protein remained to be addressed. Interestingly, our studies demonstrated that elevated CO_2 levels lead to rapid ubiquitination of the Na,K-ATPase β-subunit at the plasma membrane. To determine the ubiquitination site in Na,K-ATPase β-subunit, we conducted experiments in which all the intracellular lysines of the Na,K-ATPase β-subunit were substituted to arginines. Analysis of the data shows that only the simultaneous mutations of lysines 5 and 7, prevents the hypercapnia-induced accumulation of the polyubiquitinated Na,K-ATPase β-subunit isoforms. This finding raises the question whether ubiquitin is attached randomly to one or the other lysine or whether there is a preferred lysine residue, but when mutated, the other lysine compensates the effect. Finally it is also possible that both lysines are ubiquitinated but one of them is enough to induce Na,K-ATPase β-subunit internalization. The flexibility in the ubiquitination site is not surprising, as the reactivity of a lysine seems to be enhanced by the presence of near-by basic residues proximal to the E3 ligase binding site [140, 153, 154]. The observation that the Na,K-ATPase β-subunit gets ubiquitinated at the plasma membrane is consistent with a role of ubiquitin chains in triggering hypercapnia-induced endocytosis of the protein. Indeed, internalization of Na,K-ATPase β-subunit under hypercapnic conditions is prevented when lysines 5 and 7 of Na,K-ATPase β-subunit are replaced with arginines, demonstrating that the Na,K-ATPase β-subunit ubiquitination is absolutely required for the endocytosis of the protein.

4.3. The activity of PKC-ζ is required for hypercapnia-induced ubiquitination of the Na,K-ATPase β-subunit

Phosphorylation of a substrate may modulate its interaction with an E3 ubiquitin ligase. For some proteins, the phosphorylation sites are located close to the ubiquitination sites. Serine 11, present in the intracellular portion of the Na,K-ATPase β-subunit and proximal to lysines 5 and 7, was a potential phosphorylation site. When Na,K-ATPase β-subunit serine 11 is substituted for alanine (S11A) to prevent phosphorylation of the protein, hypercapnia-induced ubiquitination and degradation of the Na,K-ATPase β-subunit are prevented. The most likely explanation for this observation is that phosphorylation at serine 11 is required for the hypercapnia-induced ubiquitination of the Na,K-ATPase β-subunit. However, the mutation of this amino acid could have other consequences than

preventing phosphorylation of the protein, such as simply disrupting an E3 ligase degron. To better understand the role of serine 11 in the ubiquitination of the Na,K-ATPase β-subunit we conducted experiments in which we mimicked phosphorylation of the Na,K-ATPase β-subunit by replacing its serine 11 with aspartate (S11D). In this case, the hypercapnia-induced ubiquitination and degradation of the Na,K-ATPase β-subunit are preserved, suggesting that serine 11 phosphorylation might be required for hypercapnia-induced ubiquitination. There are multiple possibilities regarding the role of the phosphorylation of serine 11 of the Na,K-ATPase β-subunit in the ubiquitination of the protein. It may create a phosphodegron for the binding of an E3 ligase or it may induce conformational changes in the Na,K-ATPase β-subunit which may lead to the exposure of an existing E3 ligase degron. It has also been shown that the phosphorylation of the protein may lead to changes in the subcellular localization of the protein which may facilitate the interaction with an E3 ligase. However, the finding that Na,K-ATPase β-subunit gets ubiquitinated at the plasma membrane might argue against this possibility. One important observation is that the experiments do not show lower protein levels of the Na,K-ATPase β-subunit phosphomimic S11D than the Na,K-ATPase β-subunit wild type under basal conditions. This suggest that serine 11 is required but not sufficient to promote Na,K-ATPase β-subunit ubiquitination-driven endocytosis and degradation. Therefore, we speculate that elevated CO_2 levels may also regulate other players of the process of ubiquitination of the Na,K-ATPase β-subunit such as the E3 ligase activation.

One important issue that remained to be addressed was the identification of the kinase involved in the Na,K-ATPase β-subunit phosphorylation. Since elevated CO_2 levels activates PKC-ζ, leading to its translocation to the plasma membrane where it phosphorylates the Na,K-ATPase α-subunit [127, 128], we hypothesized that PKC-ζ might also phosphorylate the Na,K-ATPase β-subunit under hypercapnic conditions. In line with our hypothesis, the results demonstrate that PKC-ζ interacts with the Na,K-ATPase β-subunit. Since elevated CO_2 levels lead to the recruitment of PKC-ζ at the plasma membrane of alveolar epithelial cells [128], it is not surprising that we observe that hypercapnia increases the interaction between both proteins. Furthermore, interaction assays in which we employed the intracellular domain of the Na,K-ATPase β-subunit with the intracellular serines mutated to aspartates show that only serine 11 mutation impairs Na,K-ATPase β-subunit interaction with PKC-ζ. Since enzymes generally display less affinity for their products [204], this result suggests that PKC-ζ mediates Na,K-ATPase β-subunit serine 11 phosphorylation, thus confirming our previous studies. Importantly,

experiments in which PKC-ζ activity is inhibited or PKC-ζ cell expression is knocked down by the use of specific siRNA demonstrate that PKC-ζ is required for hypercapnia-induced Na,K-ATPase β-subunit endocytosis. Interestingly, we have observed that PKC-ζ interacts with the Na,K-ATPase β-subunit at normal CO_2 levels, which raises the question whether PKC-ζ may play a role in the basal turnover of the Na,K-ATPase β-subunit. However, the fact that PKC-ζ inhibition does not lead to an increase in plasma membrane Na,K-ATPase β-subunit protein abundance at basal levels does not support this speculation and further studies will be needed to understand this basal interaction between PKC-ζ and the Na,K-ATPase β-subunit.

The observed similarities in the regulation of the Na,K-ATPase α- and β-subunit localization at the plasma membrane under hypercapnic conditions, raise concerns about whether α- and β-subunit are regulated as a dimer or whether they are independently regulated. Although the Na,K-ATPase α- and β-subunit must be assembled as an heterodimer in order to be delivered to the basolateral membrane [68, 205, 206], once at the surface the Na,K-ATPase subunits have independent functions and its stability might be independently regulated [193]. We believe that our experimental data is consistent with a model in which hypercapnia directly regulates Na,K-ATPase β-subunit, independently of the Na,K-ATPase α-subunit. Indeed, our experiments have shown that PKC-ζ physically interacts with the cytosolic domain of the Na,K-ATPase β-subunit and this interaction is disrupted by the mutation of Na,K-ATPase β-subunit serine 11. Moreover our studies indicate that Na,K-ATPase β-subunit lysines 5 and 7, as well as the serine 11, are completely required for hypercapnia-induced ubiquitination-driven endocytosis and degradation of the protein. Altogether, these observations strongly suggest that Na,K-ATPase β-subunit is directly regulated by elevated CO_2 levels. Since PKC-ζ has also been shown to mediate CO_2 effects on the Na,K-ATPase α-subunit promoting its endocytosis [128], we propose that hypercapnia-induced PKC-ζ activation leads to the PKC-ζ-mediated phosphorylation of each subunit which may trigger different regulation pathways, possibly implicating different molecular players.

4.4. The proteasome activity is required for the degradation of the Na,K-ATPase β-subunit under steady-state and hypercapnic conditions

Consistent with the existence of distinct mechanisms of regulation for the plasma membrane Na,K-ATPase α- and β-subunit stability, one study done in HeLa cells has

shown that under steady-state conditions the half-life of the plasma membrane Na,K-ATPase β-subunit in this cell-line is about ~4 hours whereas the half-life of the plasma membrane Na,K-ATPase α-subunit is about ~20 hours [193], thus demonstrating that the degradation of each subunit at the plasma membrane is independently regulated. In contrast, one study in A549 cells have shown similar half-lives for both Na,K-ATPase α- and β-subunit at the plasma membrane [194]. However, this finding does not necessarily imply a shared degradation pathway.

In addition to the distinct turnover rate of the plasma membrane Na,K-ATPase α- and β-subunit in some cell-lines, evidence suggest possible differences in the degradation pathway. Previous studies have shown that the Na,K-ATPase α-subunit turnover under steady-state or hypoxic conditions is lysosome-mediated [194]. In contrast, our studies on the Na,K-ATPase β-subunit turnover showed that treatment of A549 cells with 2 different widely-employed lysosome inhibitors, chloroquine and E-64, do not prevent plasma membrane Na,K-ATPase β-subunit endocytosis and degradation under steady-state or hypercapnic conditions. On the other hand, we have found that inhibition of the proteasomal activity in A549 cells with the proteasome inhibitor MG-132 prevents endocytosis and degradation of the Na,K-ATPase β-subunit. Similarly, studies in HeLA cells have shown that the plasma membrane Na,K-ATPase β-subunit degradation is prevented by proteasome inhibitors and its prevention leads to the accumulation of ubiquitinated Na,K-ATPase β-subunit isoforms [193]. However, one needs to be careful in the interpretation of these results. First, it is known that the proteasome inhibitors have an impact on the degradation of various intracellular proteins, which may directly or indirectly affect Na,K-ATPase β-subunit stability. For instance, endocytic machinery proteins, kinases and E3 ligases may be regulated by the proteasome [207-209]. Moreover, free ubiquitin molecules are normally recycled after protein degradation by the proteasome [210]. Therefore, proteasome inhibition may eventually lead to ubiquitin depletion which may affect ubiquitin-mediated endocytosis signaling and lysosomal degradation [211, 212]. Nevertheless, without an evident effect of the lysosome inhibitors on the Na,K-ATPase β-subunit stability, and in the light of the inhibitory effects of the proteasome inhibitors on the Na,K-ATPase β-subunit degradation, at the present we believe that it is likely that the proteasome is involved in the degradation of Na,K-ATPase β-subunit under both steady-state and hypercapnic conditions. We believe that future studies oriented to further confirm this hypothesis will be of interest, since the implication of the proteasomal pathway in the degradation of plasma membrane proteins, which is generally lysosome-

mediated [213], is unusual. Nevertheless, recent evidence point to an interconnection between the degradation pathways and for example a proteasome pool associated with endosomes has been recently found to influence protein sorting [214].

Although the exact pathway of degradation of the plasma membrane Na,K-ATPase β-subunit has still to be elucidated, we have gained some knowledge regarding the molecular pathway involved in the degradation of the intracellular Na,K-ATPase β-subunit. Studies in which we employed a widely-used inhibitor of the protein synthesis, cycloheximide, allowed as to examine the turnover of the different Na,K-ATPase β-subunit isoforms. In line with studies from other groups [206], analysis of the data shows that under steady-state conditions the turnover of the core-glycosylated ER-associated Na,K-ATPase β-subunit form is faster than the turnover of the fully-glycosylated form. Interestingly, the application of proteasome inhibitor in similar experiments, does not prevent the decrease in the core-glycosylated Na,K-ATPase β-subunit protein abundance, but leads to the accumulation of a lower molecular weight form of the Na,K-ATPase β-subunit. Importantly, PNGaseF-treated deglycosylated Na,K-ATPase β-subunit protein comigrates in SDS-PAGE with this lower molecular weight form of Na,K-ATPase β-subunit accumulated in the presence of the proteasome-inhibitor, suggesting that this form might be a deglycosylated intermediate of Na,K-ATPase β-subunit. In the light of this finding we hypothesize that the core-glycosylated ER-associated Na,K-ATPase β-subunit undergoes the already well-characterized ER-associated degradation pathway (ERAD), in which ER-localized glycoproteins are retrotranslocated, deglycosylated and proteasome-degraded [196, 215, 216].

4.5. TRAF2 E3 ligase mediates the ubiquitination of the Na,K-ATPase β-subunit in hypercapnia

By specifically recognizing their substrates, the E3 ligases are the enzymes responsible for dictating the specificity of the ubiquitination process [160]. In order to identify the E3 ligase involved in hypercapnia-induced ubiquitination of Na,K-ATPase β-subunit, we conducted a protein microarray in which we screened for proteins that interact with the Na,K-ATPase β-subunit. Since the binding of an E3 ligase to its substrate is a tightly regulated event [152], in order to preserve the interaction of the E3 ligase with the Na,K-ATPase β-subunit we compensated the absence of regulation of the protein by CO_2 with an alternative approach. Based on our previous results which suggest that hypercapnia-

mediated phosphorylation of the Na,K-ATPase β-subunit serine 11 might be required for its ubiquitination, we used the Na,K-ATPase β-subunit phosphomimic (S11D) as a bait in the screening. After a thoughtful analysis of the information available in the literature about all the E3 ligases which were found to interact with the Na,K-ATPase β-subunit, we identified TRAF2 as a likely candidate. TRAF2 is a RING E3 ligase [198], well-known by its role in the activation of the NF-κβ signaling pathway [217]. TRAF2 catalytic activity has been shown to be promoted by the binding of sphingosine-1-phosphate (S1P), intracellularly produced by sphingosine kinase 1 (Sphk1) [198]. Three reasons led us to consider TRAF2 as a potential E3 ligase for the Na,K-ATPase β-subunit. First, we found a major TRAF2 binding motif (P/S/T/A)X(Q/E)E [218] in the Na,K-ATPase β-subunit intracellular domain, which comprises the lysine 7 and is in close proximity to lysine 5 and serine 11 of the Na,K-ATPase β-subunit (**Figure 43**). Second, sphingosine kinase 2 (Sphk2) was also found to significantly interact with Na,K-ATPase β-subunit in the protein microarray, and we speculated that S1P production by Sphk2, in proximity to Na,K-ATPase β-subunit may serve as the cofactor required for TRAF2 ubiquitin ligase activity. Third, TRAF2 mediates K63-linked polyubiquitination. [198] which has been shown to regulate the endocytosis and protein sorting of some plasma membrane proteins [168, 173] and could therefore regulate the ubiquitination-driven endocytosis of the Na,K-ATPase β-subunit under hypercapnic conditions.

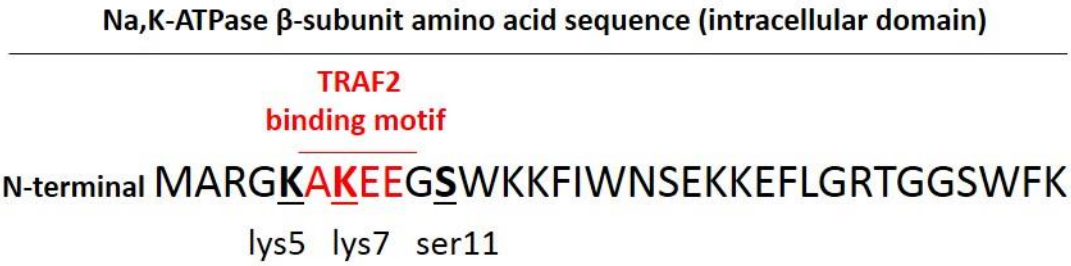

Figure 43: The amino acid sequence of the intracellular domain of the Na,K-ATPase β-subunit. The scheme shows the lysines 5 and 7 of the Na,K-ATPase β-subunit which get ubiquitinated under hypercapnic conditions. It shows the serine 11 of the Na,K-ATPase β-subunit which is required for hypercapnia-induced ubiquitination of the protein. Moreover, it shows TRAF2 binding motif present in Na,K-ATPase β-subunit which comprises the lysine 7 of the Na,K-ATPase β-subunit.

We conducted coimmunoprecipitation studies which we confirmed that TRAF2 interacts with the Na,K-ATPase β-subunit. Moreover, we demonstrated that the

overexpression of TRAF2 in A549 cells promotes the accumulation of the ubiquitinated Na,K-ATPase β-subunit isoforms. Most importantly, by *in vitro* studies we demonstrated that TRAF2 directly interacts and ubiquitinates the intracellular domain of the Na,K-ATPase β-subunit. These findings provide compelling evidence that TRAF2 is an E3 ligase of the Na,K-ATPase β-subunit. Whether TRAF2 E3 ligase activity is required for hypercapnia-induced Na,K-ATPase β-subunit endocytosis was evaluated by the cell knockdown of TRAF2 protein with the use of specific siRNA. This experiments solidly demonstrated that TRAF2 is absolutely required for hypercapnia-mediated ubiquitination-driven endocytosis of the Na,K-ATPase β-subunit.

Ubc13/Uev1A is an E2 ubiquitin conjugating enzyme complex which has been reported to interact with TRAF2 and mediate K63-linked ubiquitination of target proteins [219]. The fact that the *in vitro* ubiquitination of the Na,K-ATPase β-subunit was conducted in the presence of the Ubc13/Uev1 E2 complex suggests the possibility that Na,K-ATPase β-subunit gets ubiquitinated through K63-linked chains. Since K63-linked ubiquitination has been implicated in the regulation of protein transport [168, 173], K63-linked polyubiquitination of Na,K-ATPase β-subunit could account for the role of ubiquitination in promoting the endocytosis of the protein. Future studies oriented to elucidate the topology of Na,K-ATPase β-subunit ubiquitin chains will provide a better understanding of the CO_2-regulated Na,K-ATPase β-subunit endocytosis.

The experiments in which TRAF2 protein was depleted from cells did not show an increase in total plasma membrane abundance of Na,K-ATPase β-subunit protein. One possible explanation for this observation is that TRAF2 may not be involved in the turnover of the Na,K-ATPase β-subunit under steady-state conditions. Though required in hypercapnia-induced Na,K-ATPase β-subunit ubiquitination, TRAF2 may not be the only E3 ligase involved in the regulation of surface expression of the Na,K-ATPase β-subunit. Moreover, ubiquitination might not be the only mechanism involved in the endocytosis of the protein. Other mechanisms may account for Na,K-ATPase β-subunit endocytosis under normal or other stressed-associated conditions.

Considering the role of ubiquitination in the protein degradation pathways, it still remains to be elucidated whether hypercapnia-induced β-subunit degradation requires other ubiquitination events. Based on our studies suggesting a possible role of the proteasome in mediating hypercapnia-induced Na,K-ATPase β-subunit degradation we speculate that there might be other hypercapnia-induced Na,K-ATPase β-subunit ubiquitination steps possibly involving K48-linked polyubiquitination of the protein.

Future studies will be required to gain understanding in the mechanism(s) underlying the hypercapnia-induced TRAF2 activation. We believe that Sphk2, which has been found to interact with the Na,K-ATPase β-subunit in the protein microarray, may participate in the activation of TRAF2. Sphk2 expression, which is tightly regulated in alveolar epithelial cells, has been reported to be upregulated by ERK under hypoxic conditions [220]. Most importantly, since ERK has also been shown to be activated by hypercapnia [221] we propose a plausible mechanism in which hypercapnia-induced ERK-mediated Sphk2 activation, leads to S1P production in the proximity of the Na,K-ATPase β-subunit which activates TRAF2 E3 ligase that mediates the ubiquitination of the Na,K-ATPase β-subunit at the plasma membrane.

4.6. Concluding remarks

Previous studies have demonstrated that hypercapnia causes detrimental effects on the function of the alveolar epithelial cells such as mitochondrial dysfunction and impaired cell proliferation [203]. CO_2 levels have also been found to promote the endocytosis of the Na,K-ATPase α-subunit which leads to impaired alveolar fluid reabsorption in the lung [127, 128]. In the present studies we provide evidence of a new mechanism by which hypercapnia has adverse effects on the alveolar epithelium. By down-regulating the expression of the plasma membrane Na,K-ATPase β-subunit, hypercapnia impairs the ability of alveolar cells to interact with each other. Since new cell junctions formation is essential for the process of repairing the alveolar epithelium after ARDS, elevated CO_2 levels in the alveolar epithelium of patients with ARDS may lead to persistent dysfunction of the alveolar epithelium, which is associated with worse patient prognosis [9, 15, 16, 29, 33, 34]. Considering that Na,K-ATPase β-subunit endocytosis alone is enough to impair the formation of adherens junctions, our findings highlight the key role of the protein in alveolar epithelium as an adhesion molecule.

In the present work, we elucidate the molecular mechanism involved in hypercapnia-mediated Na,K-ATPase β-subunit down-regulation (**Figure 44**). We demonstrate that elevated CO_2 leads to PKC-ζ-mediated regulation of Na,K-ATPase β-subunit, which triggers TRAF2-mediated ubiquitination of the protein, which results in the endocytosis and degradation of Na,K-ATPase β-subunit. The decision to orient our research toward the identification of the hypercapnia-associated E3 ligase of the Na,K-ATPase β-subunit was based on the notion that E3 ubiquitin ligases determine the

specificity of the ubiquitination process by targeting the specific substrates. Considering the relevant role of Na,K-ATPase β-subunit in cell adherens junction formation in alveolar epithelial cells, the identification of the E3 ligase of the Na,K-ATPase β-subunit provides with a potential therapeutic tool to be employed not only in ARDS but also in other lung diseases in which cell adhesion events are involved, such as lung cancer and fibrosis.

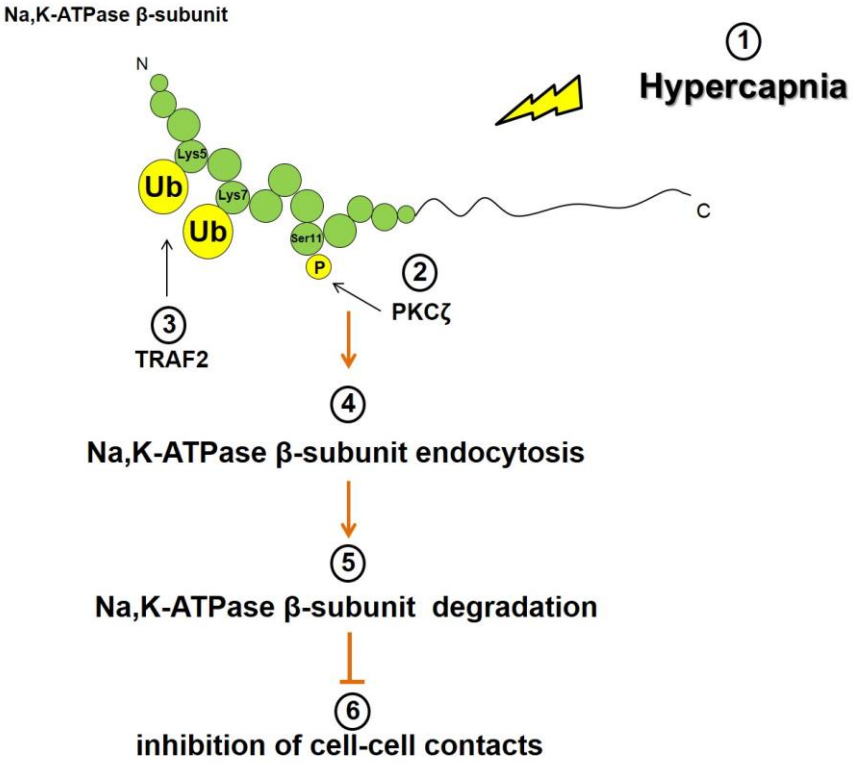

Figure 44: Model for hypercapnia-mediated inhibition of cell-cell contacts (See **section 4.6.** for detailed explanation).

5. References

1. Rubenfeld, G.D., et al., *Incidence and outcomes of acute lung injury.* N Engl J Med, 2005. **353**(16): p. 1685-93.
2. Matthay, M.A. and R.L. Zemans, *The acute respiratory distress syndrome: pathogenesis and treatment.* Annu Rev Pathol, 2011. **6**: p. 147-63.
3. Bernard, G.R., et al., *The American-European Consensus Conference on ARDS. Definitions, mechanisms, relevant outcomes, and clinical trial coordination.* Am J Respir Crit Care Med, 1994. **149**(3 Pt 1): p. 818-24.
4. Force, A.D.T., et al., *Acute respiratory distress syndrome: the Berlin Definition.* JAMA, 2012. **307**(23): p. 2526-33.
5. Bachofen, M. and E.R. Weibel, *Alterations of the gas exchange apparatus in adult respiratory insufficiency associated with septicemia.* Am Rev Respir Dis, 1977. **116**(4): p. 589-615.
6. Ware, L.B. and M.A. Matthay, *The acute respiratory distress syndrome.* N Engl J Med, 2000. **342**(18): p. 1334-49.
7. Bachofen, M. and E.R. Weibel, *Structural alterations of lung parenchyma in the adult respiratory distress syndrome.* Clin Chest Med, 1982. **3**(1): p. 35-56.
8. Meyrick, B., *Pathology of the adult respiratory distress syndrome.* Crit Care Clin, 1986. **2**(3): p. 405-28.
9. Bhattacharya, J. and M.A. Matthay, *Regulation and repair of the alveolar-capillary barrier in acute lung injury.* Annu Rev Physiol, 2013. **75**: p. 593-615.
10. Flick, M.R., A. Perel, and N.C. Staub, *Leukocytes are required for increased lung microvascular permeability after microembolization in sheep.* Circ Res, 1981. **48**(3): p. 344-51.
11. Matthay, M.A. and G.A. Zimmerman, *Acute lung injury and the acute respiratory distress syndrome: four decades of inquiry into pathogenesis and rational management.* Am J Respir Cell Mol Biol, 2005. **33**(4): p. 319-27.
12. Herold, S., N.M. Gabrielli, and I. Vadasz, *Novel aspects of acute lung injury and alveolo-capillary barrier dysfunction.* Am J Physiol Lung Cell Mol Physiol, 2013.
13. Staub, N.C., *"State of the art" review. Pathogenesis of pulmonary edema.* Am Rev Respir Dis, 1974. **109**(3): p. 358-72.
14. Staub, N.C., *Pulmonary edema due to increased microvascular permeability.* Annu Rev Med, 1981. **32**: p. 291-312.
15. Geiser, T., *Mechanisms of alveolar epithelial repair in acute lung injury--a translational approach.* Swiss Med Wkly, 2003. **133**(43-44): p. 586-90.
16. Ware, L.B., *Pathophysiology of acute lung injury and the acute respiratory distress syndrome.* Semin Respir Crit Care Med, 2006. **27**(4): p. 337-49.
17. Wiener-Kronish, J.P., K.H. Albertine, and M.A. Matthay, *Differential responses of the endothelial and epithelial barriers of the lung in sheep to Escherichia coli endotoxin.* J Clin Invest, 1991. **88**(3): p. 864-75.
18. Martin, T.R., et al., *Effects of leukotriene B4 in the human lung. Recruitment of neutrophils into the alveolar spaces without a change in protein permeability.* J Clin Invest, 1989. **84**(5): p. 1609-19.
19. Zemans, R.L., S.P. Colgan, and G.P. Downey, *Transepithelial migration of neutrophils: mechanisms and implications for acute lung injury.* Am J Respir Cell Mol Biol, 2009. **40**(5): p. 519-35.
20. Weibel, E.R., *Morphological basis of alveolar-capillary gas exchange.* Physiol Rev, 1973. **53**(2): p. 419-95.

21. Weibel, E.R., *What makes a good lung?* Swiss Med Wkly, 2009. **139**(27-28): p. 375-86.
22. Weibel, E.R., *Gas exchange: large surface and thin barrier determine pulmonary diffusing capacity.* Minerva Anestesiol, 1999. **65**(6): p. 377-82.
23. Weibel, E.R., *Morphometry of the human lung: the state of the art after two decades.* Bull Eur Physiopathol Respir, 1979. **15**(5): p. 999-1013.
24. Boitano, S., et al., *Cell-cell interactions in regulating lung function.* Am J Physiol Lung Cell Mol Physiol, 2004. **287**(3): p. L455-9.
25. Matalon, S., *Mechanisms and regulation of ion transport in adult mammalian alveolar type II pneumocytes.* Am J Physiol, 1991. **261**(5 Pt 1): p. C727-38.
26. Schneeberger, E.E. and R.D. Lynch, *Structure, function, and regulation of cellular tight junctions.* Am J Physiol, 1992. **262**(6 Pt 1): p. L647-61.
27. Taylor, A.E. and K.A. Gaar, Jr., *Estimation of equivalent pore radii of pulmonary capillary and alveolar membranes.* Am J Physiol, 1970. **218**(4): p. 1133-40.
28. Matthay, M.A., *Function of the alveolar epithelial barrier under pathologic conditions.* Chest, 1994. **105**(3 Suppl): p. 67S-74S.
29. Matthay, M.A., *The adult respiratory distress syndrome. Definition and prognosis.* Clin Chest Med, 1990. **11**(4): p. 575-80.
30. Bitterman, P.B., *Pathogenesis of fibrosis in acute lung injury.* Am J Med, 1992. **92**(6A): p. 39S-43S.
31. Lewis, J.F. and A.H. Jobe, *Surfactant and the adult respiratory distress syndrome.* Am Rev Respir Dis, 1993. **147**(1): p. 218-33.
32. Berthiaume, Y., O. Lesur, and A. Dagenais, *Treatment of adult respiratory distress syndrome: plea for rescue therapy of the alveolar epithelium.* Thorax, 1999. **54**(2): p. 150-60.
33. Ware, L.B. and M.A. Matthay, *Alveolar fluid clearance is impaired in the majority of patients with acute lung injury and the acute respiratory distress syndrome.* Am J Respir Crit Care Med, 2001. **163**(6): p. 1376-83.
34. Matthay, M.A., *Alveolar fluid clearance in patients with ARDS: does it make a difference?* Chest, 2002. **122**(6 Suppl): p. 340S-343S.
35. Mutlu, G.M. and J.I. Sznajder, *Mechanisms of pulmonary edema clearance.* Am J Physiol Lung Cell Mol Physiol, 2005. **289**(5): p. L685-95.
36. Clerici, C., *Sodium transport in alveolar epithelial cells: modulation by O2 tension.* Kidney Int Suppl, 1998. **65**: p. S79-83.
37. Matthay, M.A., C. Clerici, and G. Saumon, *Invited review: Active fluid clearance from the distal air spaces of the lung.* J Appl Physiol, 2002. **93**(4): p. 1533-41.
38. Crosby, L.M. and C.M. Waters, *Epithelial repair mechanisms in the lung.* Am J Physiol Lung Cell Mol Physiol, 2010. **298**(6): p. L715-31.
39. Schneeberger, E.E., D.V. Walters, and R.E. Olver, *Development of intercellular junctions in the pulmonary epithelium of the foetal lamb.* J Cell Sci, 1978. **32**: p. 307-24.
40. Schneeberger, E.E., *Structural basis for some permeability properties of the air--blood barrier.* Fed Proc, 1978. **37**(11): p. 2471-8.
41. Fristrom, D., *The cellular basis of epithelial morphogenesis. A review.* Tissue Cell, 1988. **20**(5): p. 645-90.
42. Takeichi, M., *Cadherins: key molecules for selective cell-cell adhesion.* IARC Sci Publ, 1988(92): p. 76-9.
43. Takeichi, M., et al., *Cadherin-dependent organization and disorganization of epithelial architecture.* Princess Takamatsu Symp, 1994. **24**: p. 28-37.
44. Angst, B.D., C. Marcozzi, and A.I. Magee, *The cadherin superfamily: diversity in form and function.* J Cell Sci, 2001. **114**(Pt 4): p. 629-41.

45. Gumbiner, B., *Cadherins: a family of Ca2+-dependent adhesion molecules.* Trends Biochem Sci, 1988. **13**(3): p. 75-6.
46. Gumbiner, B., B. Stevenson, and A. Grimaldi, *The role of the cell adhesion molecule uvomorulin in the formation and maintenance of the epithelial junctional complex.* J Cell Biol, 1988. **107**(4): p. 1575-87.
47. Gumbiner, B.M., *Regulation of cadherin adhesive activity.* J Cell Biol, 2000. **148**(3): p. 399-404.
48. Nagafuchi, A. and M. Takeichi, *Cell binding function of E-cadherin is regulated by the cytoplasmic domain.* EMBO J, 1988. **7**(12): p. 3679-84.
49. Takeichi, M., et al., *Cytoplasmic control of cadherin-mediated cell-cell adhesion.* Cold Spring Harb Symp Quant Biol, 1992. **57**: p. 327-34.
50. Perez-Moreno, M., C. Jamora, and E. Fuchs, *Sticky business: orchestrating cellular signals at adherens junctions.* Cell, 2003. **112**(4): p. 535-48.
51. Cereijido, M., R.G. Contreras, and L. Shoshani, *Cell adhesion, polarity, and epithelia in the dawn of metazoans.* Physiol Rev, 2004. **84**(4): p. 1229-62.
52. Contreras, R.G., et al., *E-Cadherin and tight junctions between epithelial cells of different animal species.* Pflugers Arch, 2002. **444**(4): p. 467-75.
53. Schneeberger, E.E. and R.D. Lynch, *Tight junctions. Their structure, composition, and function.* Circ Res, 1984. **55**(6): p. 723-33.
54. Walker, D.C., et al., *Assessment of tight junctions between pulmonary epithelial and endothelial cells.* J Appl Physiol, 1988. **64**(6): p. 2348-56.
55. Denker, B.M. and S.K. Nigam, *Molecular structure and assembly of the tight junction.* Am J Physiol, 1998. **274**(1 Pt 2): p. F1-9.
56. Overgaard, C.E., L.A. Mitchell, and M. Koval, *Roles for claudins in alveolar epithelial barrier function.* Ann N Y Acad Sci, 2012. **1257**: p. 167-74.
57. Saitou, M., et al., *Mammalian occludin in epithelial cells: its expression and subcellular distribution.* Eur J Cell Biol, 1997. **73**(3): p. 222-31.
58. Chen, Y., et al., *COOH terminus of occludin is required for tight junction barrier function in early Xenopus embryos.* J Cell Biol, 1997. **138**(4): p. 891-9.
59. LaFemina, M.J., et al., *Keratinocyte growth factor enhances barrier function without altering claudin expression in primary alveolar epithelial cells.* Am J Physiol Lung Cell Mol Physiol, 2010. **299**(6): p. L724-34.
60. Rokkam, D., et al., *Claudin-4 levels are associated with intact alveolar fluid clearance in human lungs.* Am J Pathol, 2011. **179**(3): p. 1081-7.
61. Wray, C., et al., *Claudin-4 augments alveolar epithelial barrier function and is induced in acute lung injury.* Am J Physiol Lung Cell Mol Physiol, 2009. **297**(2): p. L219-27.
62. Sun, Y., R.D. Minshall, and G. Hu, *Role of claudins in oxidant-induced alveolar epithelial barrier dysfunction.* Methods Mol Biol, 2011. **762**: p. 291-301.
63. Simet, S.M., et al., *Alcohol increases the permeability of airway epithelial tight junctions in Beas-2B and NHBE cells.* Alcohol Clin Exp Res, 2012. **36**(3): p. 432-42.
64. Gordon, R.E., D. Solano, and J. Kleinerman, *Tight junction alterations of respiratory epithelium following long-term NO2 exposure and recovery.* Exp Lung Res, 1986. **11**(3): p. 179-93.
65. Skou, J.C., *Nobel Lecture. The identification of the sodium pump.* Biosci Rep, 1998. **18**(4): p. 155-69.
66. Kaplan, J.H., *Biochemistry of Na,K-ATPase.* Annu Rev Biochem, 2002. **71**: p. 511-35.
67. Mercer, R.W., *Structure of the Na,K-ATPase.* Int Rev Cytol, 1993. **137C**: p. 139-68.

68. Tokhtaeva, E., G. Sachs, and O. Vagin, *Assembly with the Na,K-ATPase alpha(1) subunit is required for export of beta(1) and beta(2) subunits from the endoplasmic reticulum.* Biochemistry, 2009. **48**(48): p. 11421-31.
69. Blanco, G., J.C. Koster, and R.W. Mercer, *The alpha subunit of the Na,K-ATPase specifically and stably associates into oligomers.* Proc Natl Acad Sci U S A, 1994. **91**(18): p. 8542-6.
70. Lingrel, J.B. and T. Kuntzweiler, *Na+,K(+)-ATPase.* J Biol Chem, 1994. **269**(31): p. 19659-62.
71. Pressley, T.A., et al., *Amino-terminal processing of the catalytic subunit from Na(+)-K(+)-ATPase.* Am J Physiol, 1996. **271**(3 Pt 1): p. C825-32.
72. Vagin, O., S. Turdikulova, and E. Tokhtaeva, *Polarized membrane distribution of potassium-dependent ion pumps in epithelial cells: different roles of the N-glycans of their beta subunits.* Cell Biochem Biophys, 2007. **47**(3): p. 376-91.
73. McDonough, A.A., K. Geering, and R.A. Farley, *The sodium pump needs its beta subunit.* FASEB J, 1990. **4**(6): p. 1598-605.
74. Sweadner, K.J., *Isozymes of the Na+/K+-ATPase.* Biochim Biophys Acta, 1989. **988**(2): p. 185-220.
75. Sweadner, K.J., *Overview: subunit diversity in the Na,K-ATPase.* Soc Gen Physiol Ser, 1991. **46**: p. 63-76.
76. Blanco, G. and R.W. Mercer, *Isozymes of the Na-K-ATPase: heterogeneity in structure, diversity in function.* Am J Physiol, 1998. **275**(5 Pt 2): p. F633-50.
77. Mercer, R.W., et al., *Molecular cloning and immunological characterization of the gamma polypeptide, a small protein associated with the Na,K-ATPase.* J Cell Biol, 1993. **121**(3): p. 579-86.
78. Shyjan, A.W. and R. Levenson, *Antisera specific for the alpha 1, alpha 2, alpha 3, and beta subunits of the Na,K-ATPase: differential expression of alpha and beta subunits in rat tissue membranes.* Biochemistry, 1989. **28**(11): p. 4531-5.
79. Ridge, K., et al., *Alpha-2 Na,K-ATPase contributes to lung liquid clearance.* Ann N Y Acad Sci, 1997. **834**: p. 651-2.
80. Ridge, K.M., et al., *Alveolar type 1 cells express the alpha2 Na,K-ATPase, which contributes to lung liquid clearance.* Circ Res, 2003. **92**(4): p. 453-60.
81. Matthay, M.A., H.G. Folkesson, and C. Clerici, *Lung epithelial fluid transport and the resolution of pulmonary edema.* Physiol Rev, 2002. **82**(3): p. 569-600.
82. Rajasekaran, S.A., S.P. Barwe, and A.K. Rajasekaran, *Multiple functions of Na,K-ATPase in epithelial cells.* Semin Nephrol, 2005. **25**(5): p. 328-34.
83. Cereijido, M., et al., *The Na+-K+-ATPase as self-adhesion molecule and hormone receptor.* Am J Physiol Cell Physiol, 2012. **302**(3): p. C473-81.
84. Ogawa, H., et al., *Crystal structure of the sodium-potassium pump (Na+,K+-ATPase) with bound potassium and ouabain.* Proc Natl Acad Sci U S A, 2009. **106**(33): p. 13742-7.
85. Tokhtaeva, E., et al., *Identification of the amino acid region involved in the intercellular interaction between the beta1 subunits of Na+/K+ -ATPase.* J Cell Sci, 2012. **125**(Pt 6): p. 1605-16.
86. Vagin, O., E. Tokhtaeva, and G. Sachs, *The role of the beta1 subunit of the Na,K-ATPase and its glycosylation in cell-cell adhesion.* J Biol Chem, 2006. **281**(51): p. 39573-87.
87. Shoshani, L., et al., *The polarized expression of Na+,K+-ATPase in epithelia depends on the association between beta-subunits located in neighboring cells.* Mol Biol Cell, 2005. **16**(3): p. 1071-81.
88. Contreras, R.G., et al., *Relationship between Na(+),K(+)-ATPase and cell attachment.* J Cell Sci, 1999. **112 (Pt 23)**: p. 4223-32.

89. Contreras, R.G., et al., *Ouabain binding to Na+,K+-ATPase relaxes cell attachment and sends a specific signal (NACos) to the nucleus.* J Membr Biol, 2004. **198**(3): p. 147-58.
90. Gloor, S., et al., *The adhesion molecule on glia (AMOG) is a homologue of the beta subunit of the Na,K-ATPase.* J Cell Biol, 1990. **110**(1): p. 165-74.
91. Schmalzing, G., et al., *The adhesion molecule on glia (AMOG/beta 2) and alpha 1 subunits assemble to functional sodium pumps in Xenopus oocytes.* J Biol Chem, 1992. **267**(28): p. 20212-6.
92. Padilla-Benavides, T., et al., *The polarized distribution of Na+,K+-ATPase: role of the interaction between {beta} subunits.* Mol Biol Cell, 2010. **21**(13): p. 2217-25.
93. Tokhtaeva, E., et al., *Epithelial junctions depend on intercellular trans-interactions between the Na,K-ATPase beta(1) subunits.* J Biol Chem, 2011. **286**(29): p. 25801-12.
94. Vagin, O., et al., *Inverse correlation between the extent of N-glycan branching and intercellular adhesion in epithelia. Contribution of the Na,K-ATPase beta1 subunit.* J Biol Chem, 2008. **283**(4): p. 2192-202.
95. Vagin, O., G. Sachs, and E. Tokhtaeva, *The roles of the Na,K-ATPase beta 1 subunit in pump sorting and epithelial integrity.* J Bioenerg Biomembr, 2007. **39**(5-6): p. 367-72.
96. Vagin, O., et al., *The Na-K-ATPase alpha(1)beta(1) heterodimer as a cell adhesion molecule in epithelia.* Am J Physiol Cell Physiol, 2012. **302**(9): p. C1271-81.
97. Rajasekaran, S.A., et al., *Na,K-ATPase beta-subunit is required for epithelial polarization, suppression of invasion, and cell motility.* Mol Biol Cell, 2001. **12**(2): p. 279-95.
98. Rajasekaran, A.K. and S.A. Rajasekaran, *Role of Na-K-ATPase in the assembly of tight junctions.* Am J Physiol Renal Physiol, 2003. **285**(3): p. F388-96.
99. Rajasekaran, S.A., et al., *Na-K-ATPase regulates tight junction permeability through occludin phosphorylation in pancreatic epithelial cells.* Am J Physiol Gastrointest Liver Physiol, 2007. **292**(1): p. G124-33.
100. Rajasekaran, S.A. and A.K. Rajasekaran, *Na,K-ATPase and epithelial tight junctions.* Front Biosci (Landmark Ed), 2009. **14**: p. 2130-48.
101. Violette, M.I., P. Madan, and A.J. Watson, *Na+/K+ -ATPase regulates tight junction formation and function during mouse preimplantation development.* Dev Biol, 2006. **289**(2): p. 406-19.
102. Rajasekaran, S.A., et al., *Na,K-ATPase activity is required for formation of tight junctions, desmosomes, and induction of polarity in epithelial cells.* Mol Biol Cell, 2001. **12**(12): p. 3717-32.
103. Bertorello, A.M., et al., *Isoproterenol increases Na+-K+-ATPase activity by membrane insertion of alpha-subunits in lung alveolar cells.* Am J Physiol, 1999. **276**(1 Pt 1): p. L20-7.
104. Bertorello, A.M. and J.I. Sznajder, *The dopamine paradox in lung and kidney epithelia: sharing the same target but operating different signaling networks.* Am J Respir Cell Mol Biol, 2005. **33**(5): p. 432-7.
105. Ewart, H.S. and A. Klip, *Hormonal regulation of the Na(+)-K(+)-ATPase: mechanisms underlying rapid and sustained changes in pump activity.* Am J Physiol, 1995. **269**(2 Pt 1): p. C295-311.
106. Therien, A.G. and R. Blostein, *Mechanisms of sodium pump regulation.* Am J Physiol Cell Physiol, 2000. **279**(3): p. C541-66.
107. Sznajder, J.I., P. Factor, and D.H. Ingbar, *Invited review: lung edema clearance: role of Na(+)-K(+)-ATPase.* J Appl Physiol, 2002. **93**(5): p. 1860-6.

108. Vadasz, I., S. Raviv, and J.I. Sznajder, *Alveolar epithelium and Na,K-ATPase in acute lung injury.* Intensive Care Med, 2007. **33**(7): p. 1243-51.
109. Pinto-do, O.P., et al., *Short-term vs. sustained inhibition of proximal tubule Na,K-ATPase activity by dopamine: cellular mechanisms.* Clin Exp Hypertens, 1997. **19**(1-2): p. 73-86.
110. Saldias, F.J., et al., *Dopamine restores lung ability to clear edema in rats exposed to hyperoxia.* Am J Respir Crit Care Med, 1999. **159**(2): p. 626-33.
111. Lecuona, E., H.E. Trejo, and J.I. Sznajder, *Regulation of Na,K-ATPase during acute lung injury.* J Bioenerg Biomembr, 2007. **39**(5-6): p. 391-5.
112. Vadasz, I., et al., *Hypercapnia: a nonpermissive environment for the lung.* Am J Respir Cell Mol Biol, 2012. **46**(4): p. 417-21.
113. Briva, A., E. Lecuona, and J.I. Sznajder, *[Permissive and non-permissive hypercapnia: mechanisms of action and consequences of high carbon dioxide levels].* Arch Bronconeumol, 2010. **46**(7): p. 378-82.
114. Laffey, J.G. and B.P. Kavanagh, *Carbon dioxide and the critically ill--too little of a good thing?* Lancet, 1999. **354**(9186): p. 1283-6.
115. Laffey, J.G., et al., *Permissive hypercapnia--role in protective lung ventilatory strategies.* Intensive Care Med, 2004. **30**(3): p. 347-56.
116. Curley, G., M. Hayes, and J.G. Laffey, *Can 'permissive' hypercapnia modulate the severity of sepsis-induced ALI/ARDS?* Crit Care, 2011. **15**(2): p. 212.
117. Nichol, A.D., et al., *Infection-induced lung injury is worsened after renal buffering of hypercapnic acidosis.* Crit Care Med, 2009. **37**(11): p. 2953-61.
118. Kaushik, M., et al., *Extracorporeal carbon dioxide removal: the future of lung support lies in the history.* Blood Purif, 2012. **34**(2): p. 94-106.
119. Sin, D.D., S.F. Man, and T.J. Marrie, *Arterial carbon dioxide tension on admission as a marker of in-hospital mortality in community-acquired pneumonia.* Am J Med, 2005. **118**(2): p. 145-50.
120. Groenewegen, K.H., A.M. Schols, and E.F. Wouters, *Mortality and mortality-related factors after hospitalization for acute exacerbation of COPD.* Chest, 2003. **124**(2): p. 459-67.
121. Mohangoo, A.D., et al., *Prevalence estimates of asthma or COPD from a health interview survey and from general practitioner registration: what's the difference?* Eur J Public Health, 2006. **16**(1): p. 101-5.
122. Belkin, R.A., et al., *Risk factors for death of patients with cystic fibrosis awaiting lung transplantation.* Am J Respir Crit Care Med, 2006. **173**(6): p. 659-66.
123. Jones, W.D., et al., *Two chemosensory receptors together mediate carbon dioxide detection in Drosophila.* Nature, 2007. **445**(7123): p. 86-90.
124. Hashimoto, M., et al., *Arabidopsis HT1 kinase controls stomatal movements in response to CO2.* Nat Cell Biol, 2006. **8**(4): p. 391-7.
125. Hu, J., et al., *Detection of near-atmospheric concentrations of CO2 by an olfactory subsystem in the mouse.* Science, 2007. **317**(5840): p. 953-7.
126. Putnam, R.W., J.A. Filosa, and N.A. Ritucci, *Cellular mechanisms involved in CO(2) and acid signaling in chemosensitive neurons.* Am J Physiol Cell Physiol, 2004. **287**(6): p. C1493-526.
127. Briva, A., et al., *High CO2 levels impair alveolar epithelial function independently of pH.* PLoS One, 2007. **2**(11): p. e1238.
128. Vadasz, I., et al., *AMP-activated protein kinase regulates CO2-induced alveolar epithelial dysfunction in rats and human cells by promoting Na,K-ATPase endocytosis.* J Clin Invest, 2008. **118**(2): p. 752-62.
129. Hicke, L., *Ubiquitin-dependent internalization and down-regulation of plasma membrane proteins.* FASEB J, 1997. **11**(14): p. 1215-26.

130. d'Azzo, A., A. Bongiovanni, and T. Nastasi, *E3 ubiquitin ligases as regulators of membrane protein trafficking and degradation.* Traffic, 2005. **6**(6): p. 429-41.
131. Dada, L.A., et al., *Phosphorylation and ubiquitination are necessary for Na,K-ATPase endocytosis during hypoxia.* Cell Signal, 2007. **19**(9): p. 1893-8.
132. Hershko, A. and A. Ciechanover, *The ubiquitin system.* Annu Rev Biochem, 1998. **67**: p. 425-79.
133. Ciechanover, A., et al., *Activation of the heat-stable polypeptide of the ATP-dependent proteolytic system.* Proc Natl Acad Sci U S A, 1981. **78**(2): p. 761-5.
134. Ciechanover, A., et al., *Characterization of the heat-stable polypeptide of the ATP-dependent proteolytic system from reticulocytes.* J Biol Chem, 1980. **255**(16): p. 7525-8.
135. Ciechanover, A., *Intracellular protein degradation: from a vague idea through the lysosome and the ubiquitin-proteasome system and onto human diseases and drug targeting.* Bioorg Med Chem, 2013. **21**(12): p. 3400-10.
136. Metzger, M.B., V.A. Hristova, and A.M. Weissman, *HECT and RING finger families of E3 ubiquitin ligases at a glance.* J Cell Sci, 2012. **125**(Pt 3): p. 531-7.
137. Scheffner, M., U. Nuber, and J.M. Huibregtse, *Protein ubiquitination involving an E1-E2-E3 enzyme ubiquitin thioester cascade.* Nature, 1995. **373**(6509): p. 81-3.
138. Ciechanover, A., *The ubiquitin-proteasome pathway: on protein death and cell life.* EMBO J, 1998. **17**(24): p. 7151-60.
139. Huibregtse, J.M., et al., *A family of proteins structurally and functionally related to the E6-AP ubiquitin-protein ligase.* Proc Natl Acad Sci U S A, 1995. **92**(7): p. 2563-7.
140. Deshaies, R.J. and C.A. Joazeiro, *RING domain E3 ubiquitin ligases.* Annu Rev Biochem, 2009. **78**: p. 399-434.
141. Joazeiro, C.A. and T. Hunter, *Biochemistry. Ubiquitination--more than two to tango.* Science, 2000. **289**(5487): p. 2061-2.
142. Lu, J.Y., et al., *Functional dissection of a HECT ubiquitin E3 ligase.* Mol Cell Proteomics, 2008. **7**(1): p. 35-45.
143. Lorick, K.L., et al., *RING fingers mediate ubiquitin-conjugating enzyme (E2)-dependent ubiquitination.* Proc Natl Acad Sci U S A, 1999. **96**(20): p. 11364-9.
144. Ozkan, E., H. Yu, and J. Deisenhofer, *Mechanistic insight into the allosteric activation of a ubiquitin-conjugating enzyme by RING-type ubiquitin ligases.* Proc Natl Acad Sci U S A, 2005. **102**(52): p. 18890-5.
145. Meek, D.W. and U. Knippschild, *Posttranslational modification of MDM2.* Mol Cancer Res, 2003. **1**(14): p. 1017-26.
146. Merlet, J., et al., *Regulation of cullin-RING E3 ubiquitin-ligases by neddylation and dimerization.* Cell Mol Life Sci, 2009. **66**(11-12): p. 1924-38.
147. Gao, M. and M. Karin, *Regulating the regulators: control of protein ubiquitination and ubiquitin-like modifications by extracellular stimuli.* Mol Cell, 2005. **19**(5): p. 581-93.
148. Kawakami, T., et al., *NEDD8 recruits E2-ubiquitin to SCF E3 ligase.* EMBO J, 2001. **20**(15): p. 4003-12.
149. Glickman, M.H. and A. Ciechanover, *The ubiquitin-proteasome proteolytic pathway: destruction for the sake of construction.* Physiol Rev, 2002. **82**(2): p. 373-428.
150. Willems, A.R., et al., *Cdc53 targets phosphorylated G1 cyclins for degradation by the ubiquitin proteolytic pathway.* Cell, 1996. **86**(3): p. 453-63.
151. Deshaies, R.J., *Phosphorylation and proteolysis: partners in the regulation of cell division in budding yeast.* Curr Opin Genet Dev, 1997. **7**(1): p. 7-16.

152. Hunter, T., *The age of crosstalk: phosphorylation, ubiquitination, and beyond.* Mol Cell, 2007. **28**(5): p. 730-8.
153. Beal, R., et al., *Surface hydrophobic residues of multiubiquitin chains essential for proteolytic targeting.* Proc Natl Acad Sci U S A, 1996. **93**(2): p. 861-6.
154. Yamano, H., et al., *The role of the destruction box and its neighbouring lysine residues in cyclin B for anaphase ubiquitin-dependent proteolysis in fission yeast: defining the D-box receptor.* EMBO J, 1998. **17**(19): p. 5670-8.
155. Winget, J.M. and T. Mayor, *The diversity of ubiquitin recognition: hot spots and varied specificity.* Mol Cell, 2010. **38**(5): p. 627-35.
156. Ikeda, F., N. Crosetto, and I. Dikic, *What determines the specificity and outcomes of ubiquitin signaling?* Cell, 2010. **143**(5): p. 677-81.
157. Metzger, M.B., et al., *RING-type E3 ligases: Master manipulators of E2 ubiquitin-conjugating enzymes and ubiquitination.* Biochim Biophys Acta, 2013.
158. Ye, Y., et al., *Ubiquitin chain conformation regulates recognition and activity of interacting proteins.* Nature, 2012. **492**(7428): p. 266-70.
159. Komander, D. and M. Rape, *The ubiquitin code.* Annu Rev Biochem, 2012. **81**: p. 203-29.
160. Burger, A.M. and A.K. Seth, *The ubiquitin-mediated protein degradation pathway in cancer: therapeutic implications.* Eur J Cancer, 2004. **40**(15): p. 2217-29.
161. Pickart, C.M. and M.J. Eddins, *Ubiquitin: structures, functions, mechanisms.* Biochim Biophys Acta, 2004. **1695**(1-3): p. 55-72.
162. Pickart, C.M. and D. Fushman, *Polyubiquitin chains: polymeric protein signals.* Curr Opin Chem Biol, 2004. **8**(6): p. 610-6.
163. Raasi, S. and C.M. Pickart, *Ubiquitin chain synthesis.* Methods Mol Biol, 2005. **301**: p. 47-55.
164. Weissman, A.M., *Themes and variations on ubiquitylation.* Nat Rev Mol Cell Biol, 2001. **2**(3): p. 169-78.
165. Xu, P., et al., *Quantitative proteomics reveals the function of unconventional ubiquitin chains in proteasomal degradation.* Cell, 2009. **137**(1): p. 133-45.
166. Pickart, C.M., *Targeting of substrates to the 26S proteasome.* FASEB J, 1997. **11**(13): p. 1055-66.
167. Bremm, A. and D. Komander, *Synthesis and analysis of K11-linked ubiquitin chains.* Methods Mol Biol, 2012. **832**: p. 219-28.
168. Clague, M.J. and S. Urbe, *Ubiquitin: same molecule, different degradation pathways.* Cell, 2010. **143**(5): p. 682-5.
169. Ciechanover, A., D. Finley, and A. Varshavsky, *The ubiquitin-mediated proteolytic pathway and mechanisms of energy-dependent intracellular protein degradation.* J Cell Biochem, 1984. **24**(1): p. 27-53.
170. Finley, D., *Recognition and processing of ubiquitin-protein conjugates by the proteasome.* Annu Rev Biochem, 2009. **78**: p. 477-513.
171. De Duve, C. and R. Wattiaux, *Functions of lysosomes.* Annu Rev Physiol, 1966. **28**: p. 435-92.
172. Grant, B.D. and J.G. Donaldson, *Pathways and mechanisms of endocytic recycling.* Nat Rev Mol Cell Biol, 2009. **10**(9): p. 597-608.
173. Lauwers, E., C. Jacob, and B. Andre, *K63-linked ubiquitin chains as a specific signal for protein sorting into the multivesicular body pathway.* J Cell Biol, 2009. **185**(3): p. 493-502.
174. Kirkin, V., et al., *A role for ubiquitin in selective autophagy.* Mol Cell, 2009. **34**(3): p. 259-69.
175. Geisler, S., et al., *PINK1/Parkin-mediated mitophagy is dependent on VDAC1 and p62/SQSTM1.* Nat Cell Biol, 2010. **12**(2): p. 119-31.

176. Lazrak, A., A. Samanta, and S. Matalon, *Biophysical properties and molecular characterization of amiloride-sensitive sodium channels in A549 cells.* Am J Physiol Lung Cell Mol Physiol, 2000. **278**(4): p. L848-57.
177. Wodopia, R., et al., *Hypoxia decreases proteins involved in epithelial electrolyte transport in A549 cells and rat lung.* Am J Physiol Lung Cell Mol Physiol, 2000. **279**(6): p. L1110-9.
178. Fernandez, A.L., et al., *Chronic alcohol ingestion alters claudin expression in the alveolar epithelium of rats.* Alcohol, 2007. **41**(5): p. 371-9.
179. Zhou, B., et al., *Troglitazone attenuates TGF-beta1-induced EMT in alveolar epithelial cells via a PPARgamma-independent mechanism.* PLoS One, 2012. **7**(6): p. e38827.
180. Giard, D.J., et al., *In vitro cultivation of human tumors: establishment of cell lines derived from a series of solid tumors.* J Natl Cancer Inst, 1973. **51**(5): p. 1417-23.
181. Dobbs, L.G., *Isolation and culture of alveolar type II cells.* Am J Physiol, 1990. **258**(4 Pt 1): p. L134-47.
182. Lim, K.L., et al., *Parkin mediates nonclassical, proteasomal-independent ubiquitination of synphilin-1: implications for Lewy body formation.* J Neurosci, 2005. **25**(8): p. 2002-9.
183. Chadee, D.N., T. Yuasa, and J.M. Kyriakis, *Direct activation of mitogen-activated protein kinase kinase kinase MEKK1 by the Ste20p homologue GCK and the adapter protein TRAF2.* Mol Cell Biol, 2002. **22**(3): p. 737-49.
184. Laemmli, U.K., *Cleavage of structural proteins during the assembly of the head of bacteriophage T4.* Nature, 1970. **227**(5259): p. 680-5.
185. Fang, L.P., et al., *Hydrogen sulfide attenuates epithelial-mesenchymal transition of human alveolar epithelial cells.* Pharmacol Res, 2010. **61**(4): p. 298-305.
186. Amato, M.B., et al., *Effect of a protective-ventilation strategy on mortality in the acute respiratory distress syndrome.* N Engl J Med, 1998. **338**(6): p. 347-54.
187. Broccard, A.F., et al., *Protective effects of hypercapnic acidosis on ventilator-induced lung injury.* Am J Respir Crit Care Med, 2001. **164**(5): p. 802-6.
188. Feihl, F. and C. Perret, *Permissive hypercapnia. How permissive should we be?* Am J Respir Crit Care Med, 1994. **150**(6 Pt 1): p. 1722-37.
189. Sharabi, K., et al., *Sensing, physiological effects and molecular response to elevated CO2 levels in eukaryotes.* J Cell Mol Med, 2009. **13**(11-12): p. 4304-18.
190. Rodrigo, C. and G. Rodrigo, *Subarachnoid hemorrhage following permissive hypercapnia in a patient with severe acute asthma.* Am J Emerg Med, 1999. **17**(7): p. 697-9.
191. Mutlu, G.M., et al., *Severe status asthmaticus: management with permissive hypercapnia and inhalation anesthesia.* Crit Care Med, 2002. **30**(2): p. 477-80.
192. Vagin, O., J.A. Kraut, and G. Sachs, *Role of N-glycosylation in trafficking of apical membrane proteins in epithelia.* Am J Physiol Renal Physiol, 2009. **296**(3): p. F459-69.
193. Yoshimura, S.H., et al., *Fast degradation of the auxiliary subunit of Na+/K+-ATPase in the plasma membrane of HeLa cells.* J Cell Sci, 2008. **121**(Pt 13): p. 2159-68.
194. Lecuona, E., et al., *Ubiquitination participates in the lysosomal degradation of Na,K-ATPase in steady-state conditions.* Am J Respir Cell Mol Biol, 2009. **41**(6): p. 671-9.
195. Petaja-Repo, U.E., et al., *Newly synthesized human delta opioid receptors retained in the endoplasmic reticulum are retrotranslocated to the cytosol, deglycosylated, ubiquitinated, and degraded by the proteasome.* J Biol Chem, 2001. **276**(6): p. 4416-23.

196. Tsai, B., Y. Ye, and T.A. Rapoport, *Retro-translocation of proteins from the endoplasmic reticulum into the cytosol.* Nat Rev Mol Cell Biol, 2002. **3**(4): p. 246-55.
197. Haglund, K. and I. Dikic, *The role of ubiquitylation in receptor endocytosis and endosomal sorting.* J Cell Sci, 2012. **125**(Pt 2): p. 265-75.
198. Alvarez, S.E., et al., *Sphingosine-1-phosphate is a missing cofactor for the E3 ubiquitin ligase TRAF2.* Nature, 2010. **465**(7301): p. 1084-8.
199. Scherer, D.C., et al., *Signal-induced degradation of I kappa B alpha requires site-specific ubiquitination.* Proc Natl Acad Sci U S A, 1995. **92**(24): p. 11259-63.
200. Grzesik, B.A., et al., *Efficient gene delivery to primary alveolar epithelial cells by nucleofection.* Am J Physiol Lung Cell Mol Physiol In Press.
201. Kelm, K.B., et al., *The internalization of yeast Ste6p follows an ordered series of events involving phosphorylation, ubiquitination, recognition and endocytosis.* Traffic, 2004. **5**(3): p. 165-80.
202. Leger, J., et al., *Conversion of serine to aspartate imitates phosphorylation-induced changes in the structure and function of microtubule-associated protein tau.* J Biol Chem, 1997. **272**(13): p. 8441-6.
203. Vohwinkel, C.U., et al., *Elevated CO(2) levels cause mitochondrial dysfunction and impair cell proliferation.* J Biol Chem, 2011. **286**(43): p. 37067-76.
204. Ubersax, J.A. and J.E. Ferrell, Jr., *Mechanisms of specificity in protein phosphorylation.* Nat Rev Mol Cell Biol, 2007. **8**(7): p. 530-41.
205. Tokhtaeva, E., et al., *Subunit isoform selectivity in assembly of Na,K-ATPase alpha-beta heterodimers.* J Biol Chem, 2012. **287**(31): p. 26115-25.
206. Tokhtaeva, E., G. Sachs, and O. Vagin, *Diverse pathways for maturation of the Na,K-ATPase beta1 and beta2 subunits in the endoplasmic reticulum of Madin-Darby canine kidney cells.* J Biol Chem, 2010. **285**(50): p. 39289-302.
207. Lee, H.W., et al., *Ubiquitination of protein kinase C-alpha and degradation by the proteasome.* J Biol Chem, 1996. **271**(35): p. 20973-6.
208. Smith, L., et al., *Activation of atypical protein kinase C zeta by caspase processing and degradation by the ubiquitin-proteasome system.* J Biol Chem, 2000. **275**(51): p. 40620-7.
209. Li, X., Y. Yang, and J.D. Ashwell, *TNF-RII and c-IAP1 mediate ubiquitination and degradation of TRAF2.* Nature, 2002. **416**(6878): p. 345-7.
210. Hershko, A., et al., *ATP-dependent degradation of ubiquitin-protein conjugates.* Proc Natl Acad Sci U S A, 1984. **81**(6): p. 1619-23.
211. Melikova, M.S., K.A. Kondratov, and E.S. Kornilova, *Two different stages of epidermal growth factor (EGF) receptor endocytosis are sensitive to free ubiquitin depletion produced by proteasome inhibitor MG132.* Cell Biol Int, 2006. **30**(1): p. 31-43.
212. Carter, S., S. Urbe, and M.J. Clague, *The met receptor degradation pathway: requirement for Lys48-linked polyubiquitin independent of proteasome activity.* J Biol Chem, 2004. **279**(51): p. 52835-9.
213. Piper, R.C. and J.P. Luzio, *Ubiquitin-dependent sorting of integral membrane proteins for degradation in lysosomes.* Curr Opin Cell Biol, 2007. **19**(4): p. 459-65.
214. Gorbea, C., et al., *A protein interaction network for Ecm29 links the 26 S proteasome to molecular motors and endosomal components.* J Biol Chem, 2010. **285**(41): p. 31616-33.
215. Meusser, B., et al., *ERAD: the long road to destruction.* Nat Cell Biol, 2005. **7**(8): p. 766-72.

216. Leichner, G.S., et al., *Dislocation of HMG-CoA reductase and Insig-1, two polytopic endoplasmic reticulum proteins, en route to proteasomal degradation.* Mol Biol Cell, 2009. **20**(14): p. 3330-41.
217. Xia, Z.P. and Z.J. Chen, *TRAF2: a double-edged sword?* Sci STKE, 2005. **2005**(272): p. pe7.
218. Ye, H., et al., *The structural basis for the recognition of diverse receptor sequences by TRAF2.* Mol Cell, 1999. **4**(3): p. 321-30.
219. Liu, J., et al., *Site-specific ubiquitination is required for relieving the transcription factor Miz1-mediated suppression on TNF-alpha-induced JNK activation and inflammation.* Proc Natl Acad Sci U S A, 2012. **109**(1): p. 191-6.
220. Schnitzer, S.E., et al., *Hypoxia enhances sphingosine kinase 2 activity and provokes sphingosine-1-phosphate-mediated chemoresistance in A549 lung cancer cells.* Mol Cancer Res, 2009. **7**(3): p. 393-401.
221. Welch, L.C., et al., *Extracellular signal-regulated kinase (ERK) participates in the hypercapnia-induced Na,K-ATPase downregulation.* FEBS Lett, 2010. **584**(18): p. 3985-9.

6. Acknowledgement

First I would like to express my gratitude to Prof. Dr. Werner Seeger for giving me the opportunity to do my PhD studies at the Faculty of Medicine of University of Giessen and for his support during my research.

I am also grateful to Prof. Dr. Martin Diener for his co-supervision and support.

I am especially grateful to Dr. István Vadász for his constant support and advice. I deeply appreciate his encouragement throughout my studies and his positive attitude which made my work much more enjoyable. His open discussions and critical comments have given me the opportunity to grow as a scientist.

Thanks to all the members of the laboratory for providing a nice working atmosphere and for the support throughout my studies. Thanks to Miriam Wessendorf for her technical support.

My special thanks to Prof. Dr. Iasha Sznajder for his immense support and advice. He has been a great mentor and his feedback has guided me troughout my PhD studies.

I would also like to thank the members of the laboratory of the Prof. Dr. Iasha Sznajder at Northwestern University for their support throughout my work and for sharing experimental protocols and materials. My special thanks to Dr. Laura Dada, Lynn Welch and Dr. Markus Queisser.

I am also thankful to Dr. Marcelo Salierno for his help with the microscopy studies.

I am also very grateful to the MBML committee, Dr. Rory Morty, Dr. Dorothea Peters and Dr. Florian Veit. Thanks to all my MBML colleagues, especially Christin Becker for her help and advice.

I would like to thank my grandparents for their love and constant support. Thanks to all my family members. I also like to thank my friends from Giessen and Buenos Aires for believing in me and making my life happier.

Finally, I dedicate this work to my parents. I am deeply thankful for their unconditional love, advice, help, understanding and patience.